Quantitative Seismic Reservoir Characterization of Mehar Block, Lower Indus Basin, Pakistan.

Muhammad Usama Kamran
(02112013004)

M.Phil. (Geophysics)
2020-2022

Department of Earth Sciences Quaid-I-Azam University, Islamabad

Credential

It is endorsed that Mr. Muhammad Usama Kamran conceded out the work delimited in this dissertation in my observation and is conferred for the grade of M.Phil. (Geophysics) by the department of Earth Sciences in contentment of the degree provisions.

Commended By:

Dr. Aamir Ali (Chairperson)
Associate Professor,
Department of Earth Sciences,
Quaid-i-Azam University, Islamabad.

External Examiner

Salutation

The principal praise with prodigious appreciation is for none but Almighty Allah, who is the foundation of potency, acquaintance, capability and opportunity. His supremacy is all around this world and the world hereafter. His will was there for sure to commence this study and influence it to the adequately customary work. A lot of obligation, durood and salaam to Almighty Allah, Prophet (PBUH) and his family. May the continuation of His blessings remain forever on all of us. The forever living, the forever existing, and the greatest, the Allah.

I would like to acknowledge my teacher and supervisor Dr. Aamir Ali, Chairperson, Department of Earth Sciences, who is worth mentioning here because of his guidance and professional assertiveness throughout the progression towards accomplishment of my dissertation. Furthermore, the part and support of my family members, friends and all other connected masses is likewise appreciable. Thanks to all concerned with the innermost of my heart.

Muhammad Usama Kamran

Abstract

The exploitation of a reservoir can be enhanced significantly by means of reservoir characterization. The objective of this dissertation is to use the seismic and well log data of Mehar Block, Lower Indus Basin, Pakistan in order to demarcate and subsequently characterize the reservoir formation (i.e. Ranikot). The techniques used for this analysis includes seismic structural interpretation, wireline log analysis, seismic inversion analysis (P-impedance and S-impedance), and LMR attributes (lambda-rho ($\lambda\rho$) and mu-rho ($\mu\rho$)). Furthermore, porosity sections have been generated using cross plot analysis and machine learning approach, namely, Probabilistic Neural Networking (PNN). To analyze the spatial distribution of water saturation, Deep Feed-forward Neural Networking (DFFN) approach has been used. The structural seismic interpretation reveals that the regime of the Mehar block is compressional in nature as confirmed by the presence of thrust faulting. The wireline log analysis of the wells Mehar-01, 02 and 03 indicates that the effective porosity (PHIE) in the zone of interest in Mehar-01 is 7.3%, total porosity (PHIT) is 8.1%, shale volume (Vsh) is 10%, and hydrocarbon potential (HS) is 58.2%. In case of Mehar-02, the PHIE in the zone of interest has been estimated to be 7.6%, Vsh is 25%, PHIT is 13% and HS is 68%. Two zones have been demarcated in Mehar-03 well indicating PHIE values of 5.3% and 11.9%, total porosity is 7.8% and 17.9%, shale volume is 11.9% and 12%, and hydrocarbon saturation is 51.2% and 72% respectively. The values from the model-based inversion (MBI), maximum likelihood, and bandlimited inversion indicates low impedance in the zone of interest within the Ranikot Formation. This spatially identified zone is further confirmed by the low values of the $\lambda\rho$ sections (derived from each inversion model) indicating presence of hydrocarbons while the moderate values in the same zone from the $\mu\rho$ sections depict the presence of sand. The spatial distribution of effective porosity using PNN and cross plots depicts high values in the reservoir formation. Furthermore, the DFFN based water saturation values indicate relatively low saturation values in the zone of interest.

Table of Contents

List of Figures

List of Tables

Chapter 1 Introduction

1.1) Research Work Implication

The role of energy sector in progression of development for any country is of great significance. Pakistan is a developing country, so it is a matter of great concern for its economic growth to explore its energy resources. The term "Primitive" attributes indicate to attributes that only quantify a single characteristic. "Hybrid" attributes are generated by relating these primitive attributes through statistical, neural network, or mathematical execution (Taner, 2001).

For the exploration of energy resources, reservoir characterization is the route to approach towards the development of field. Reservoir characterization entails the integration of all the possible techniques that may be brought in use to analyze the field for purpose of development. Seismic interpretation of the reservoir is best way to quantitatively host its properties. To acquire an oil field, reservoir characterization plus model composition are pre-requisite steps (Mahapatra et al., 2003).

Petrophysical analysis on well data leads us to a comprehensive geological and geophysical aspect of the reservoir. The workflow of petrophysics, when followed, enriches our study of reservoir with useful parameters including the zones of interest in sense of hydrocarbon potential. Moreover, the lithological perspective of the reservoir is also briefed by the evaluation of porosities, shale volume and saturation of hydrocarbon and water. As seismic characteristics are much responsive to horizontal fluctuations in geology, though they are likewise comparatively responsive to horizontal deviations in noise (Oyeyemi et al., 2015).

The purpose of research revolves around the quantitative characterization of reservoir of the study area i.e Mehar block, Lower Indus Basin. Various seismic techniques were applied to the 3D data of the respected area to reach the analysis of reservoir quantification. These include the attribute analysis, facies analysis, petrophysical analysis, inversion analysis and porosity sections. The key resolution of analysis of wireline logs is to customize the existing data, regulated to the finest standard and approximating maximum precise quantitative standards of the wireline log parameters incorporating shale volume, net pay, water saturation, porosity and lithology (Cannon, 2016). The attribute analysis of the respected area visualizes the seismic interpretation. The attributes better illustrate the presence and extent of faults, depositional environment, channels and overall structure of the study area.

1.2) Data Set

The data set approved by DGPC (Directorate General of Petroleum Concession) by the verification of LMKR contained the following elements,

- Well data
    1. Well tops
    2. Well headers data
    3. Digital well data
        a) Mehar-01.las
        b) Mehar-02.las
        c) Mehar-03.las
- Seismic data
    1. OMV Mehar 3D
        (a) PSTM data
        (b) 3 points Grids

Three wells of Mehar have been shown in the table below with their latitude, longitude and authoritative depths.

Table 1.1: Table of well data

Well's Name	Mehar-01	Mehar-02	Mehar-03
Latitude	27.45119006ºN	27.45119000ºN	27.42814722ºN
Longitude	67.55493803ºE	67.55493806ºE	67.50905278ºE
Depth	3570m	3940m	3970m

The locality of study area lies in the Kirthar Fold Belt which is surrounded by Kirthar Fore Deep from the east, Sibbi trough on the Northern side and Axial zone (Ophiolite belt) in the western side. The Figure (1.1) shows the regional location of Mehar Block, Southern Lower Indus Basin.

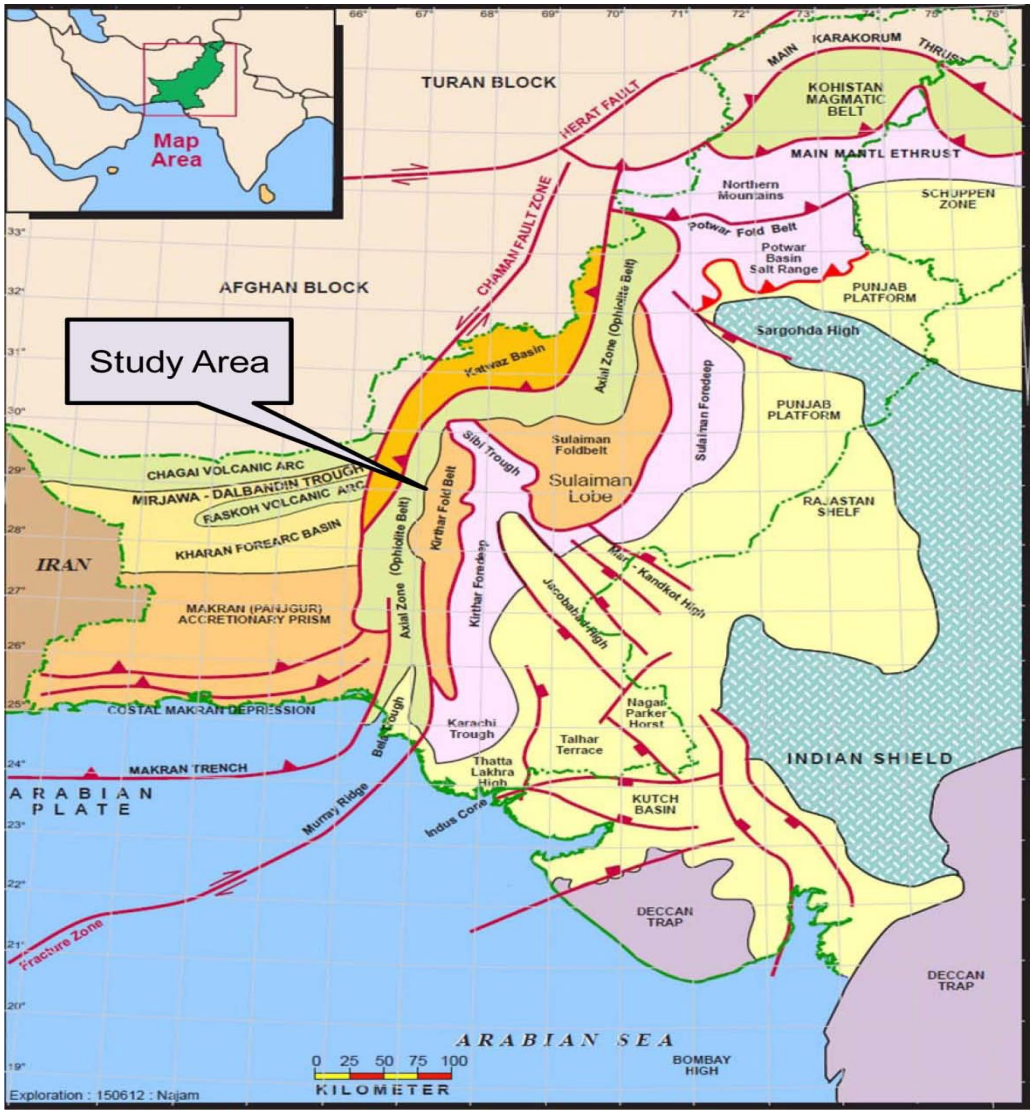

Fig (1.1) Local map of Study Area, Lower Indus Basin, Pakistan, demonstrating the regional sight (Abrar Ahmad et, al 2012.)

1.3) History of Exploration

Petronas operated Mehar gas field, Lower Indus basin, Pakistan. This block is a collaborative venture of GHPL, ZPCL, OPL and Petronas. The Mehar-01 well of this block is the breakthrough in 2003, (as a gas condensate) from the formation (Pab sandstone) in cretaceous age. In 2005, the Mehar-02 well, which also examined for gas and condensate, revised this discovery. In Mehar-03 well, gas and condensate were also identified in 2012. The Mehar field's development and production lease was granted in December of 2013 and the field presently offering 36 MMSCFD and 2906 BCPD from its wells. The field is owned by Orient Petroleum Limited, which has a post-commercial working interest of 11.8421 percent, and Zaver Petroleum Company Limited, which has a working interest of 3.9474 percent.

1.4) Base Map

The base map of Mehar block is shown in Figure (1.2) below with adequate spacing of inline and crosslines. Three wells are displayed on the base map i.e. Mehar-01, Mehar-02 and Mehar-03.

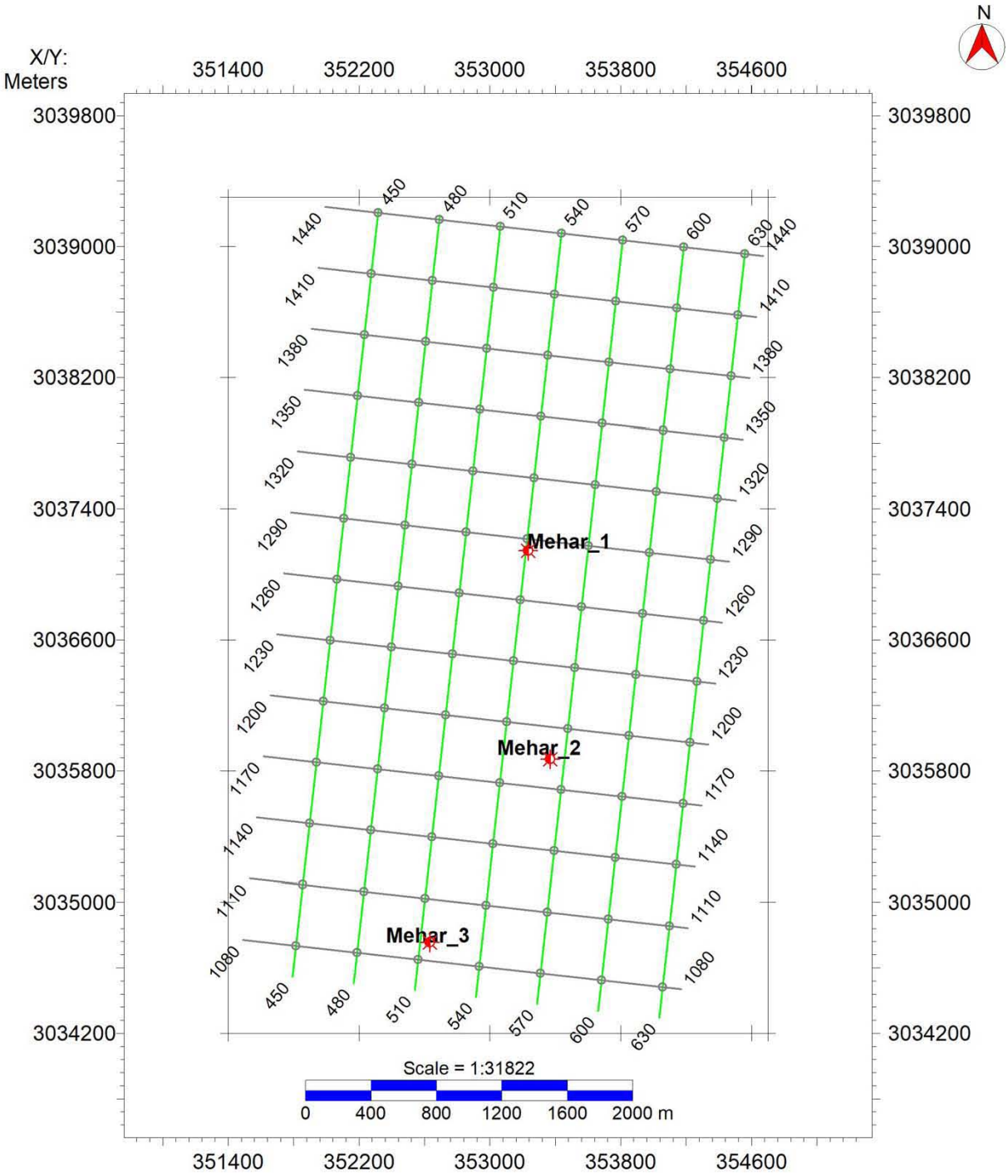

Fig (1.2) Base map of Study area demonstrating the geographical position of Mehar-01, 02 and 03

1.5) Research Objectives

The resolution of my research is to characterize the reservoir quantitatively by exercising seismic techniques including,

- Seismic Interpretation for the idealization of geological features in the respected area. Evaluating the Hydrocarbon potential zones by using Petrophysical analysis.
- Post-stack seismic inversion on given data to have an individual as well as comparison study of Model Base, Maximum Likelihood (Sparse Spike) and Bandlimited models. Porosity and Impedance slices of Model-base, Sparse-spike (Maximum Likelihood) and Bandlimited Inversion on the basis of cross plots.
- Porosity section evaluation by using Probabilistic Neural Networking (PNN). Water saturation evaluated by using Deep Feed-forward Network (DFFN).

1.6) Research Methodology

The methodology adopted to achieve the forementioned aims leads with the analysis of data. The well log data was exploited in marking the zones of hydrocarbon via petrophysical analysis. The data of three given wells were loaded on Power Log Software and then the required parameters were evaluated. The petrophysical analysis of well data gave statistical information about reservoir potential by marking the zones of interest. The comprehensive workflow of the study area is presented underneath in the figure (1.3).

The synthetic seismogram generated to validate the seismic sections with marked horizons. The interpretation and facies modeling are completed using IHS Kingdom Suite. Post-stack seismic Inversion analysis along with the types including Model-based, Bandlimited and Sparse-spike (Maximum likelihood) was computed using Hampson Russel Suite (HRS). The correlation of Model-based inversion came out to be 99.7%, Maximum Likelihood with 97.3% and that of Bandlimited inversion with 93.3%.

The porosity sections are furthermore anticipated for equivalent varieties of inversion by operating practice of Probabilistic Neural Network (PNN). The consequences of porosities attained from PNN are meticulously relatable with those achieved from petrophysical analysis. The porosity sections of Model based, Maximum likelihood and Bandlimited inversion are also configured and in addition to porosity sections, the slices of the Model-based, Maximum likelihood and Bandlimited inversion in terms of together porosity and impedance, are correspondingly demonstrated.

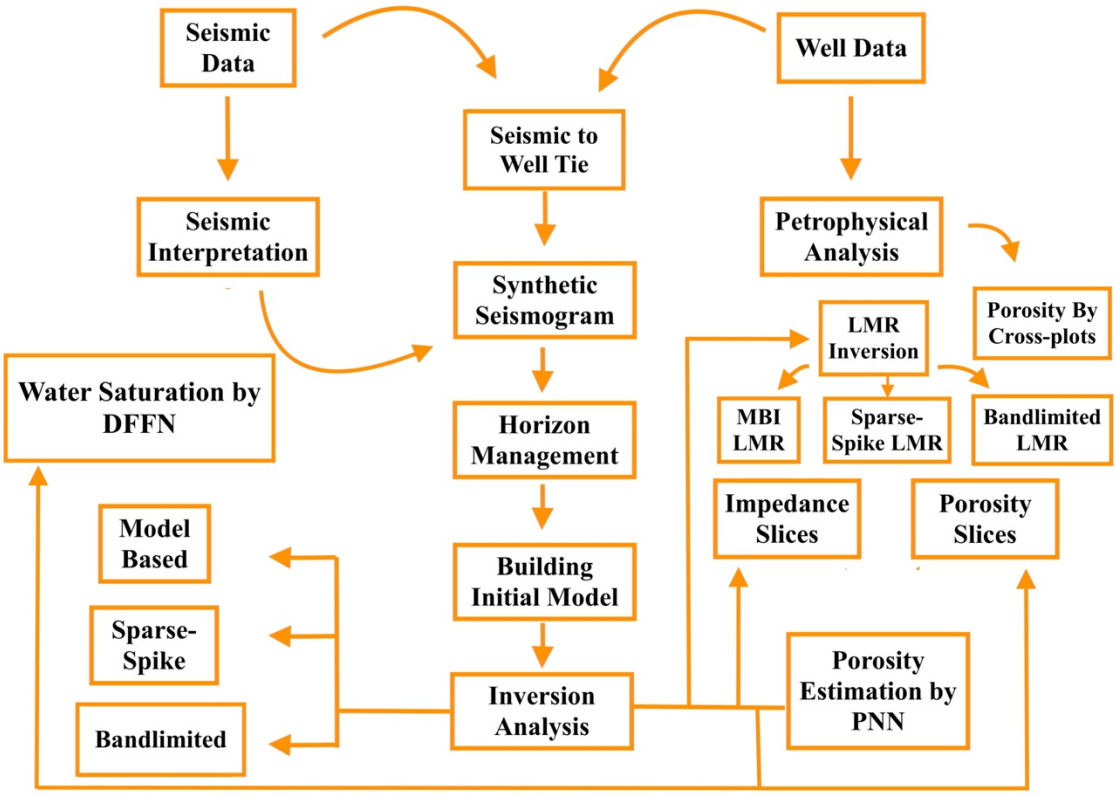

Fig (1.3) Over-all Workflow of the Research Methodology representing the hierarchy of steps obeyed for the accomplishment of study.

Chapter 2 Geology, Tectonics and Stratigraphy

2.1) Regional Illustration of Study Area

The area of research lies in Sindh with average dimensions of 1600km and 300km in length and width respectively. The major hydrocarbon producing field of Pakistan is Indus basin which is further elaborated into Lower, Upper and Middle Indus Basin. The east and west of Indus basin is dominated by Pakistan and India, respectively. In terms of structural features, the presence of foredeep with depression, platform, outer and inner fold belts are significant (Memon and Siddiqui, 2005). Kohat-Potwar plateau is the second name of Upper Indus basin and it is in the south surrounded by Sargodha high and in the north by Main Boundary Thrust (MBT). Middle Indus basin is situated between Sargodha high and Jacobabad high, north to south respectively. The main regions included in this basin are, Sulaiman foredeep, Sulaiman fold belt and Punjab Platform (Khadri, I.B., 1995).

2.2) Geology and Tectonics

Gas field of Mehar is situated in western region of Kirthar fold and thrust range, that lies in Lower part of Indus Basin, Pakistan. The central Indus basin sorrounds Lower Indus Basin in the north whereas Sulaiman fold belt is situated in northwest and fold belt of Kirthar is present in west. Rifting of the Indian plate over the Gondwana land causing the uplifting and tilting towards east are the controlling tectonic activities for the change in structures as well as stratigraphy of Lower part of Indus Basin (Daud et al., 2011). Lower Indus basin contain major oil fields of Pakistan. Geographically, the Lower Indus Basin lies in Sindh, Pakistan, with an aerial extension of 24º-28ºN and 68ºE to 20ºS. The Figure (2.1) represents the basin wise distribution of Pakistan.

Mehar Block lies in boundary of Kirthar Fold Belt. We better know that KFB is a deformation zone tresnding from north east and verging from east, so, on its north is Sulaiman belt, in its west is Chaman Fault, Kirthar Foredeep on the east and in the south is Indus delta. (Shakir et al., 2022). Kirthar Foredeep form the KFB, contains the significant source for the generation of oil and gas (Szeliga et al., 2009).

Fig. (2.1) Basin Wise Illustration of Pakistan with Dark shaded Zone 3 including Lower Indus basin (Hanif et al., 2014)

Kirthar fold belt is situated on the south-west region of the Indian plate. Its tectonic feature trends the structure and stratigraphy towards north south. Sulaiman fold-belt following the deformed boundary (western) of Indian plate, Kirthar fold belt is thought to be similar deformation the rocks present in this region are deposited by the Triassic age and following till now. The western part of Kirthar Fold Belt that arms with Baluchistan Basin, is considered as the most deformed western region of Indus Basin. The good petroleum system of this region contains reservoirs including Pab sandstone, Mughal Kot, Suimain Limestone, Ranikot, out of which Pab sandstone is considered as the largest field among this region in terms of hydrocarbon potential. The geological study of this region reveals the presence of anticlinal structures. Other discoveries of Kirthar belt include Mehar, Jhal Magsi, Mazarani, Bhit, Sari, Badhra, Bhit and Hundi (Daud et al., 2011). In below Figure (2.2), structure, locality and lithostratigraphy of KFB can be idealized.

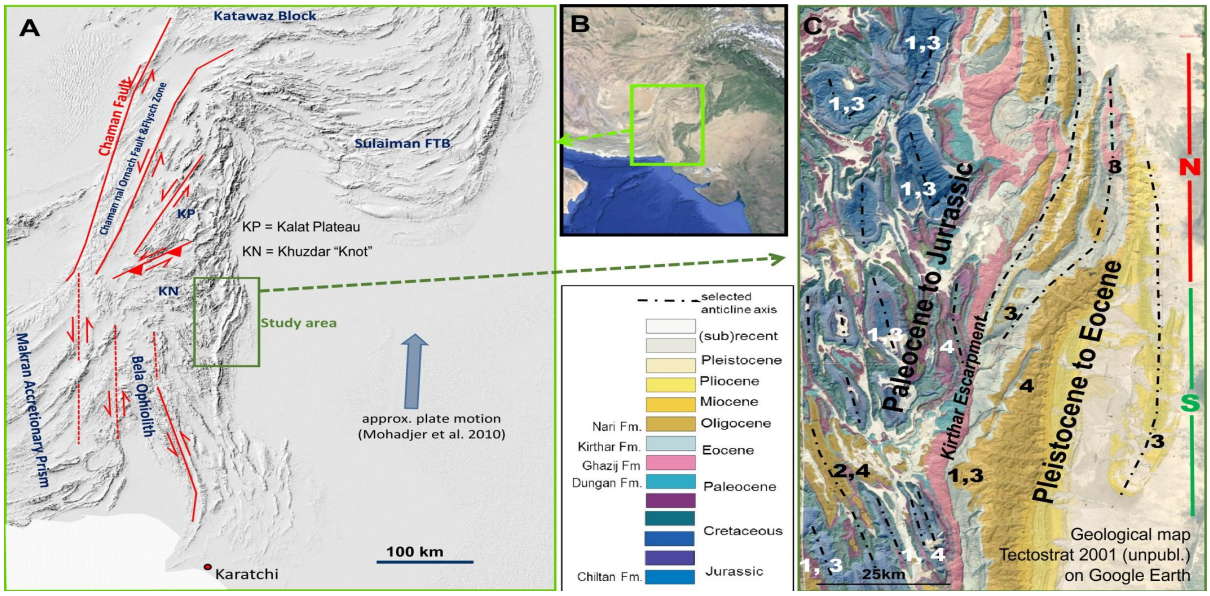

Fig. (2.2) A-wider structural sketch of Kirthar Fold Belt area, B-Locality of KFB in Google Earth image, C-Geological map of the study area in terms of lithostratigraphy (Ralph Hinsch et al., 2018)

The tectonic map with representation of the study area is shown in the Figure (2.3). The yellow block is showing the location of the study area, lying deep in the Kirthar fold belt.

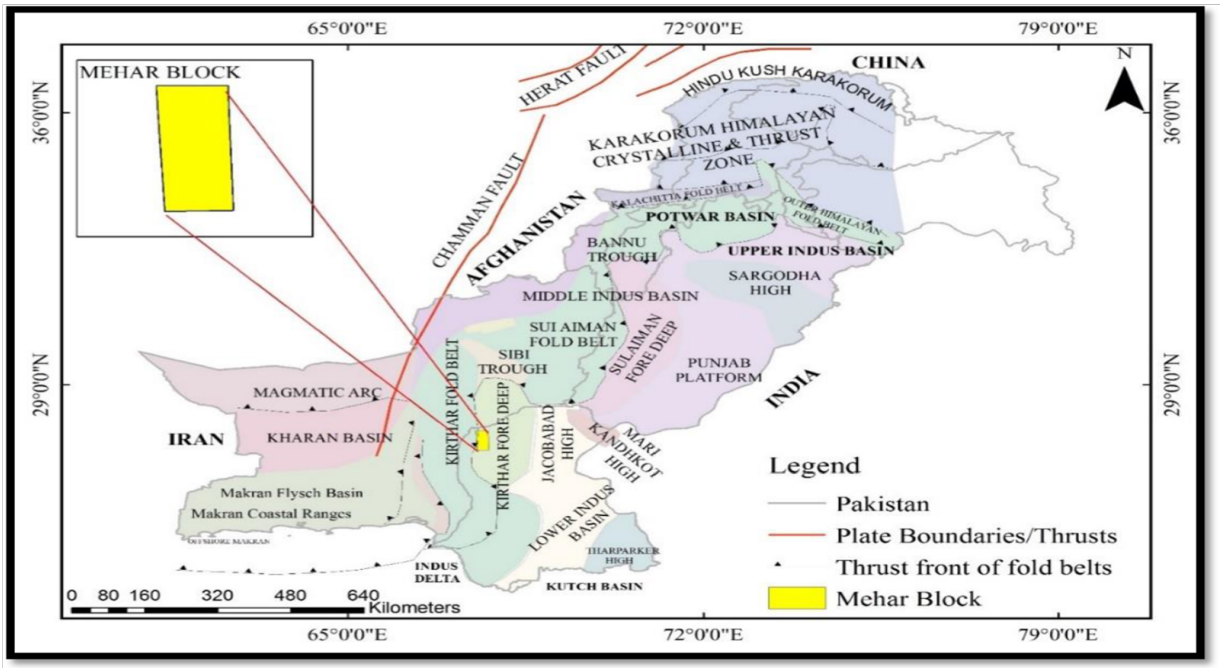

Fig. (2.3) Tectonic map of Pakistan, showing fold belts with thrust boundaries. The yellow block in the map represents Mehar block region (Shakir et, al. 2021).

The fields contain by Kirthar Foredeep include Zamzama, Miano, Rehmat, Bhit, Mehar, and Mazarani, Gambat and Badhra (Ahmad et al., 2004; Arshad et al., 2013; Mahmud & Aziz, 2002).

2.3) Stratigraphy

In lower Indus basin, Mehar block is a gas containing field. In this block, Sembar formation and shales of lower Goru from cretaceous age are acting as source rock. The formations including Pab, Mughal Kot and Lower Ranikot have sandstones that are the proven reservoirs of Mehar Block. The cap rock in the petroleum play of this block have shales from upper Ranikot. The detailed stratigraphic chart of the research area is shown in Figure (2.4).

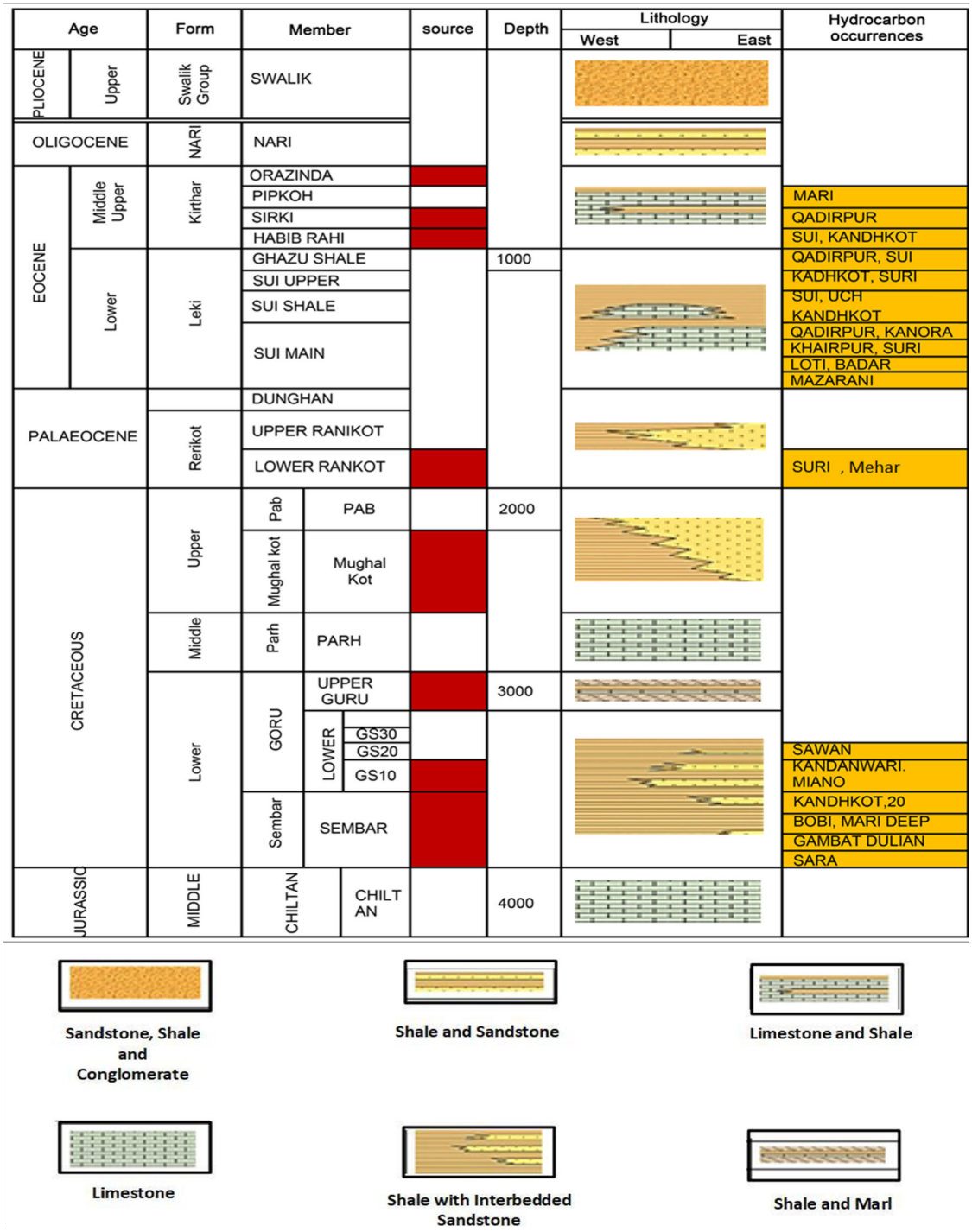

Fig. (2.4) Stratigraphical demonstration of formation and their ages in Lower Indus Basin (Shakir, et al. 2021)

2.4) Petroleum Settings

A petroleum system is thought to be a container of hydrocarbon's source, a good potential of reservoir and a seal for the trap of petroleum (either gas or oil or both). From geological perspective, a petroleum system is a combination of oil field which is being controlled by several geological functions in the respected region (Stonley, 1995). It is of the great significance for a petroleum system that development of hydrocarbons in the source rock with their accumulation in the reservoir by the aid of seal rock, is being done timely and efficiently.

2.4.1) Source Rock

A source rock is what which have the ability to produce hydrocarbons. Shales of Sembar and lower Goru formation of cretaceous age act as the source rocks. Other than shale, there also lies sandstone and siltstone. The western part of the formation is in excess of siltstone and shale but in the eastern part, sandstone is dominant. The thickness, in Mehar block of Sembar formation varies in range from 142-270m. While, the overall thickness of Sembar formation ranges from 10-270m and its deposition was occurred in the marine environment (Iqbal and Shah, 1980). The reason that we consider Sembar formation as the main source rock is its level of maturity.

2.4.2) Reservoir Rock

The reservoir formations in the Lower Indus Basin are Mughal kot and Pab (sandstone), from Cretaceous age, Ranikot and Sui Main Limestone of Paleocene and Eocene ages respectively. It is seen that the quality of the reservoir is of low standard towards western basin, but due to massive erosion eastwards and Cretaceous rock's truncation, the thickness enhances in the west (Wandrey et al., 2004). The main potential reservoir in the study area is Ranikot, whose thickness varies between 360-330m and is decreased following the south.

2.4.3) Seal Rock

A seal rock plays an important part in preserving the hydrocarbon in any petroleum play by setting a trap with certain lithological units. And the seal in study area is governed by shales which are interbedded by sand. In the formational settings of study area, upper Ranikot is the seal for the sands of Lower Ranikot and Pab formations. Furthermore, carbonates of Dunghan and Sui Main Limestone are capped by shales of Ghazij formation of Eocene age.

Chapter 3 Wireline Log Analysis

The wireline log analysis stipulates us the key features to quantitatively characterize the reservoir potential. In fact, it is the quantitative measure of hydrocarbon potential in the given domain. However, the interaction of rocks with fluids along with evaluation of rock's properties is known as petrophysics. (Tiab et al, 2004). Well log data is the tool to reach the petrophysical aspect of the area under consideration. The techniques of well logging have been in use largely due to their contribution in characterizing the reservoir in every possible way (Lovell, et al.1999). The data of well logging, through following the required workflow, quantifies the actual presence of water or hydrocarbon (either oil or gas or both) in the study area (Asquith and Krygowski, 2004). The frequent use of well logs is made to evaluate the reservoir to get enough information and also to identify the thickness (Abd El-Gawad, 2007).

The Resistivity, Density and Neutron Log are the paramount logs for completion of petrophysical analysis of any reservoir. With the help of these logs, the information about lithology, porosity, effective porosity, permeability, thickness and saturation of both hydrocarbon and water can be figured out (Van Wagoner, et. Al 1990). The parameters that are gained by petrophysical analysis including porosity, permeability volume of shale, saturation of water and hydrocarbon, help us to evaluate petroleum system of any respected domain (Singha et al., 2016).

3.1) Data Set

The well data given by DGPC consisted of three wells i.e. Mehar-1, Mehar-2 and Mehar-3. The files of the well data were present in LAS format that contained different geophysical logs. These logs mainly include Gamma Ray log, Caliper log, Spontaneous Potential log, Density log, Neutron log and Resistivity logs. The additional files that were required for proper petrophysical analysis, including well headers and formation tops, were also present in the data. The petrophysical analysis for the characterization of reservoir have been performed for all of the three wells.

3.2) Methodology

Initially three tracks are being made to approach rest of the required logs that give the actual required parameters for reservoir characterization. These tracks are,

I. Lithology track
II. Resistivity track
III. Porosity track

3.3) Lithology track

Lithology track, secondly known as correlation track, is comprised of Gamma Ray (GR) log, Spontaneous Potential (SP) log and Caliper log. The diameter of borehole is calibrated by Caliper log. Gamma Ray log is utilized in identifying the lithology (specifically volume of shale). And Spontaneous Potential indicates zones of permeability and also used in evaluating the formation water resistivity.

3.4) Resistivity track

In Resistivity track, Later Log Deep (LLD), Later Log Shallow (LLS) and MSFL logs are used. The separation between the two logs i.e. LLD and LLS, is of great concern while picking the zone of interest.

3.5) Porosity track

While in density track, Sonic Log (DT), Density Log (RHOB) and Neutron Log (NPHI) is used. These logs are used to optimize reservoir parameters including porosities (total and effective) and permeability.

On running all these tracks, we aim towards the evaluation of further parameters for reservoir characterization in terms of petrophysical analysis. Volume of shale, Total and effective porosity and then saturation of water and hydrocarbon.

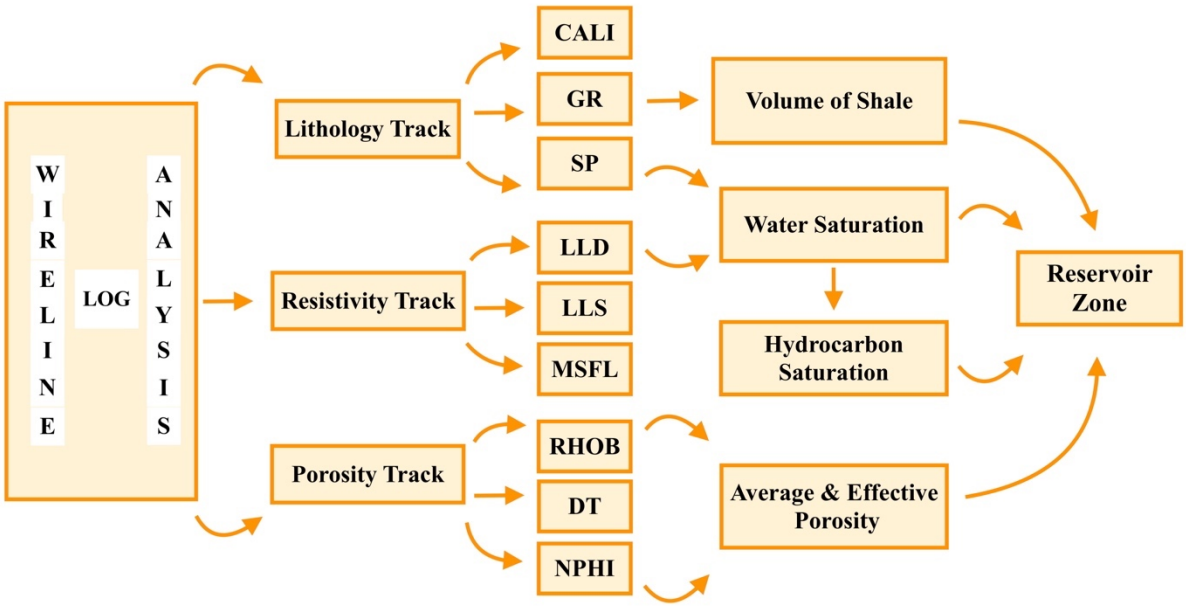

Fig (3.1) Track-wise distribution of logs on the basis of their functionality.

3.6) Reservoir Properties

3.6.1) Volume of Shale

The subsurface is highly heterogeneous in terms of lithology. There come repetitions of lithologies e.g. shale with carbonates or shale with sands etc. So, the calculation for volume of shale is of great concern in identifying lithology. Shale may contain minerals of radioactive nature (e.g. ^{40}K) which emit radioactive radiations. Hence, by using GR log from well log data, volume of shale can be directly calculated. The measurements of GR log response are taken in API (American Petroleum Institution) values. Another method of calculating volume of shale is using logs in combination i.e. Neutron-Density or Resistivity-GR log (Stefansson and Steingrimsson, 1980). The volume of shale can be calculated by using the formula,

$$V_{sh} = \frac{GR_{log} - GR_{min}}{GR_{max} - GR_{min}} \quad (3.1)$$

Here, V_{sh} = Volume of shale, GR_{log} = Gamma ray log, GR_{min} = minimum value of GR log, GR_{max} = maximum value of GR log.

3.6.2) Porosity Evaluation

The measure of porosity for any reservoir is of great mean in terms of quantitative characterization of hydrocarbon potential. It is so because fluid containing rock bodies must have pores in them. So, porosity of a rock body is the quantitative measure of its pore continuance. The normal range of porosity found in the reservoir lies between 5% and 30%. The effect of grain in terms of its size, pattern of packing, shape and level of compaction all are significant. Porosity is calculated using geophysical logs including Density log, Neutron log and Sonic log (Arason, 1993).

We need to calculate effective and total porosity for which density porosity is needed. And we can easily compute density porosity by using Density log because we know that Density log better provide bulk density of the formation. We use the following formula for calculating Density Porosity (PHID),

$$\varphi_D = \frac{\rho_M - \rho_B}{\rho_M - \rho_F} \quad (3.2)$$

where, φ_D = Porosity density, ρ_M = Matrix density, ρ_B = Bulk density and ρ_F = Fluid density. φ_M depends on lithology in the formation which is under consideration i.e. for Sandstone, it is 2.65 g/cm^3 and for limestone it is between 2.71 g/cm^3 and 2.87 g/cm^3 depending upon the nature of limestone.

The main aim after evaluating porosity density is to approach effective and total porosity. For effective porosity we need Neutron log with porosity density and volume of shale. The mathematical relation for effective porosity is,

$$\varphi_E = \frac{(\varphi_D + \varphi_N)}{2} * (1 - V_{sh}) \quad (3.3)$$

Here, φ_E = PHIE = Effective porosity, φ_D = PHID = Porosity density, φ_N = NPHI = Neutron log and V_{sh} = volume of shale. The plot of effective porosity and total porosity (φ_T) help in picking the zone of interest in terms of hydrocarbon potential. Total porosity is the average of porosity density and Neutron porosity log and can be expressed as,

$$\varphi_T = \frac{\varphi_D + \varphi_N}{2} \quad (3.4)$$

The standard scales taken for best log plots are described in following,

GR log ⇒ 1 - 150 API (American Petroleum Institution), CALI log ⇒ 2 - 24 in (inches), LLD & LLS log ⇒ 0.2 - 2000 Ω (ohm), RHOB log ⇒ 1.95 - 2.95 g/cc (gram per cubic centimeter), NPHI log ⇒ 0.45 - –0.15 v/v (volumetric ratio), PHIE and PHIT log ⇒ 0 - 0.4 v/v, other than these, V_{sh}, Saturation of water and hydrocarbon are also volumetric ratios and their scales are same i.e. 0 - 1 v/v.

3.6.3) Water Saturation Evaluation

Down the surface, the presence of water is subjected to the presence of pores, in fact interconnected pores. So, it is obvious that water saturation is the ratio between volume of pores to volume of water. Archie equation (Archie 1942, 1952) is used to find water saturation of the reservoir formation. The required parameters for the implementation of Archie equation can be calculated by using data of spontaneous potential log and resistivity log (Campion and Rahmanian, 1990), and the equation is represented as,

$$S_w = \left[\frac{F * R_w}{R_t}\right]^{1/n} \quad (3.5)$$

Here, S_w = Saturation of water, **F =** Formation factor, R_w = Resistivity of water, R_t = rock resistivity and n = exponent of saturation.

Formation factor can be calculated using the formula,

$$F = \frac{a}{\varphi_E^m} \tag{3.6}$$

Where, a = Tourtosity factor, φ_E = Effective porosity and m = factor of cementation.

When we get water saturation by following the above methodology, we can find hydrocarbon saturation by using the relation, $S_H = 1 - S_W$, where, S_H representing the saturation of Hydrocarbon.

3.7) Results of Wireline Log Analysis

Three wells were interpreted on the basis of geophysical logs given in the data. The zones that are found noticeable in sense of hydrocarbon potential in the three given wells are displayed below with their quantitative analysis.

3.7.1) Mehar-1

Ranikot formation as a reservoir in the well Mehar-01 exhibits the following results of petrophysical parameters. The following table shows the parameters that are required for petrophysical analysis.

Table (3.1) Results of Petrophysical Analysis of Mehar-01

Mehar - 01	Volume of Shale V_{SH}	Effective Porosity φ_E	Total Porosity φ_T	Hydrocarbon Saturation S_H	Water Saturation S_W	Zone Thickness (m)
% age	10.0	7.3	8.1	58.2	41.8	5

The figure (3.2) is the well log display of the Mehar-01 well with evaluated saturation of hydrocarbon and water.

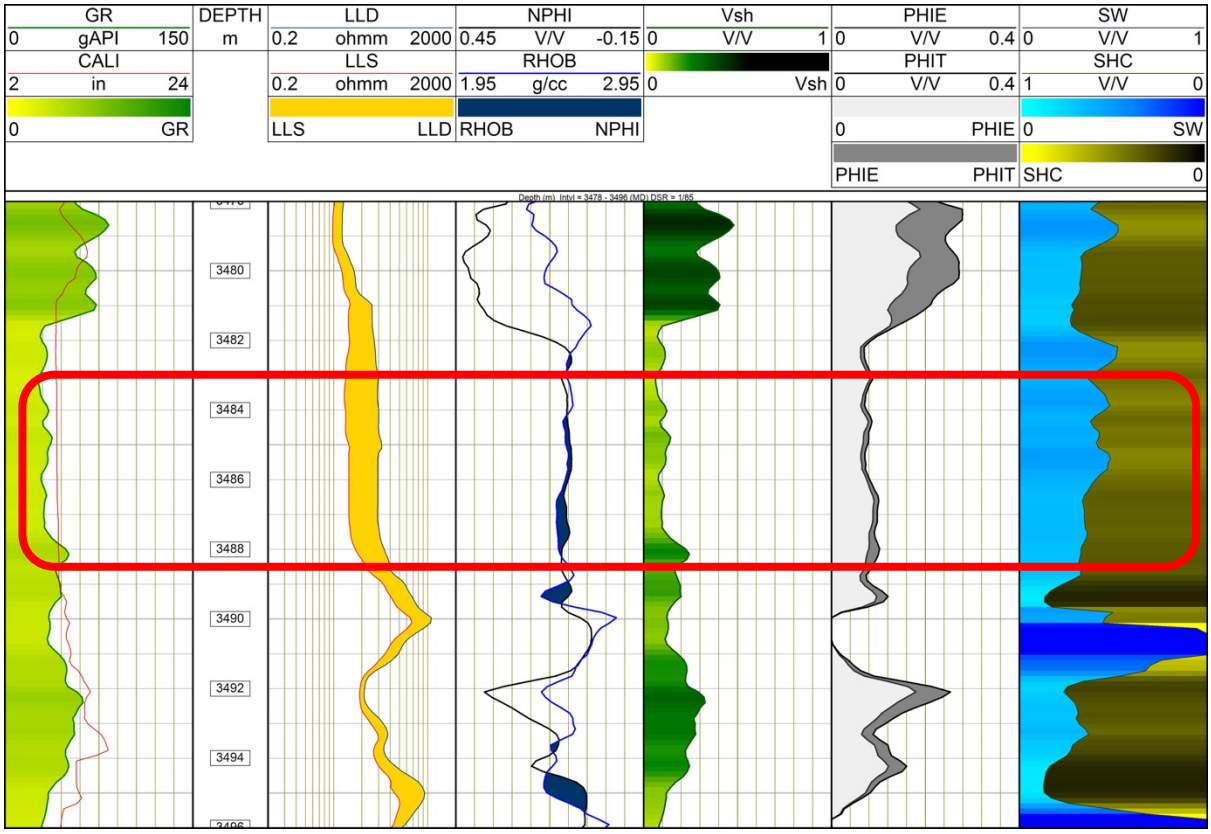

Fig (3.2) Petrophysical analysis of Mehar-01 (Ranikot) with marked zone of interest.

From the figure shown above, the plot of each curve better justifies the potential zone of the reservoir in the respected well.

3.7.2) Mehar-02

Another zone marked in the Ranikot formation right below the depth of the zone marked in the well-01. In well-2, the depth of potential zone comes out to be 5 meters. The table below shows the potential of hydrocarbon in numeric values. The hydrocarbon saturation in well-02 is greater than that of Mehar -01.

Table (3.2) Results of Petrophysical Analysis of Mehar-02

Mehar - 02	Volume of Shale V_{SH}	Effective Porosity φ_E	Total Porosity φ_T	Hydrocarbon Saturation S_H	Water Saturation S_W	Zone Thickness (m)
% age	25.3	7.6	13.0	68.9	31.1	5

The Figure (3.3) below displays the petrophysical analysis of Mehar-02 with rectangle in red indicating the zone of interest.

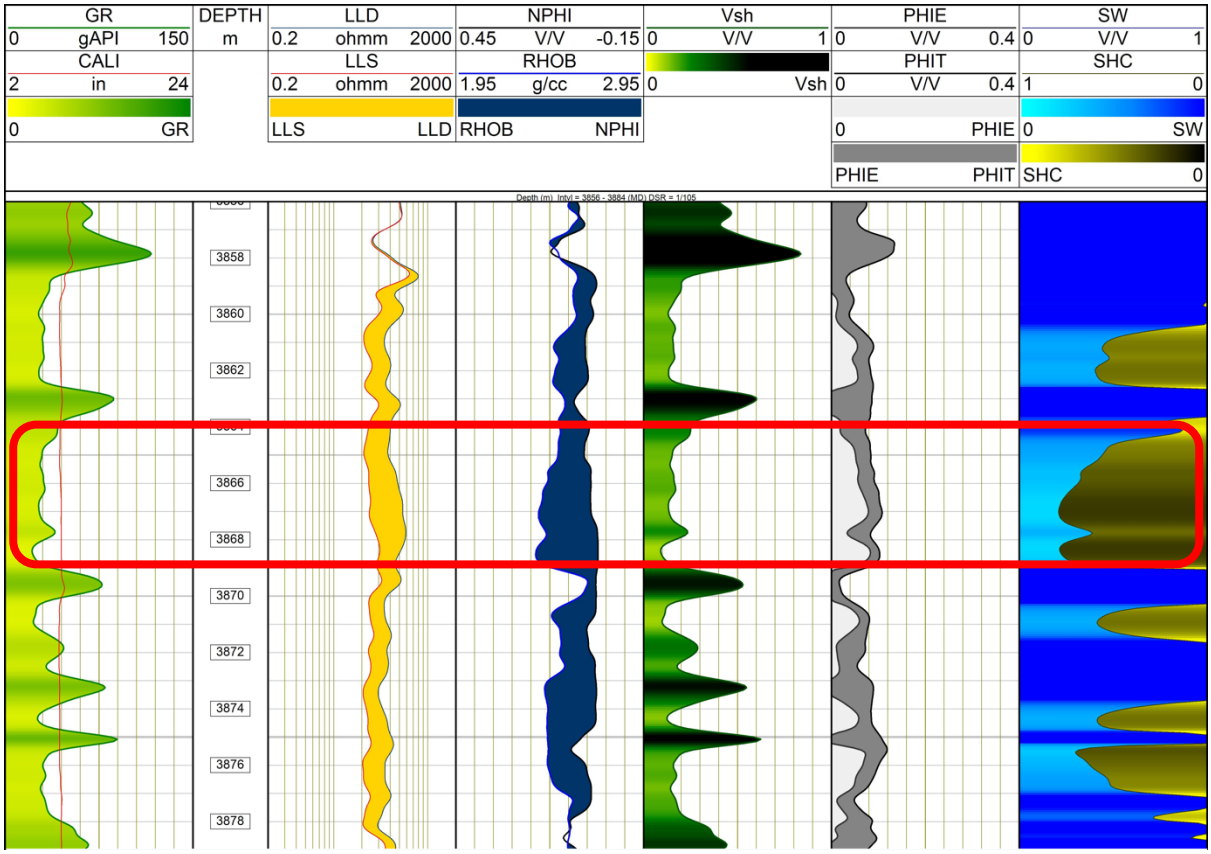

Fig (3.3) Petrophysical analysis of Mehar-02 (Ranikot) with marked zone of interest

3.7.3) Mehar-03 (Zone-1)

The workflow of petrophysics is also applied on well-03 of Mehar block. Two zones were marked in this well, both of which shows appreciable potential of hydrocarbon. This zone is from Pab formation and of 21 meters of thickness. The table below shows the results of petrophysical analysis of Mehar-03.

Table (3.3) Results of Petrophysical Analysis of Mehar-03

Mehar - 03 Zone-1	Volume of Shale V_{SH}	Effective Porosity φ_E	Total Porosity φ_T	Hydrocarbon Saturation S_H	Water Saturation S_W	Zone Thickness (m)
% age	11.9	5.3	7.8	51.2	48.8	21

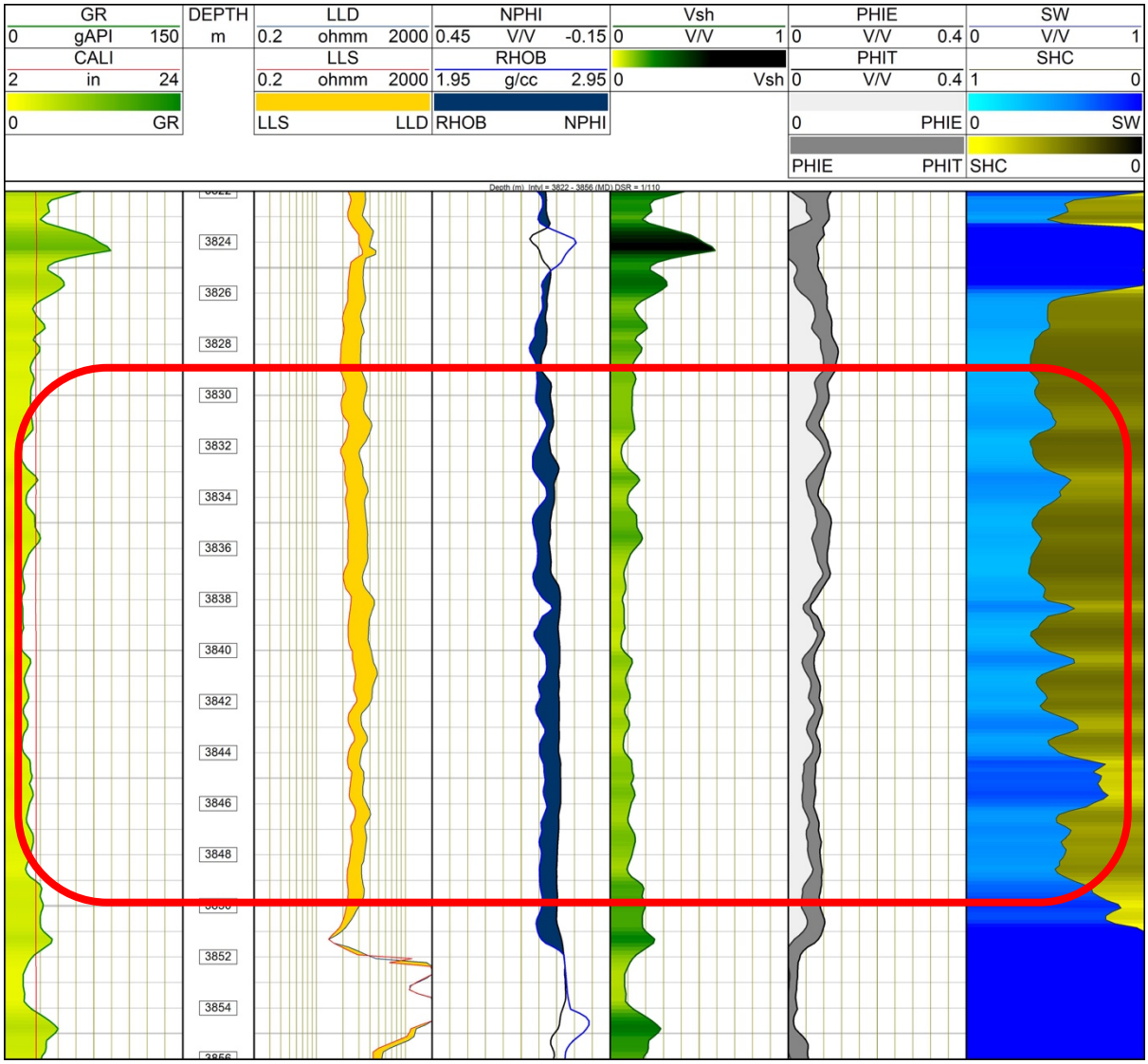

Fig (3.4) Petrophysical analysis of Mehar-03 (Pab) with marked zone of interest

3.7.4) Mehar-03 (Zone-2)

The zone found in Ranikot formation of Mehar-03 is of 7 meters of reservoir potential. The table shown below contain the results of petrophysical analysis of Ranikot formation in Mehar-03.

Table (3.4 Results of Petrophysical Analysis of Mehar-03

Mehar - 03 Zone-2	Volume of Shale V_{SH}	Effective Porosity φ_E	Total Porosity φ_T	Hydrocarbon Saturation S_H	Water Saturation S_W	Zone Thickness (m)
% age	12.0	11.9	17.9	72.2	27.8	7

The following figure (3.5) shows the results of petrophysical analysis in Ranikot formation of Mehar-03.

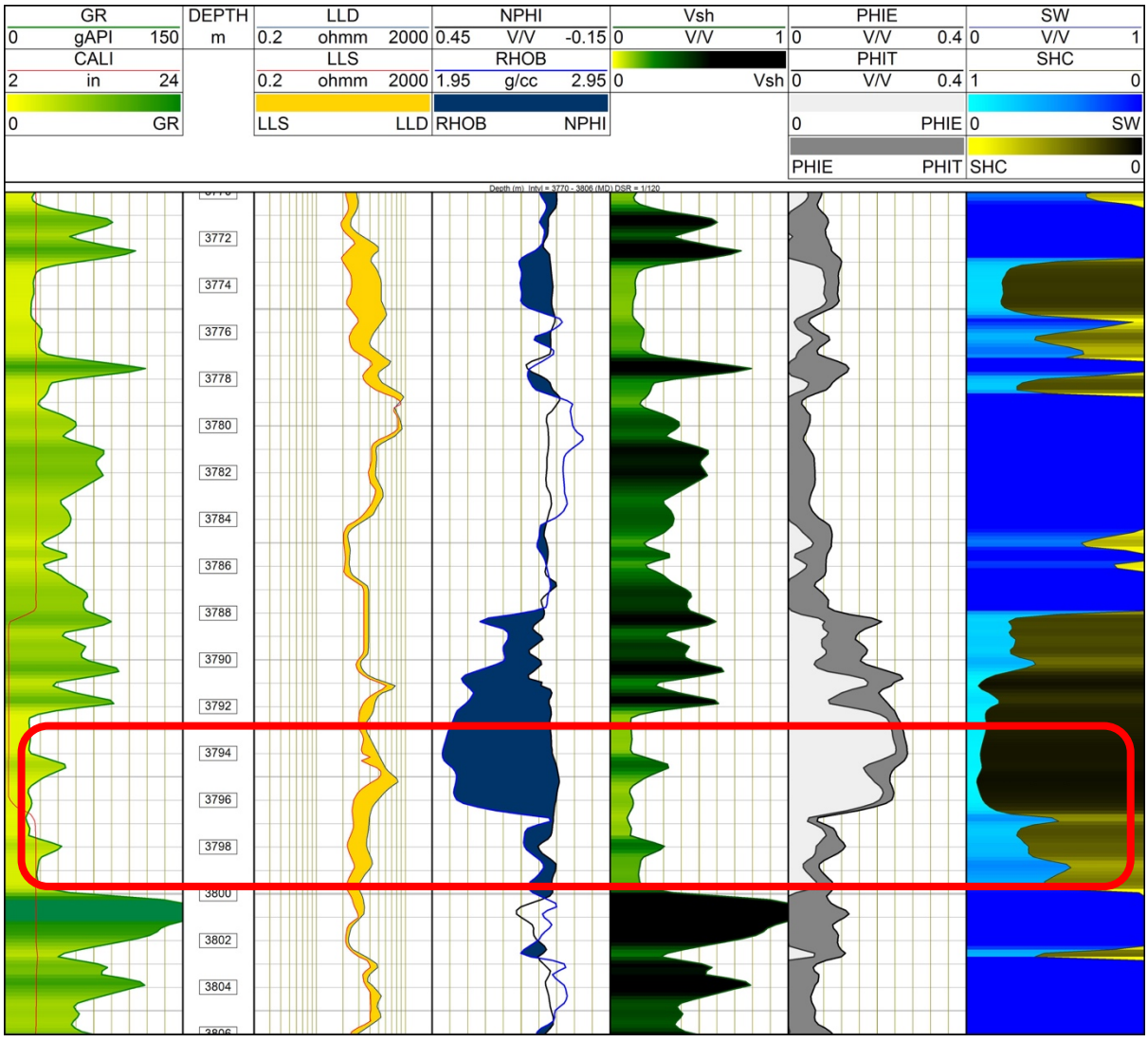

Fig (3.5), Petrophysics analysis of Ranikot formation of Mehar-03

Chapter 4 Seismic Structural Interpretation

The assessment of subsurface reflectors is the principal errand in structural interpretation of seismic data. It is the utmost prerequisite that to recognize about the foundations of geological and geometrical features of the interpretation in terms of structure. An adequate structural interpretation and its conclusions are meaningful in idealizing the geology of the subsurface. (Badley, 1985). Extraction of geological information from raw data is the primary goal of seismic interpretation. Stratigraphic variation and the identification of direct hydrocarbons are now part of the interpretive process extension. Extraction of seismic characteristics and direct and inverse modelling of structures are further contemporary interpretation techniques. In hydrocarbon exploration of together oil and gas, interpretation is contemplated as a suggestive means. Interpretations from numerous scientific experiments are typically not unique. (Avseth et al., 2005).

Mapping the region's large-scale structure is the first step in seismic interpretation. The essential component of this structural interpretation is the construction of faults plus horizons with planes. The interpreter creates horizons by choosing and moving a reflector across the volume (Bakker, 2002). In order to extract subsurface information about stratigraphy, structure, rock physics and possibly reservoir fluid fluctuations in time and space, seismic interpretation transforms the geological meaning of seismic data (Liner, 1999).

4.1) Organization of Interpretation

The interpretation is completed by using algorithms of IHS Kingdom software and Hampson-Russell Suite. On creation of project, the seismic data in SEG Y format was imported in the software. The data of three wells in LAS format was also loaded in the same project to display wells on the base map and seismic sections. The following workflow describes the stepwise demonstration of structural interpretation.

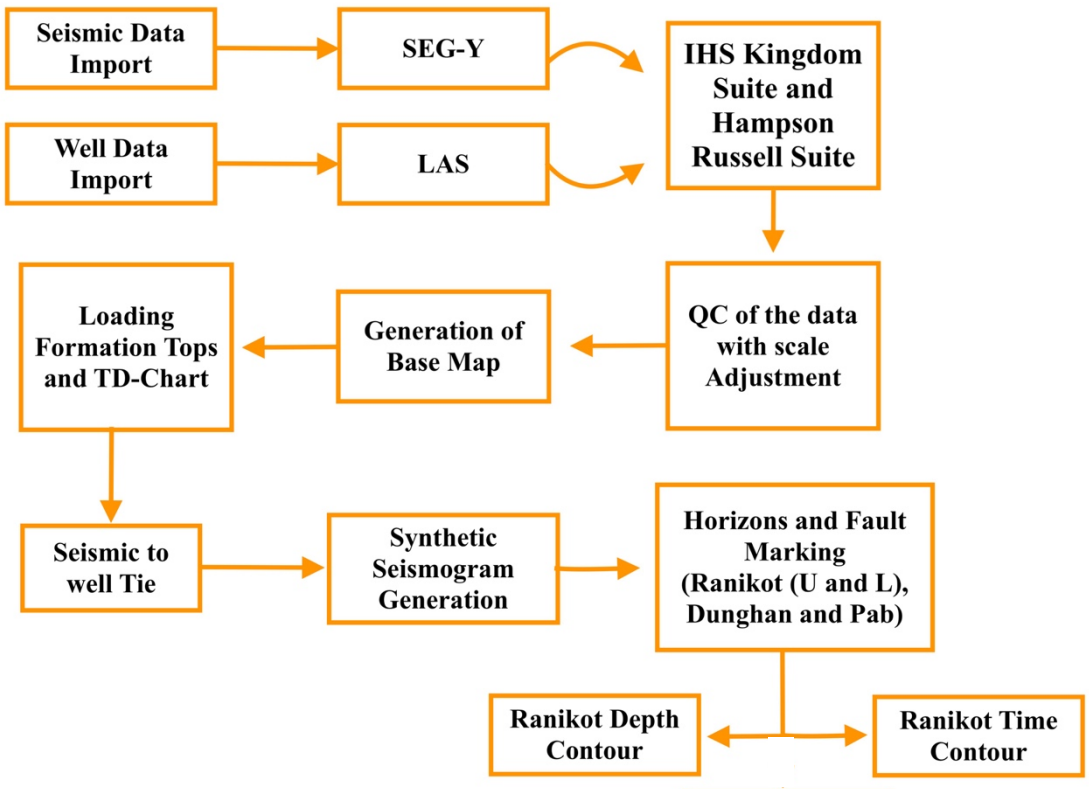

Fig (4.1) General Workflow of Interpretation adopted for the configuration of depth and time contours.

4.2) Base Map Configuration

The first step in procession of seismic interpretation is the generation of seismic base map. It is a representation of geographical data. It comprises the positioning of leasing and concession boundaries, wells, sites of seismic survey, and other cultural data with a geographic reference such as latitude and longitude and is a configuration of the seismic lines in the studied area. Three wells i.e. Mehar-01, Mehar-02 and Mehar-03 are shown according to their geographic positions. The following Figure (4.2) is showing the base map with in-lines and crosslines with adequate numeric display.

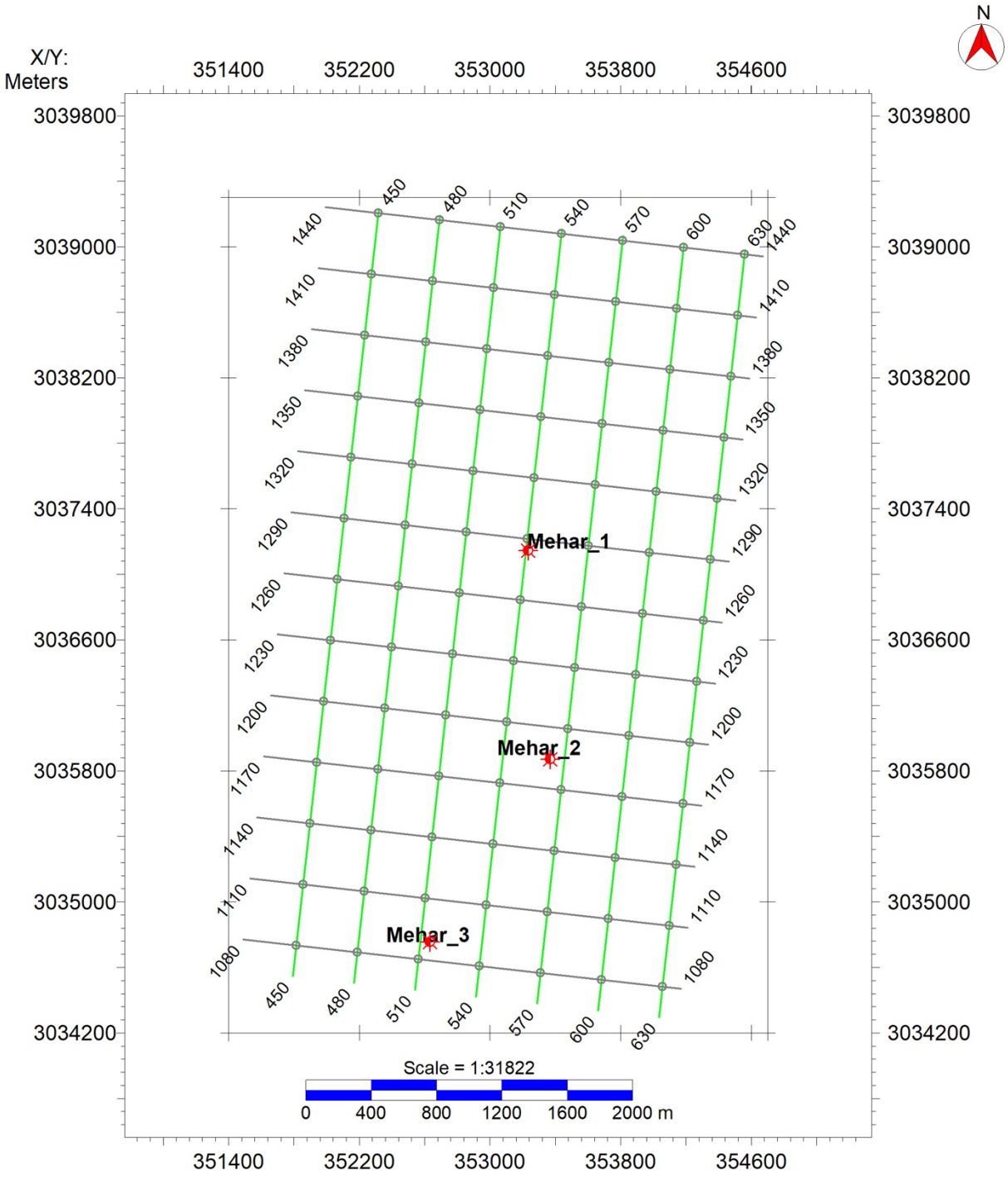

Fig (4.2) Base Map of the Study Area showing wells Mehar-01, 02 and 03 with adequate number of inline and crosslines

4.3) Foundation of Synthetic Seismogram

Synthetic seismogram is the 1D-forward modeling approach that envisage precise location of reflectors upon seismic sections with the backing of density (RHOB) and Acoustic impedance (DT) logs. We can practice several techniques for correlation of well to seismic although corresponding synthetic seismogram amid seismic lines stands frequently cast-off.

The logs used under this method are Gamma ray log (GR) as a reference log, RHOB as a density log and Sonic log (DT) as evidence of velocity in the layers of subsurface. We get the reflectivity series (RC) by the cross of Density and Velocity log. Their product (i.e. RC) is then convolved with the extracted seismic wavelet for the generation of synthetic seismogram. The following figure (4.3) is the representation of synthetic seismogram.

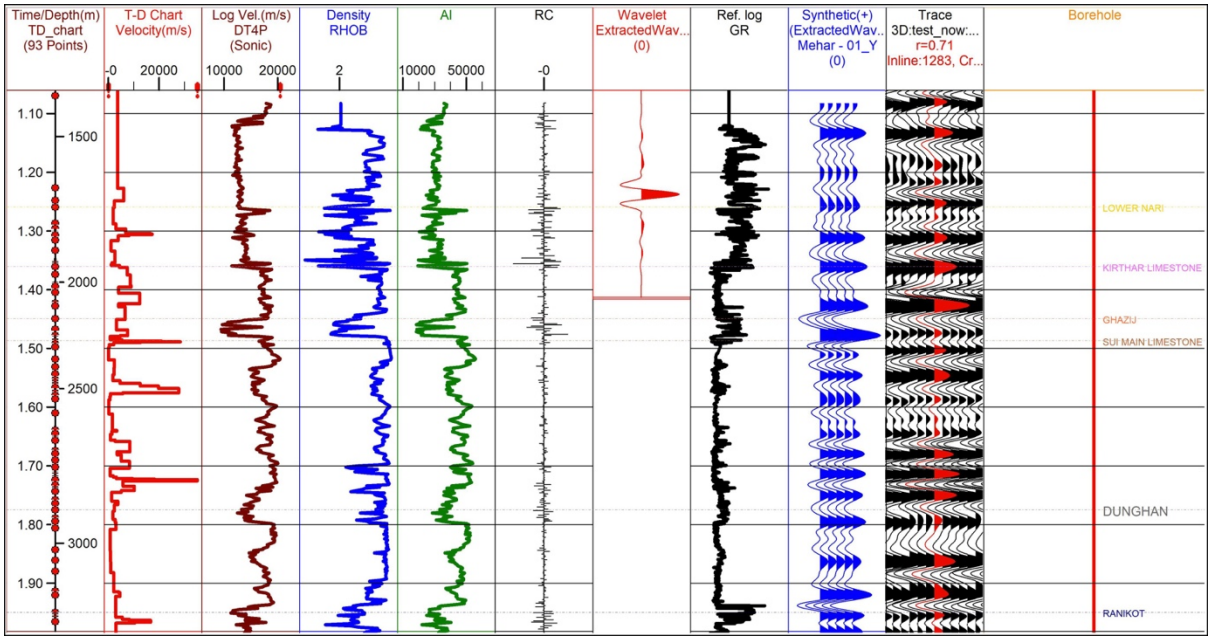

Fig (4.3) Synthetic Seismogram of Mehar-01 (seismic tie to well Mehar-01) with correlation of 71% corresponding with the formations.

4.4) Horizon Marking and Consideration of Seismic Interpretation

The horizons are marked along the seismic sections including Ranikot, Dunghan and Pab formations. The Ranikot is further divided into upper Ranikot and Lower Ranikot. Upper Ranikot is mainly shales and in that of lower Ranikot is sand. As, the Mehar block of Lower Indus basin has reverse or thrust faulting, it is on, so basis is called a compressional regime. The dispersion in the seismic reflection data on the right side of seismic sections is an evident of the presence of thrust faulting in the respected area.

The details of seismic features in 3D data is definitely more comprehensive, sharp and consistent. The major thrust faulting is being confirmed by the 3D data structural interpretation on seismic data with synthetic seismogram on well Mehar-01 of the Mehar block. The following Figure (4.4) is the demonstration on seismic line (inline 1280 and crossline 424) of seismic section.

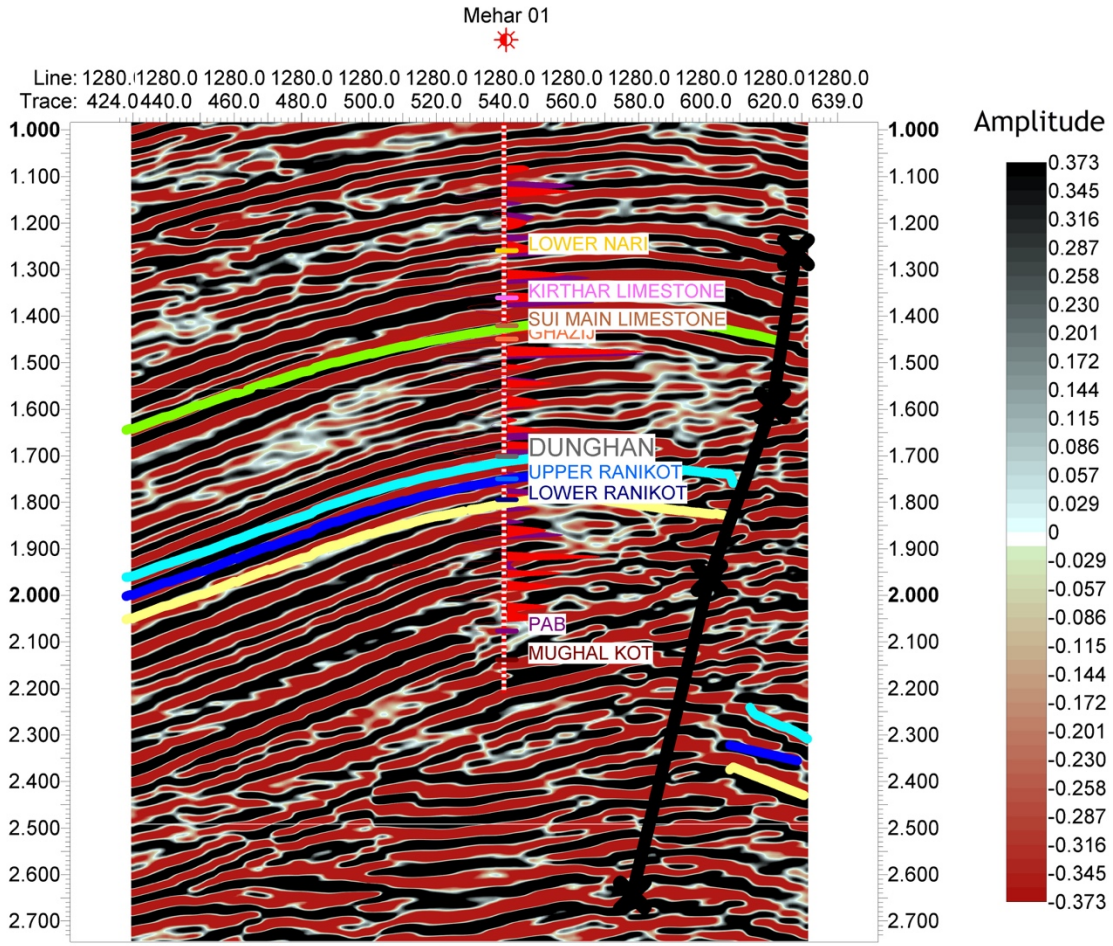

Fig (4.4) Seismic inline 1280 with horizons marked on the seismic section displaying thrust faulting.

4.5) Contour Map of Reservoir Formation (U and L Ranikot)

The term "contouring" refers to more than just mathematical approximation of grid data and uniting of equivalent values. A contour map of seismic represents geological features with distinct layers and a defined chronostratigraphic horizon. Depositional morphology and structural dynamics of geological features are depicted by seismic contours (C. Nanda, 2016). The Ranikot formation's time and depth contour maps demonstrate horizontal variation in the formation and a broad NS-EW trend in the structure of subsurface with closed contours pointing east. The Mehar-01, Mehar-02, and Mehar-03 wells in the map indicates an anticlinal feature with one limb that is signposted by a structural constriction at a depth of 3300 meters and a least time of 1.75 seconds (dipping in the east). Compared to other dark blue zones on these maps, the horizon in the west appears to be farther away. The time and depth contours map of Upper Ranikot formation are shown in the Figure's underneath. The sands of Lower Ranikot identified as reservoir in the Mehar region are the objective concern of this study. The longitudinal fluctuation of the horizon is represented by temporal and depth contour maps of

the lower Ranikot formation. The geological trends in subsurface structure swing from the west to the east. Both time and contour maps display a mild anticline in an eastern direction with individual time and depth values, which is considered as an advantageous environment for the sequestration of hydrocarbons. The time and depth contours map of Lower Ranikot formation are shown in the figure's underneath.

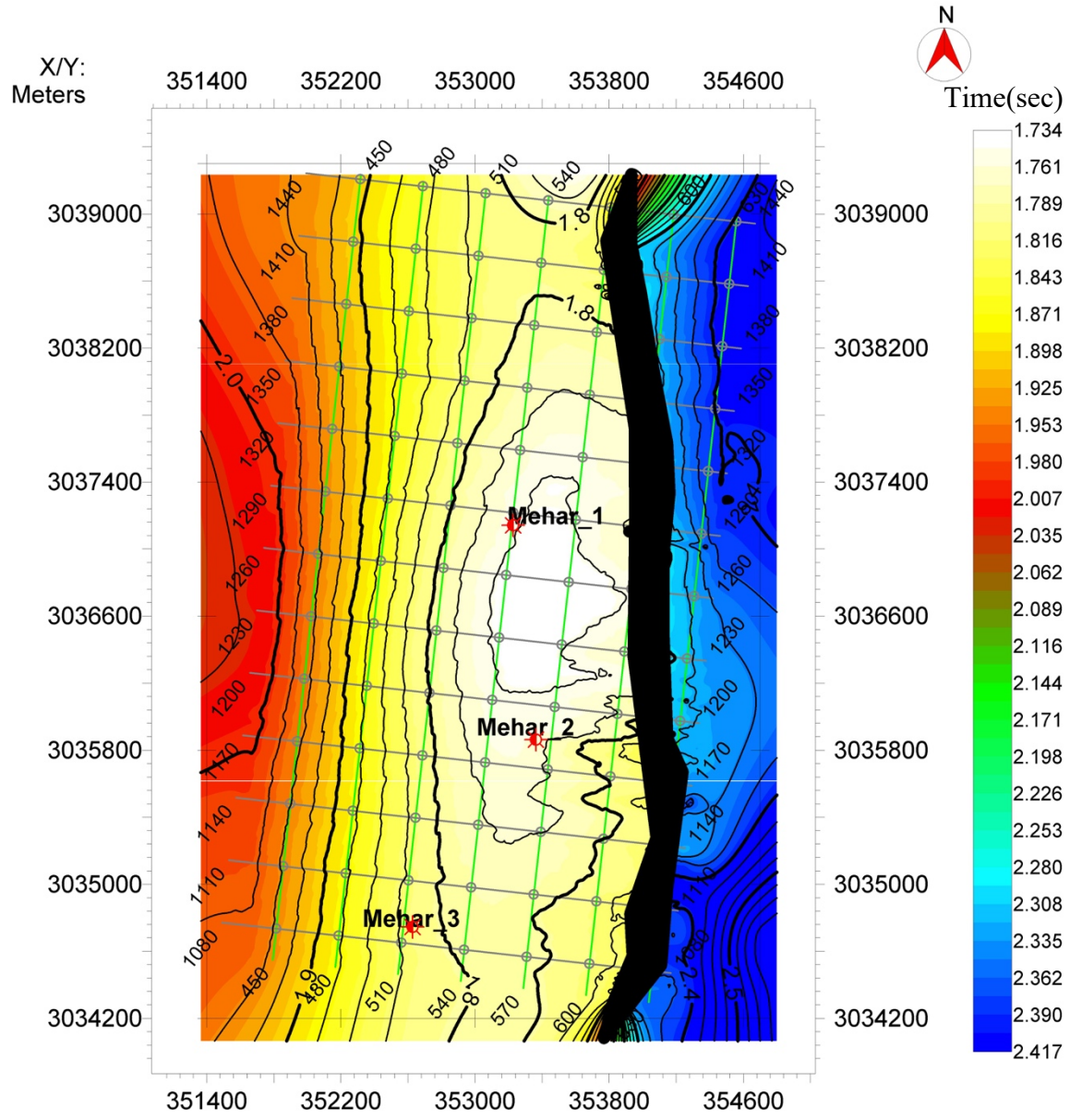

Fig (4.5) Time contour map of Upper Ranikot Formation

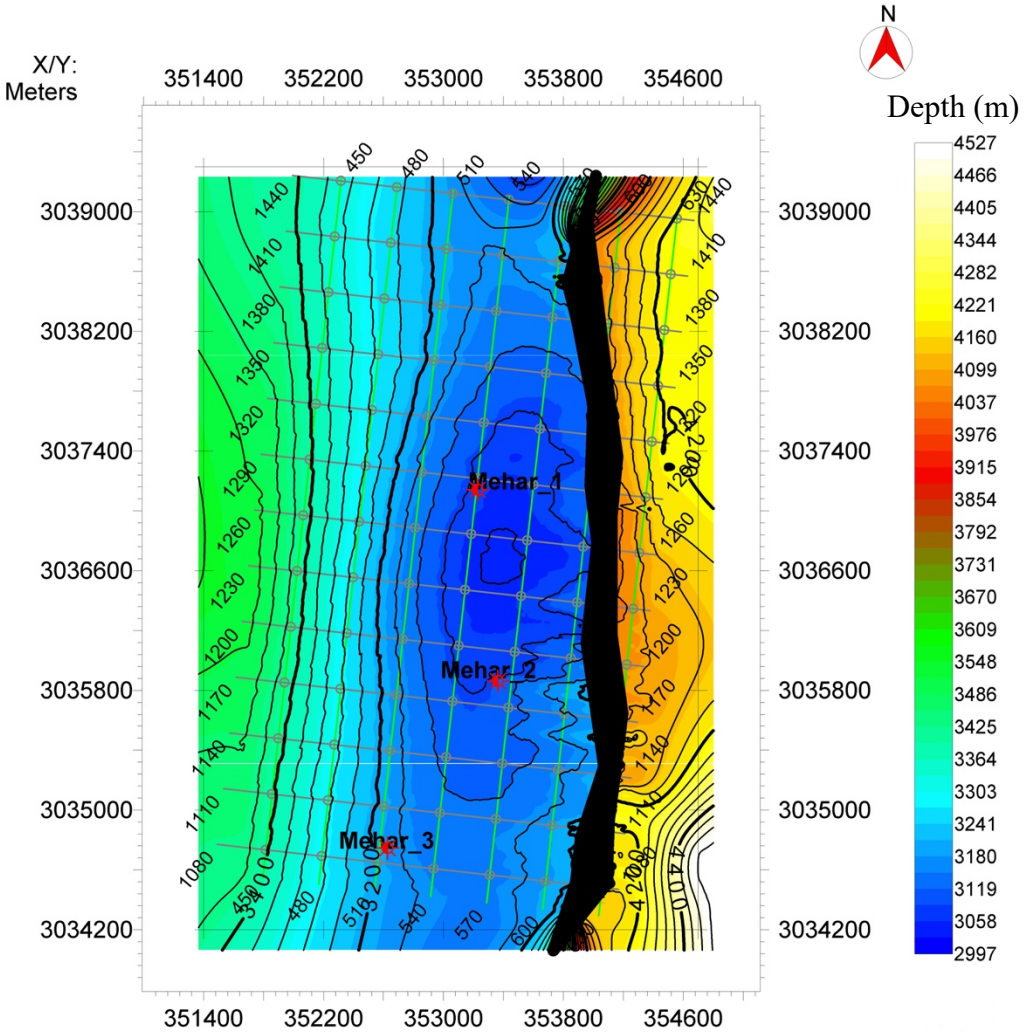

Fig (4.6) Depth contour map of Upper Ranikot Formation

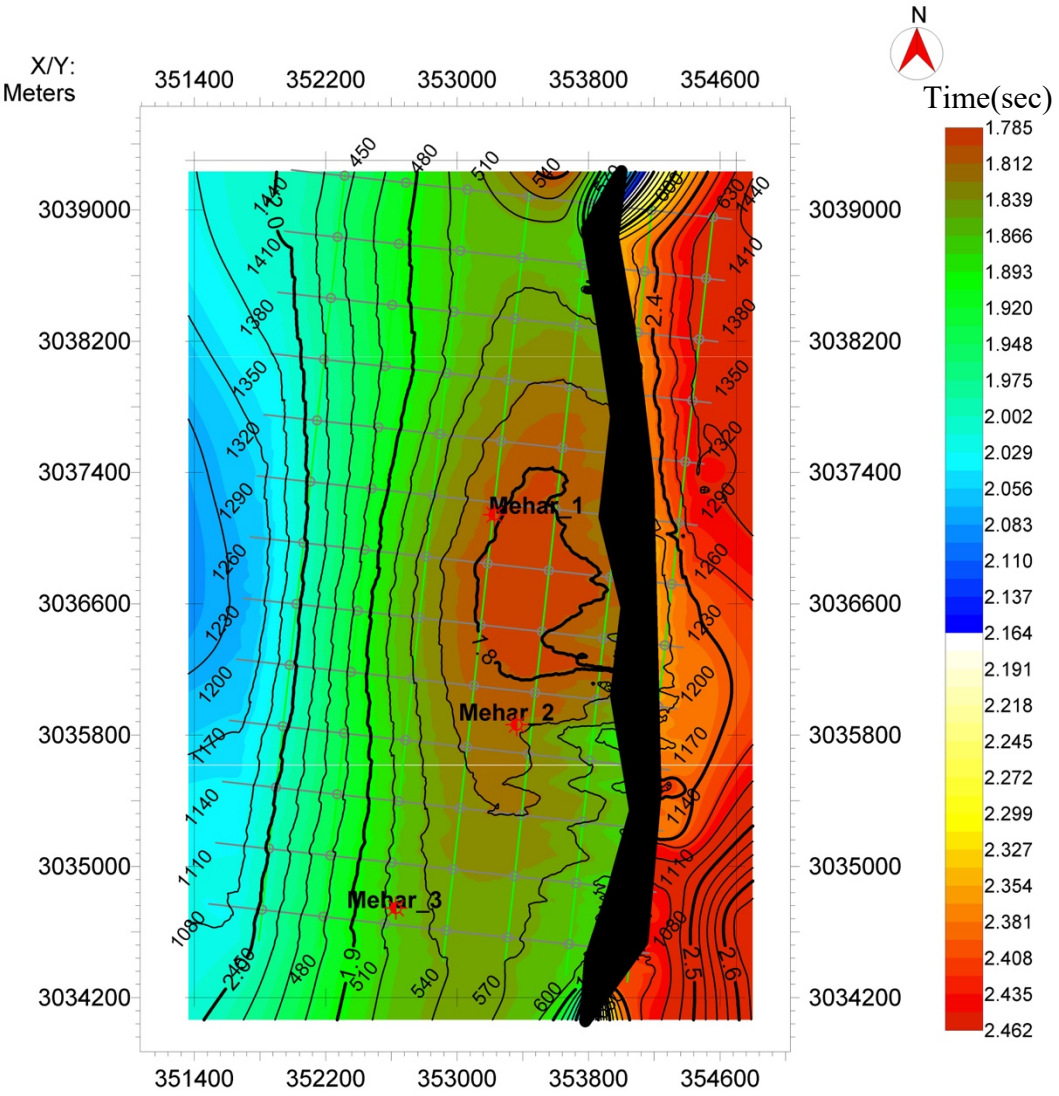

Fig (4.7) Time Contour map of Lower Ranikot Formation

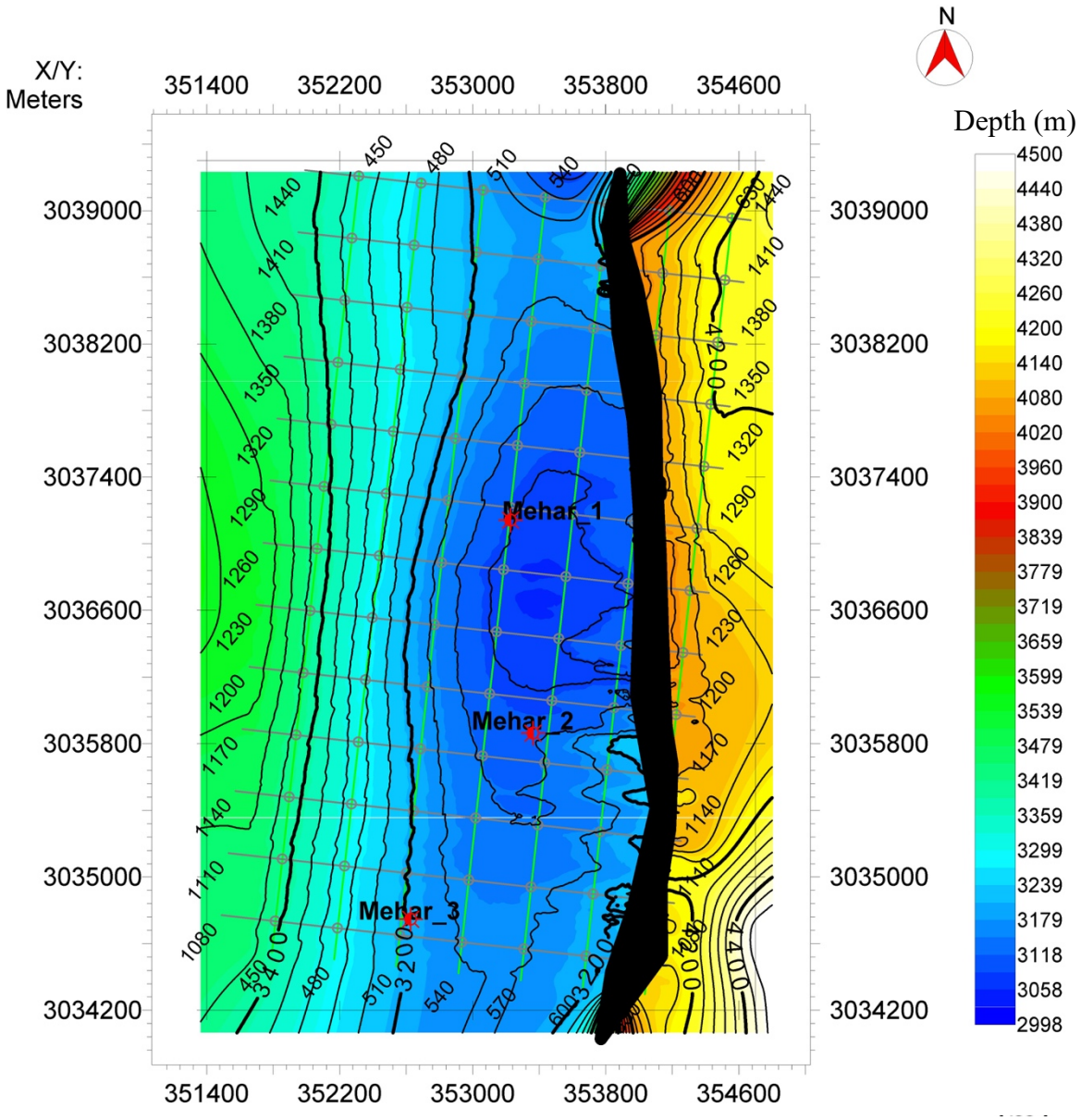

Fig (4.8) Depth Contour map of Lower Ranikot Formation

Chapter 5 Seismic Inversion Analysis

To guesstimate rock parameters, exclusively acoustic impedance, seismic inversion is frequently employed in the processing and interpretation of seismic reflection data. Seismic inversion can correspondingly be used for reservoir characterization, well planning and in monitoring the changes in properties of rocks while production or inoculation of field (e.g. net pay, porosity). Seismic inversion's leading goal is to deconvolute seismic data to confiscate the wavelet impression before transforming the output into an acoustic impedance (AI). Depending on the imperial relationship, a layer feature called acoustic impedance can be utilized to define reservoir characteristics including density, porosity, fluid saturation for the space between wells (Kumar et, al. 2016). Model Parameters stand customized till the model equivalence amid experimental data. Conclusive geological model contributes for approximation of the dissemination of reservoir characteristics (Vecken and Da Silva, 2004).

Physical characteristics of reservoir and that of lithological units are distinguished by the seismic data. The seismic inversion can directly be correlated with well log data and is also conscientious for the modification of property of interface into stratigraphic property. Following the so procedure, reservoir characterization can be idealized by the interpretation in terms of seismic and geological aspects fixed from seismic plus inverted data (Li., 2014).

Seismic inversion, on both pre- and post-stack data, can be pertained. Several seismic inversion techniques, including model-based, sparse-spike, band-limited, and colored inversion, can be used with post-stack data, depending on the goals as well as expediency of the data. When doing post stack seismic inversion, stack data was used as an input, and all sounds were eliminated by maintaining the real amplitude in the essential data (Da Silva et, al. 2004). The correlation between well data and seismic data is crucial for seismic inversion because it improves resolution and yields accurate data on physical parameters. A statistical analysis of seismic and well data is seismic inversion (Maurya and Sarkar, 2016).

The types of inversion that are studied during the research are as follows,

- Model based inversion
- Bandlimited inversion
- Sparse spike inversion

5.1) Phases monitored for Computation of Inversion

The software Hampson Russell Suite (HRS) was employed for the computation of Inversion. For post-stack inversion on HRS, we are required to load the data firstly with conditional and

standard parametric settings. We simultaneously start with seismic and well data loading. Then comes the progression of horizon marking. Once we marked the horizons, we head towards the wavelet extraction which is extracted using seismic data. The extracted wavelet is then convolved with the reflectivity series for converting seismic amplitude volume to impedance volume. As, the preferred way is to avoid the wave which is estimated theocratically and to adopt the one which is being extracted by the seismic data (Cooke and Cantt,2010).

The general workflow which was adopted for the computation of inversion is shown in Figure (5.1).

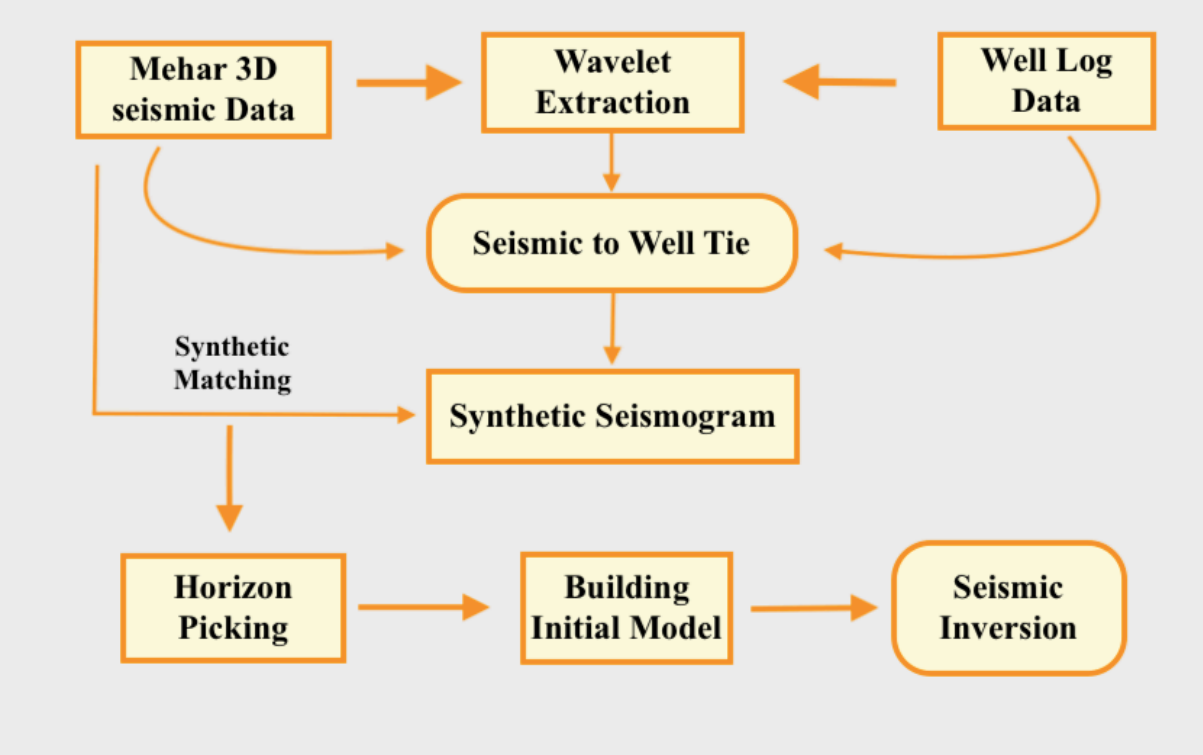

Fig (5.1) Generalized workflow of inversion indicating the steps followed for building inversion models

The time window from 1700 to 1900 inclosing traces of inline and crosslines from seismic data is considered for the extraction of wavelet. Lithology inclusion of the respected time window is Shale and sand of Ranikot sandstone of Pab formation. The wavelet extracted is shown in Figure (5.2).

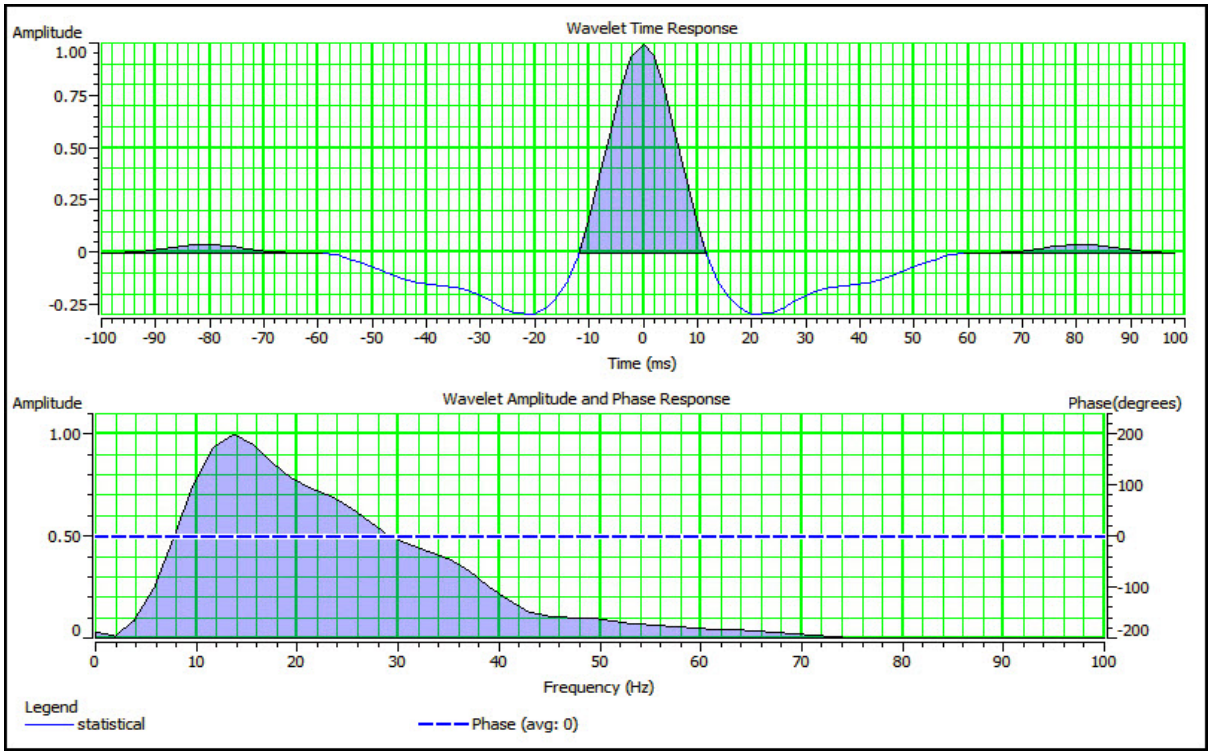

Fig (5.2) Extracted Statistical wavelet using seismic data

5.2) Low Frequency Model (LFM)

Acoustic impedance may be relative or absolute depending upon the condition. In relative acoustic impedance, there is no need of LFM as the relative properties of certain layers and is used as a qualitative interpretation tool. But in case of absolute acoustic impedance, there is demand of constructing a low frequency model as it designates the absolute property of layer. The background information of relevant data is contained by low frequencies and hence required in techniques of seismic inversion (Kumar & Negi., 2016). It also assists in understanding of both qualitative and quantitative interpretation. Besides, LFM provides a better information even in terms of gradual changes that occur in the formation under consideration. In order to procure absolute acoustic impedance, the component of low frequency is incorporated in the algorithm of inversion (Cooke and Cant., 2010). Before

building the initial model, it is necessary to make a tie between seismic and well data which is displayed in the following Figure.

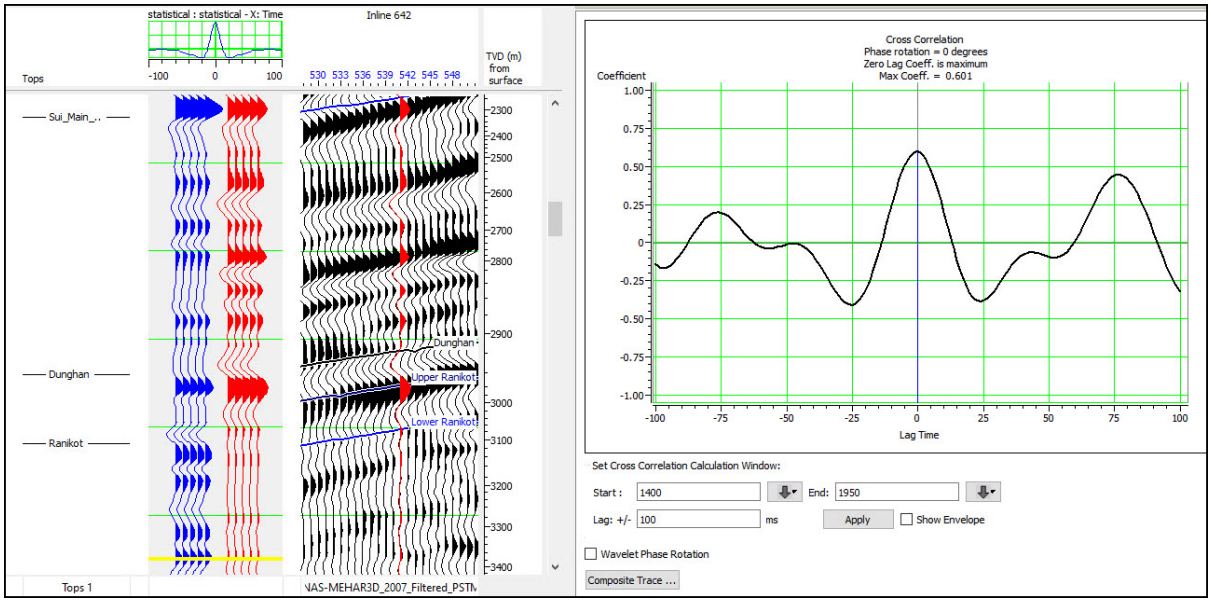

Fig (5.3) Seismic to well tie using Mehar-01 and inline 642

We make low frequency models by means of well data to support our results. The Initial model of P-impedance and S-Impedance based on well-01 of the study area i.e. Mehar-01 is shown in the succeeding figures. The model distinctly shows the leaning of amplitude fluctuations in the reservoir formation i.e. Ranikot.

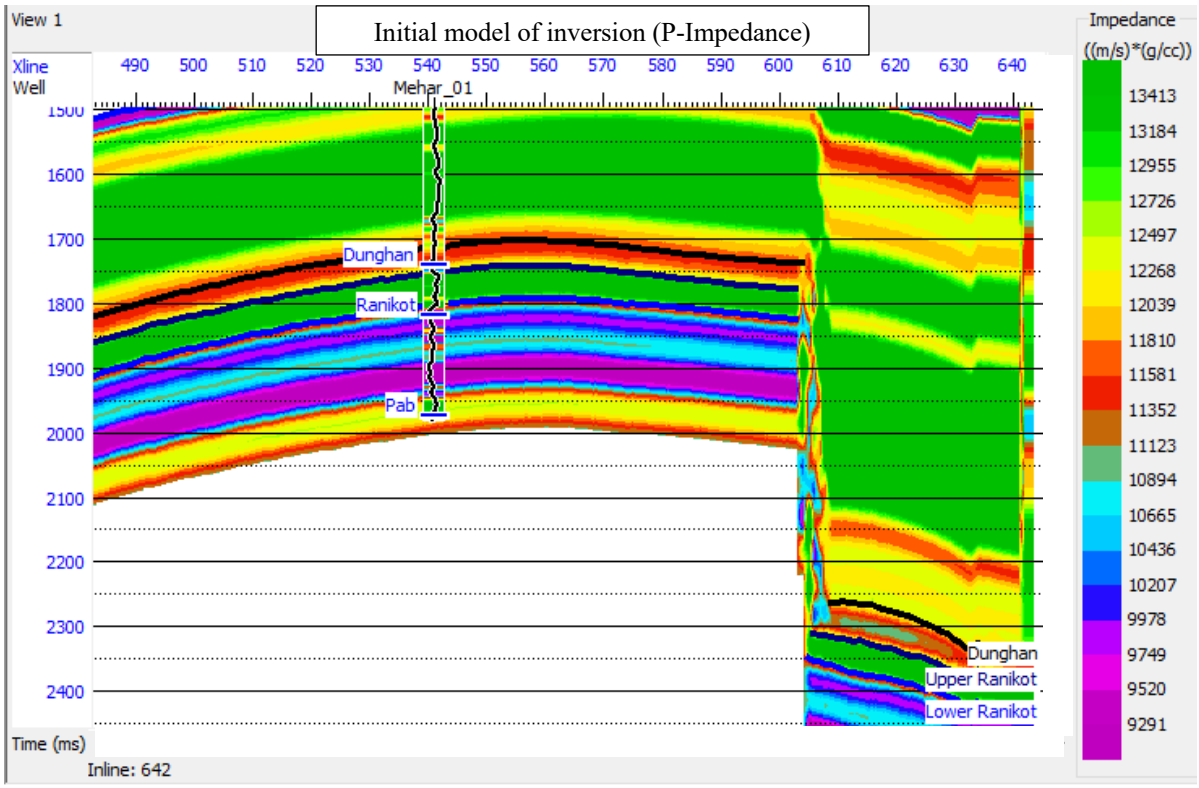

Fig (5.4) Initial P-impedance model of inversion using Mehar-01

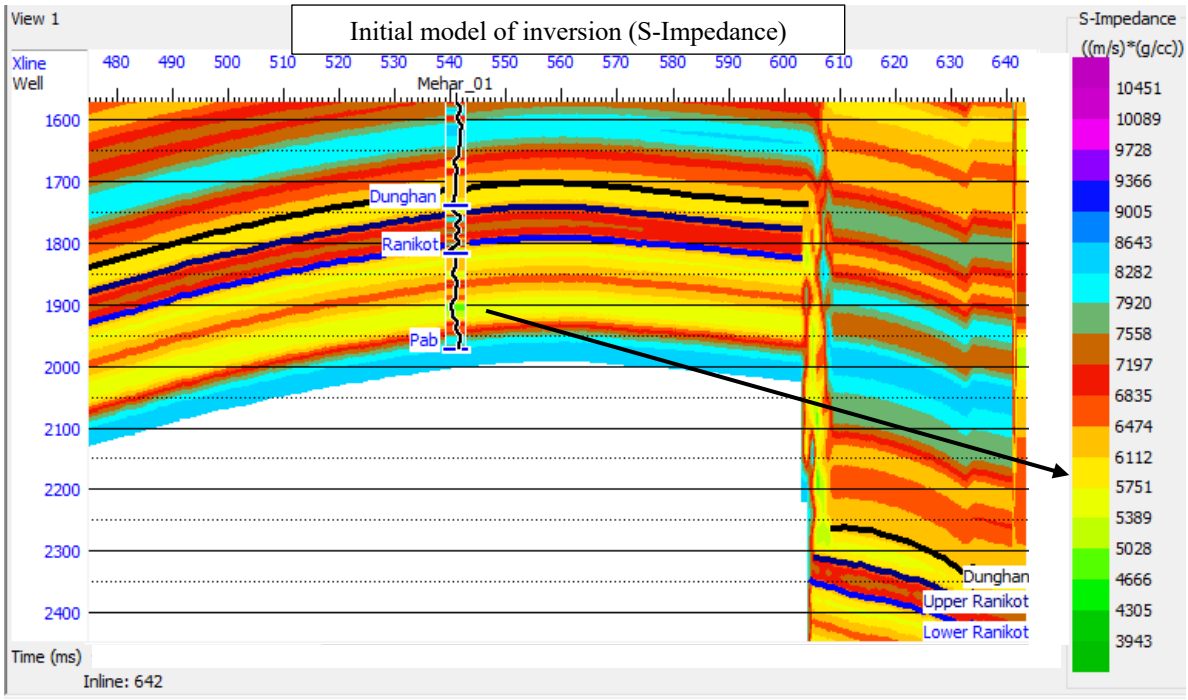

Fig (5.5) Initial S-impedance model of inversion

5.3) Inversion Analysis

The workflow of inversion is pertained on the three basic types of inversion including Model based, Maximum likelihood and Bandlimited inversion. The results of these inversions alongwith their respected correlations based on P-impedance and S-impedance, are discussed in the subsequent manner.

5.3.1) Model Based Inversion

Generalized linear inversion (GLI) is an algorithm that operates frequently till the obtained results balance the seismic data within the necessary limits and is contemplated to be the most stable well-thought-out linear model (Das et, al. 2017). In Model-based inversion, we develop the seismic trace by the convolution of source wavelet and the reflectivity of earth, amid the factor of noise (Mallick, 1995). The ensuing shown relation is the fundamental representation of seismic trace in terms of source wavelet and reflection coefficient with noise factor and source wavelet,

$$S(t) = \text{Noise} + RC * W(t) \quad (5.1)$$

The correlation of Model-based inversion is 99.6% and is represented in the figure (4.5) below with trace equivalency.

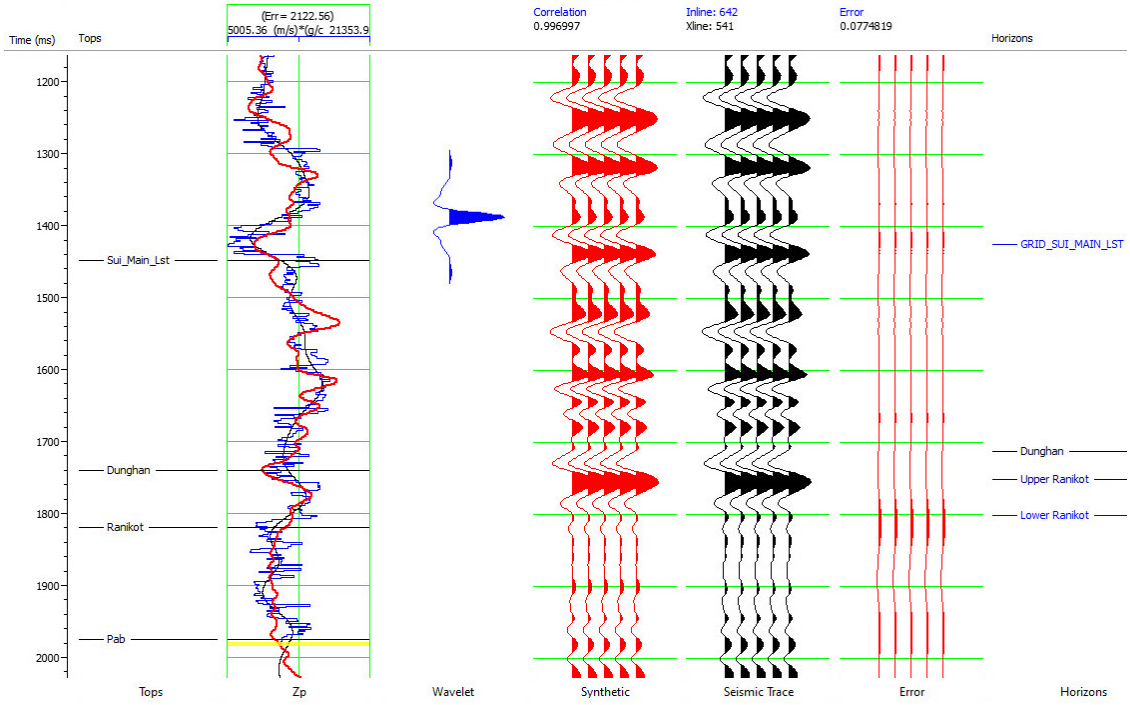

Fig (5.6) Correlation of Model-based Inversion (P-Impedance)

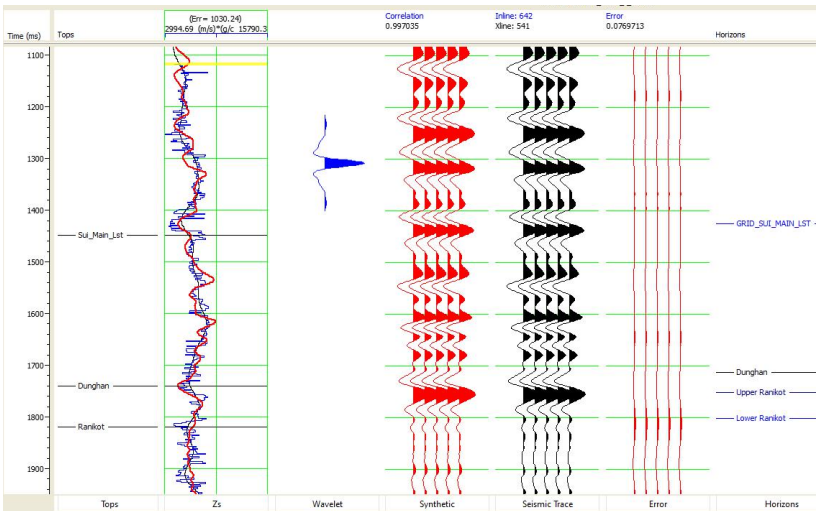

Fig (5.7) Correlation of Model-based Inversion (S-Impedance)

The chasing Figures (5.8) and (5.9) characterizes the results proposed by Model-based inversion, when applied on the given 3D cube of Mehar area under definite time window i.e 1700-1900. The colored scale bar noticeably spectacles the impedance variations in the formations incorporating upper Ranikot, lower Ranikot and Dunghan.

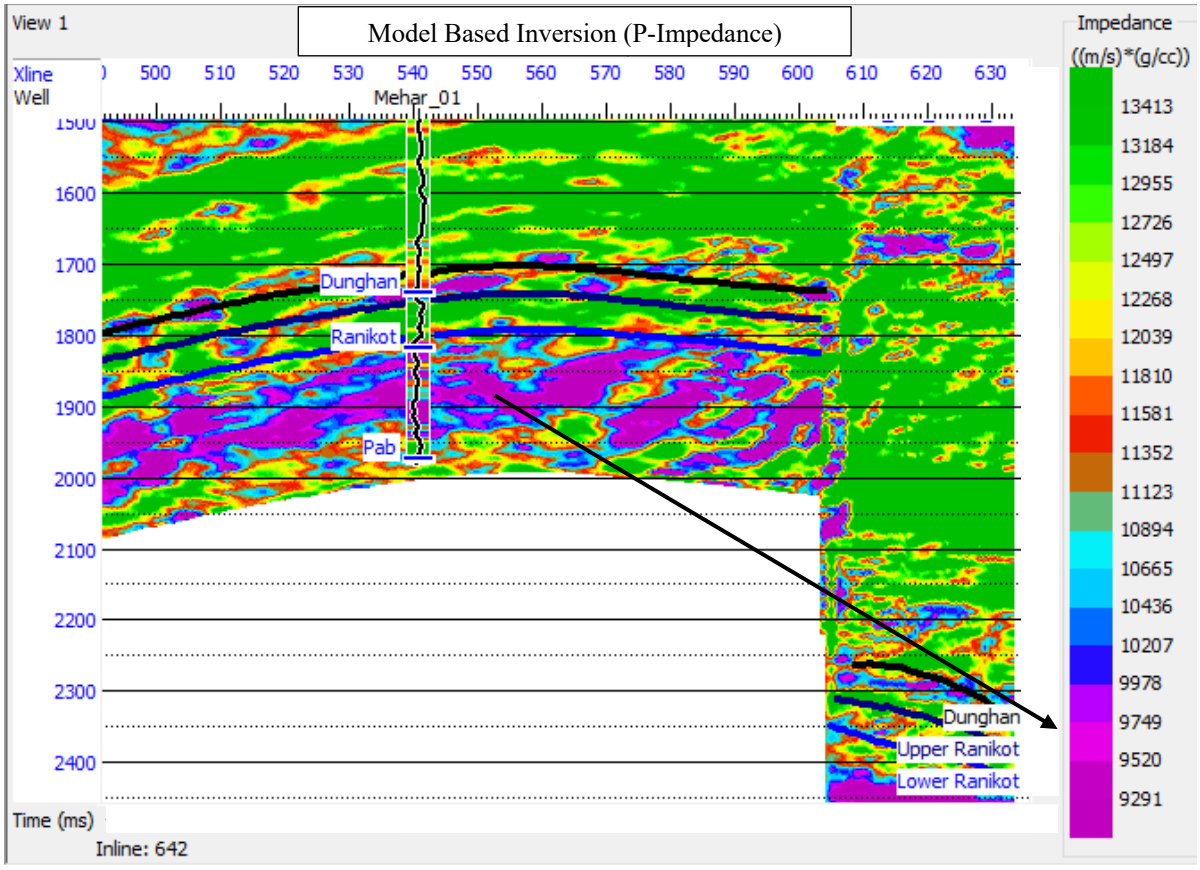

Fig (5.8) Results of Model-based Inversion (P-Impedance) showing low values of impedance

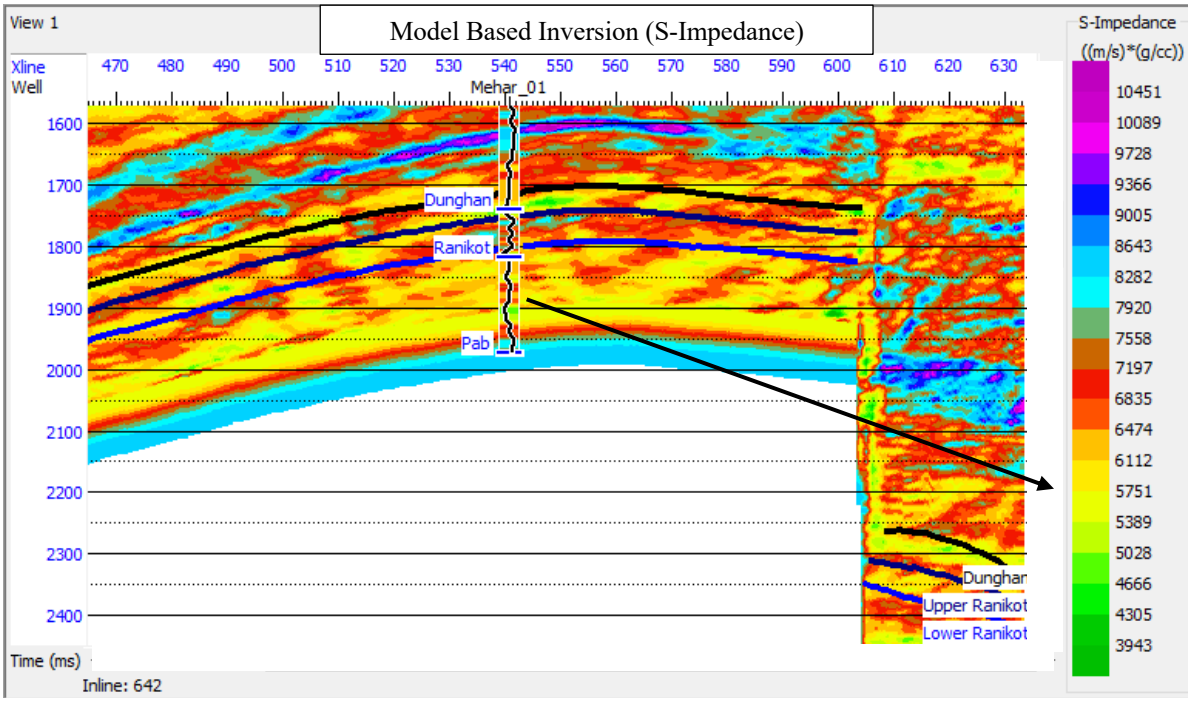

Fig (5.9) Sectional view of Model-based Inversion on the basis of S-Impedance

The continuity in terms of impedance can be seen in the same Figure where the reservoir formation is lying. However, the continuity in impedance is breaking at above or below the

reservoir formation which is evident of the presence of reservoir in the formation. As described in the workflow of inversion, the wavelet is estimated firstly and then the initial model of impedance is generated. Then this initial model with certain updates is shaped into model-based inversion which have least errors. The horizontal layers of impedance change with relative to wells, while the vertical layers may constant in terms of impedance or may change linearly. Vertical layers are frequently utilized while examining the impedance of reservoir.

5.3.2) Sparse Spike Inversion

The sparse-spike inversion can be computed using two algorithms including maximum likelihood (sparse-spike) or linear programming. In accordance with the hypotheses that key lithological boundaries imply significant events in reflectivity series. These significant occurrences occur on top of minor ones (noise). The spikes on the reflectivity series are major events. Wavelet when estimated, can be utilized to compute reflectivity series after improving it. This process is repeated so that the errors can be minimized. The purpose of low frequency modeling is that in the absence of low frequency, final data can show some false impedance layers. And the reasons we miss low frequencies from seismic data are that due to the problem of ground roll, we don't record them. Some limitations of geophones also miss to record low frequencies. And often we consciously remove them during processing, considering them noise. We can add low frequencies to our data by means of geological model, velocity analysis of seismic data and by filtered sonic log. The convenient way is to make use of combination of sonic and seismic velocity data. We can add low frequency to the data while computing impedance model or reflectivity. The Figures (5.10) and (5.11) displays the results of sparse spike inversion.

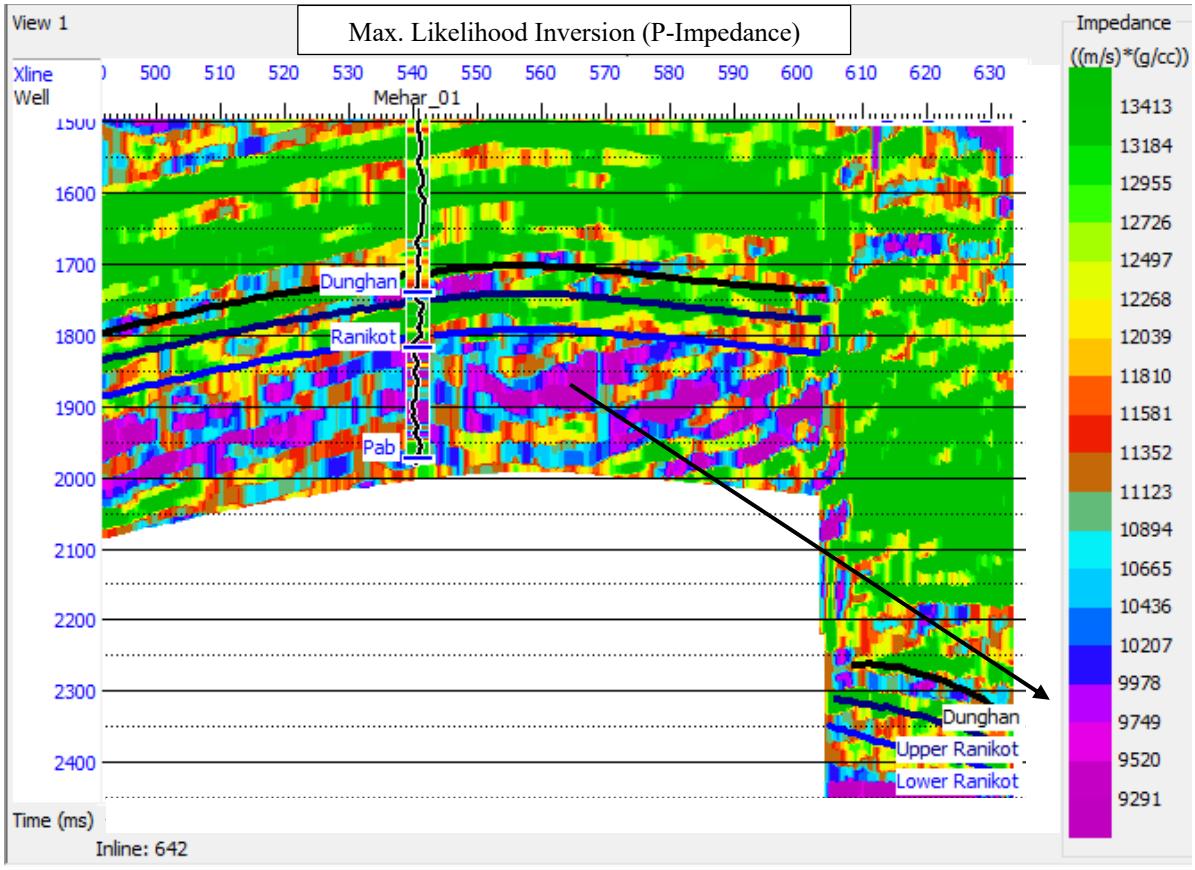

Fig (5.10) Results of Maximum Likelihood Inversion (P-Impedance) with low impedance values

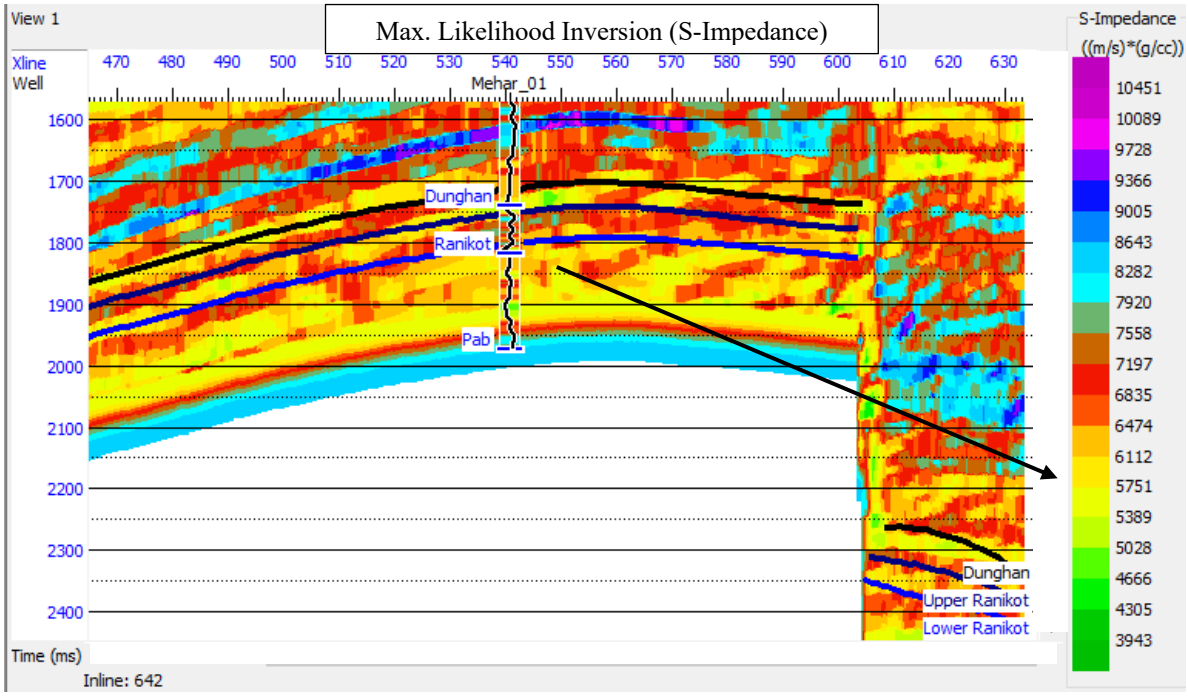

Fig (5.11) Sectional view of Maximum Likelihood Inversion (S-Impedance)

With each subsequent reflection coefficient added to a single trace, sparse reflectivity is generated until the desired set of outputs is reached. The correlation of Sparse-spike inversion (Maximum Likelihood) is shown in the below figures.

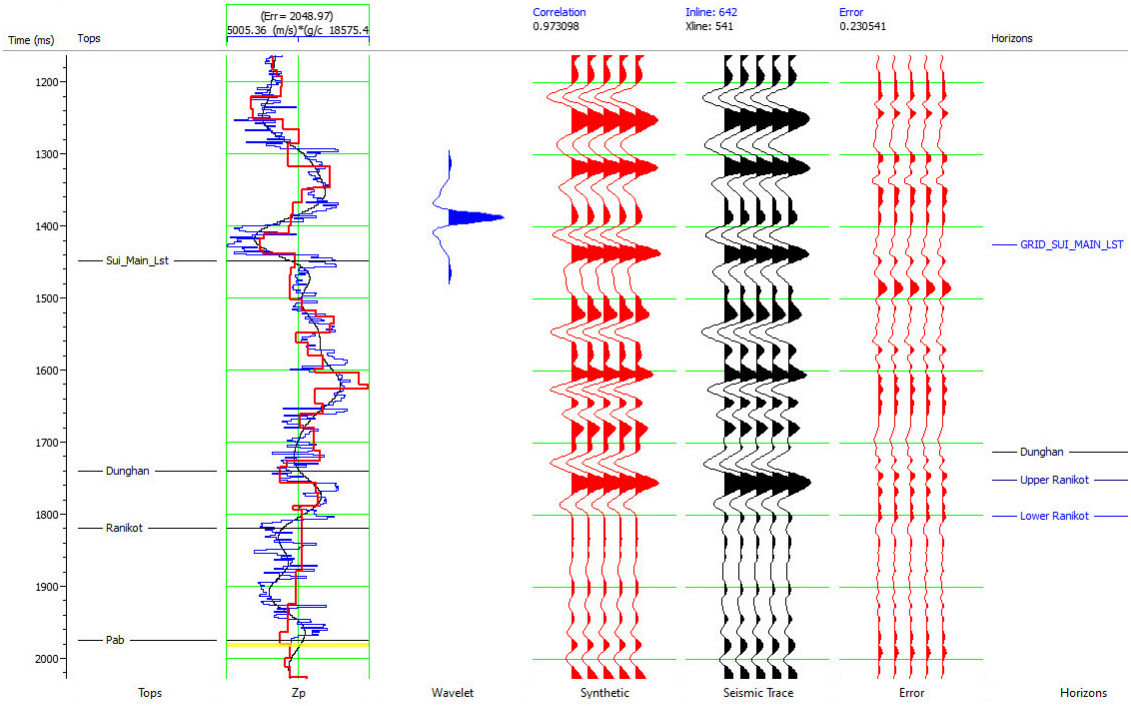

Fig (5.12) Correlation of Maximum likelihood Inversion (P-Impedance)

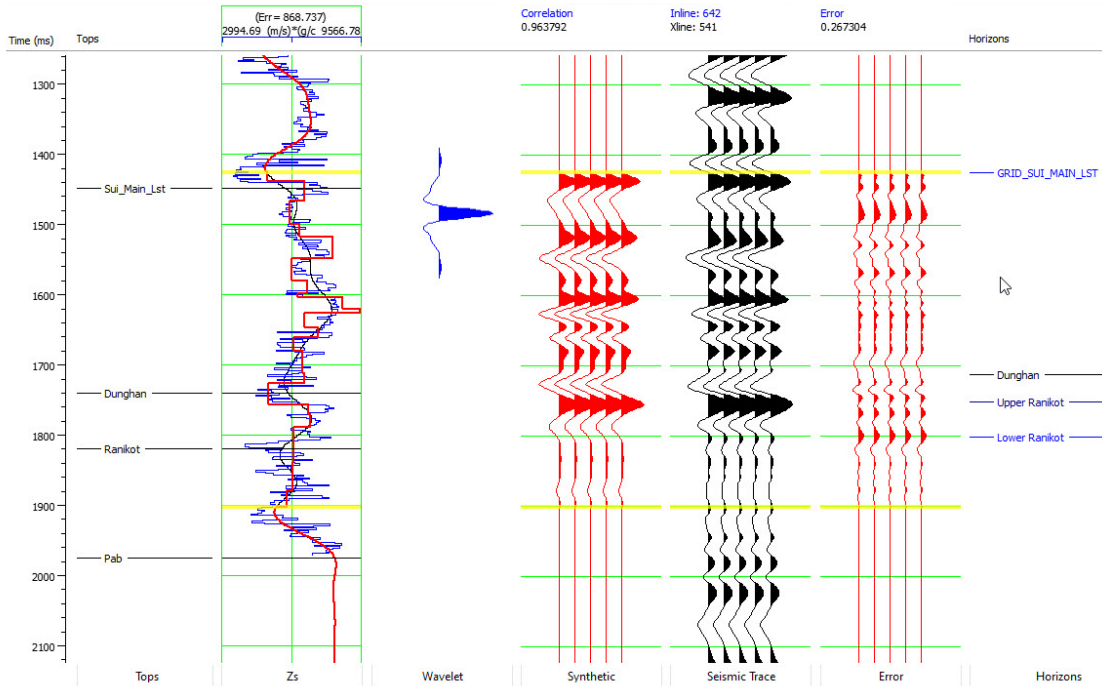

Fig (5.13) Correlation of Maximum likelihood Inversion (S-Impedance)

This form of reflectivity in the broad spectrum has steadily changed until the synthetic and actual traces coincide. This technique starts the broadband seismic inversion process with a sparse reflection coefficient (Maurya., S.P 2016).

5.3.4) Bandlimited Inversion

Band limited inversion is the transformation of post-stack data into velocity of seismic wave, density and acoustic impedance. Band-limited inversion is related to the seismic trace for the estimation of impedance. The interface is quickly identified by band limited inversion, which also follows the general trend of the initial geological model, but it is unable to address the impedance of reservoir. The correlation of band limited inversion is 0.933 and shown in the following Figure (5.14).

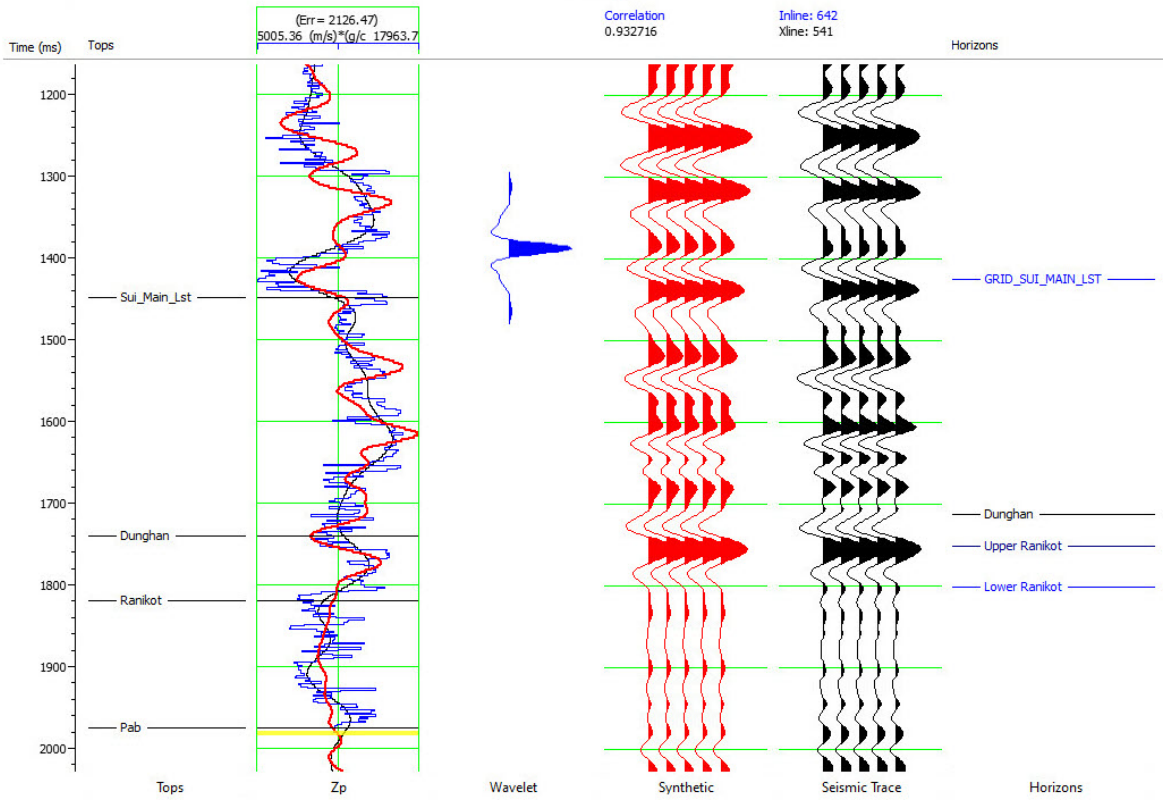

Fig (5.14) Correlation of Bandlimited Inversion (P-Impedance)

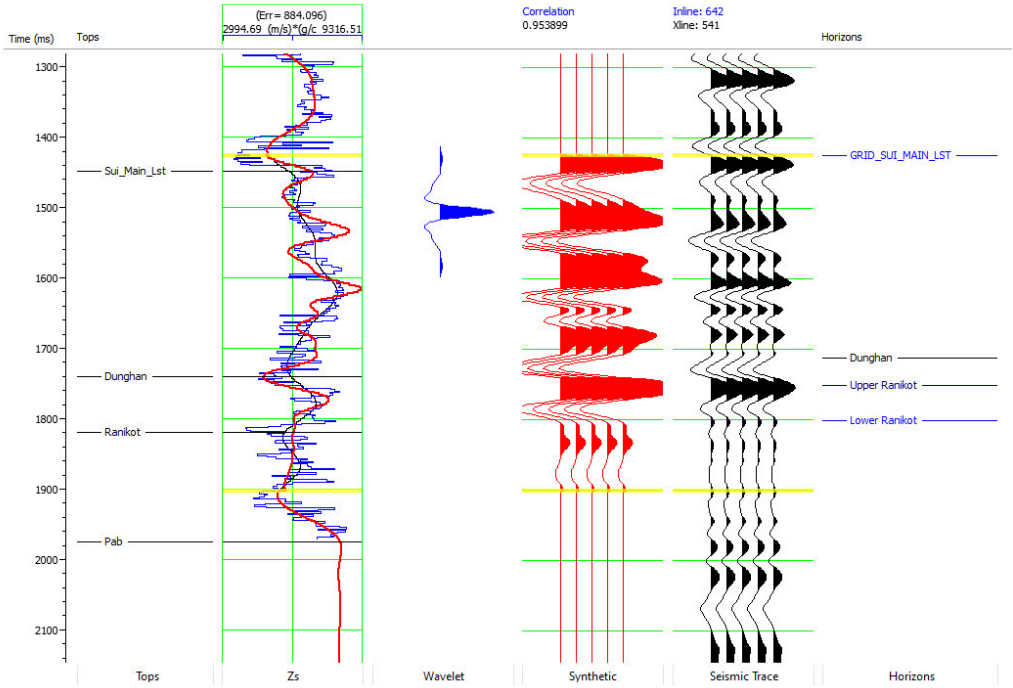

Fig (5.15) Correlation of Bandlimited Inversion for S-Impedance model

The interpretation is undertaken by the inverted P-impedance which identifies faults and geological trends. The following Figure (5.16) and (5.17) represents the results of bandlimited inversion on the root of P-impedance and S-impedance respectively.

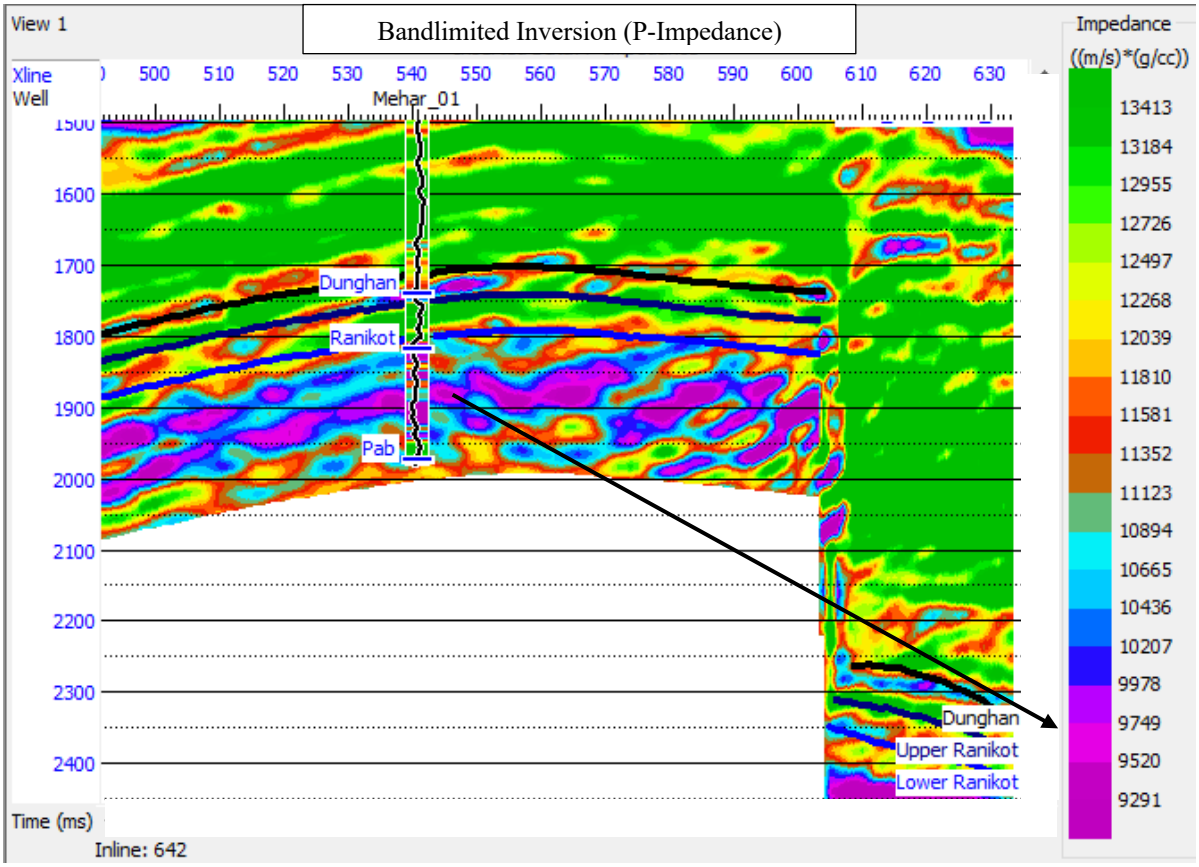

Fig (5.16) Sectional view of Results of Band Limited Inversion (P-Impedance)

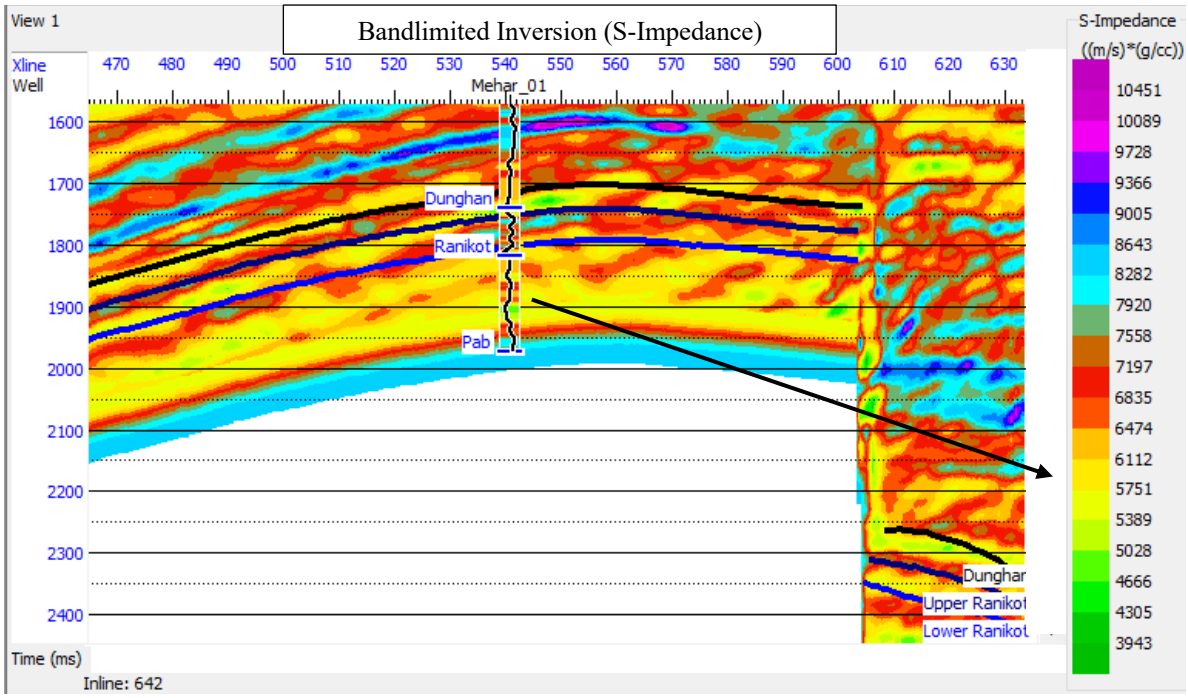

Fig (5.17) Results of Band Limited Inversion (S-Impedance)

5.3.5) Comparative study of Inversion Modes

The correlation of Model Based Inversion is 99.7 screening it to the best visualization in terms of impedance. Whereas, correlation of that of Sparse-spike (maximum likelihood) and Bandlimited came out to be 97.3 and 93.2 respectively. The common attribute found in all of the three applied types of inversion is that they depict low impedance on the reservoir formation providing the exhibition of hydrocarbon potential in the respected domain. The comparative pictural representation of inversion types is shown below in the following Figure.

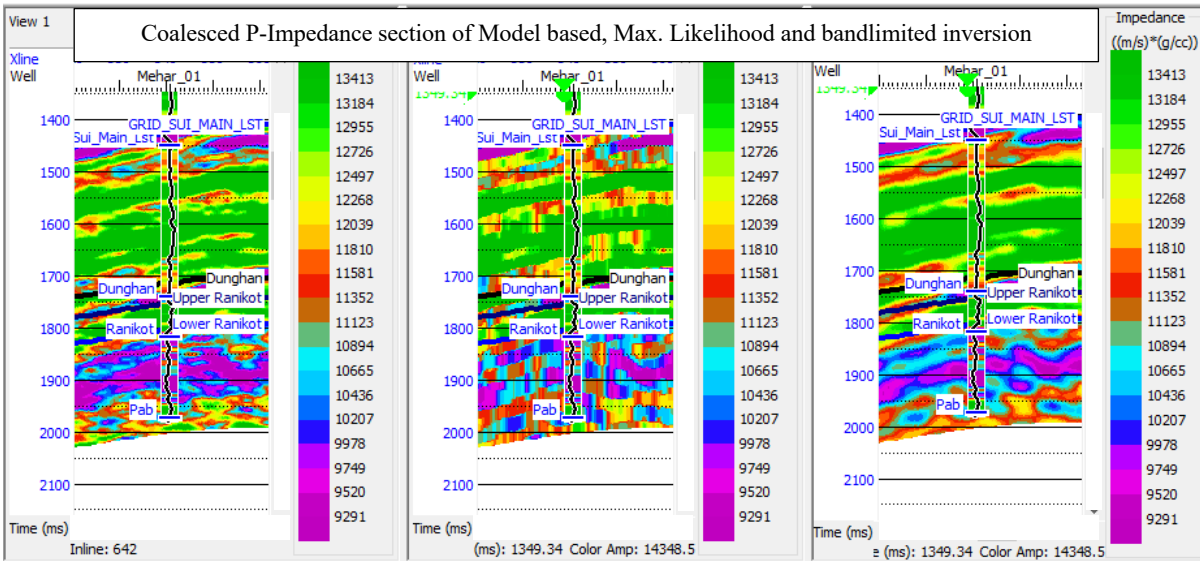

Fig (5.18) Coalesced Demonstration of P-Impedance Model based, Maximum likelihood and Bandlimited inversion

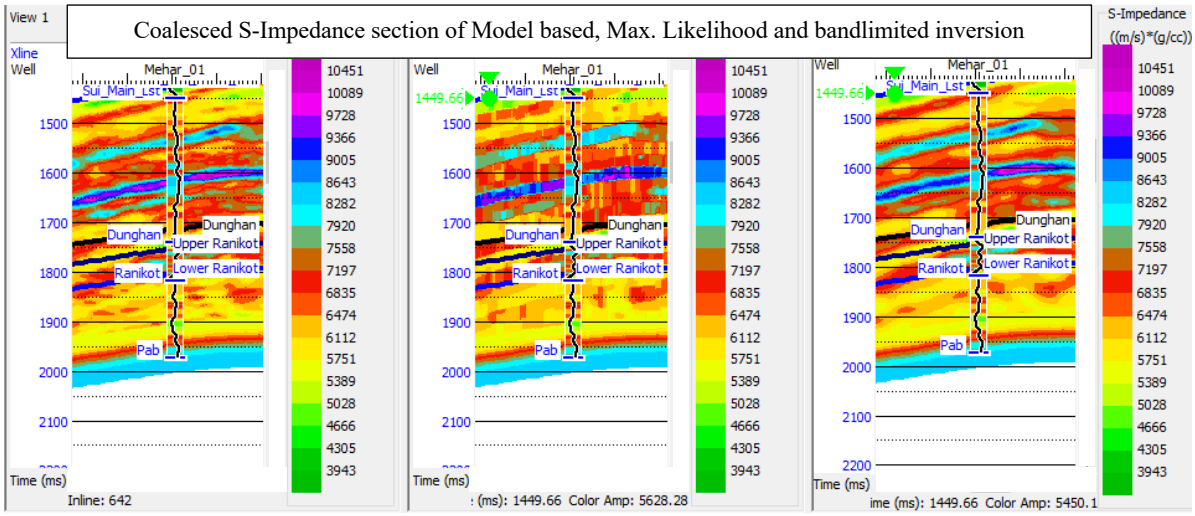

Fig (5.19) Coalesced Demonstration of S-Impedance Model based, Maximum likelihood and Bandlimited inversion

5.4) Porosity Modeling on the basis of Cross-plots

The porosity sections are made by cross plots on Model based, Maximum likelihood and Bandlimited inversion. The models of porosity sections are represented below in the succeeding Figures. The slices of these models are also configured on the basis of porosity and impedance.

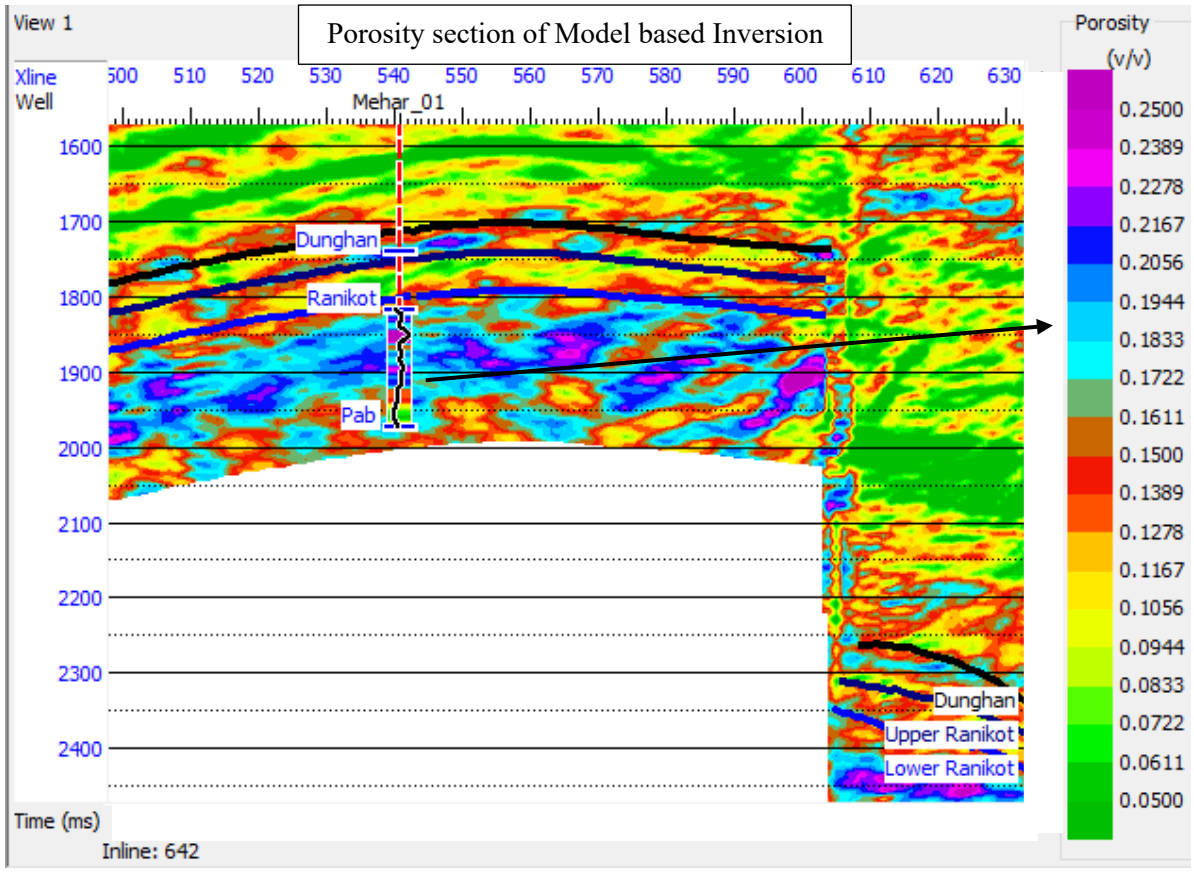

Fig (5.20) Porosity section of Model-Based Inversion with indicating of corresponding values

The slice of porosity section showing two wells i.e Mehar-01 and Mehar-02 of MBI is shown below in Figure (5.21) below.

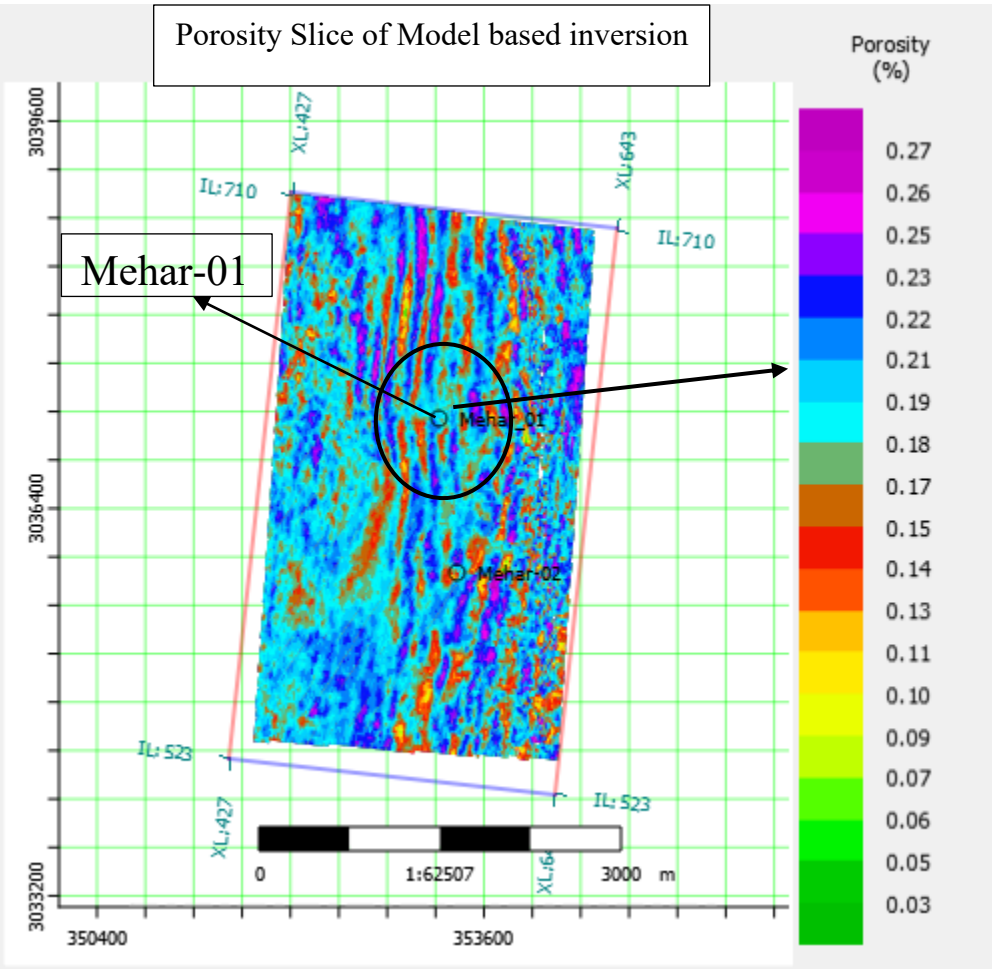

Fig (5.21) Porosity slice of Model-based Inversion

The slice section of MBI on the basis of impedance by using cross plots is depicted in the following Figure (5.22).

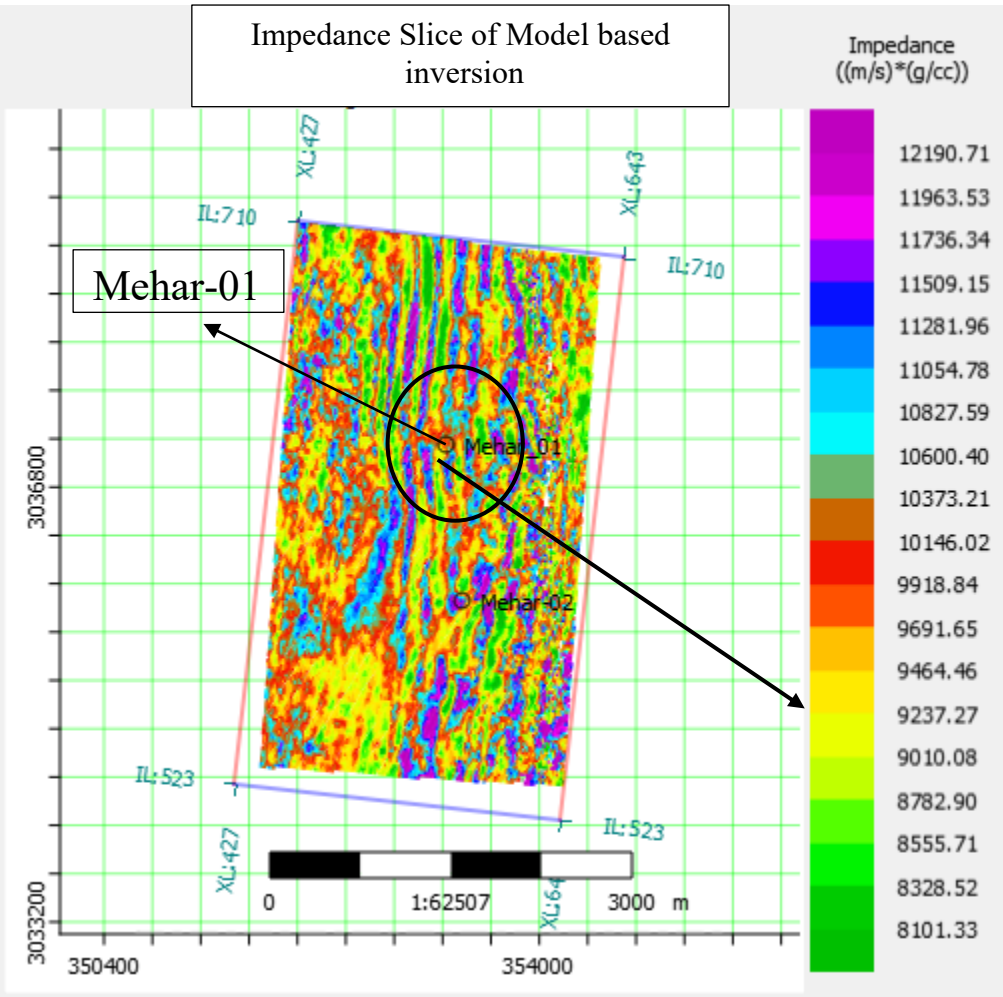

Fig (5.22) Impedance Slice of MBI

The porosity section of Sparse-spike (Maximum likelihood) inversion and its slice section on the basis of porosity and impedance are also featured with the assistance of cross plots and the results are shown in the following Figure (5.23).

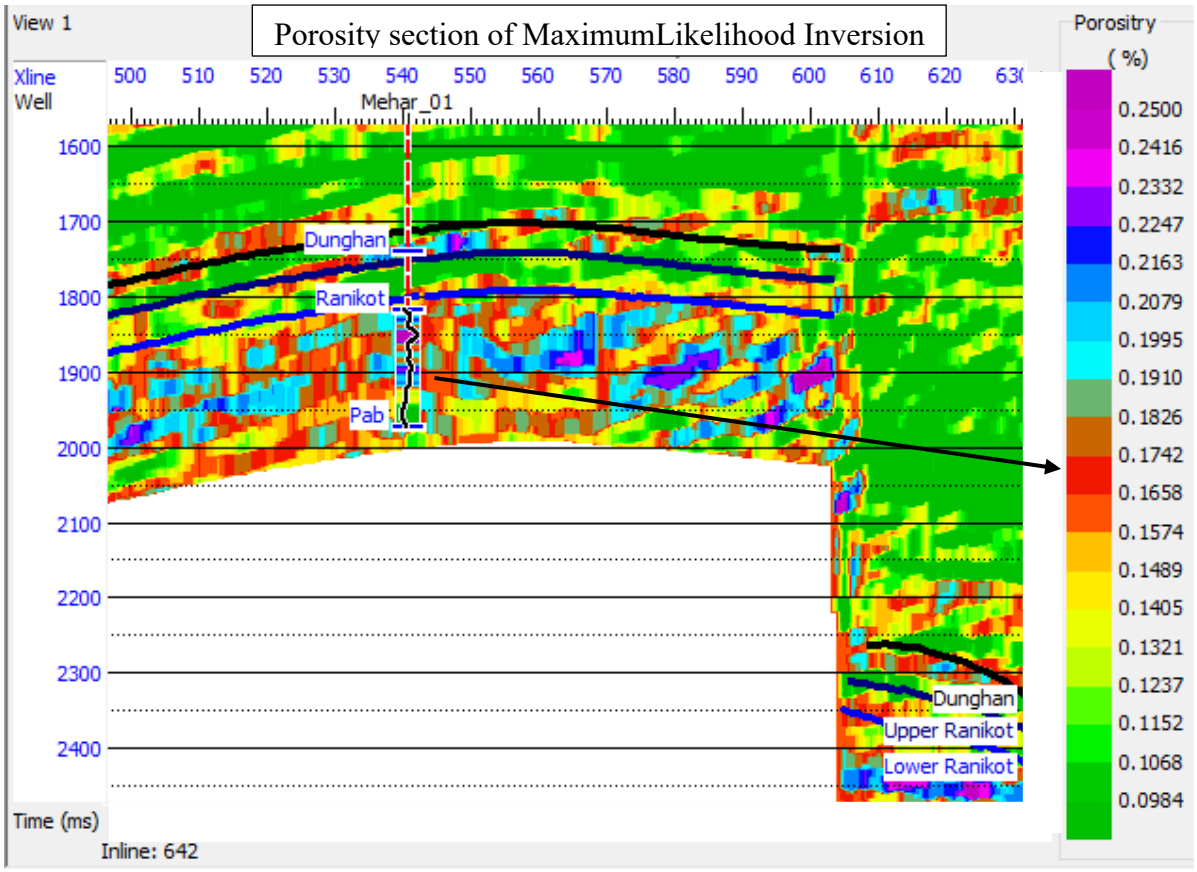

Fig (5.23) Porosity section of Maximum Likelihood Inversion

The porosity and impedance slice of Maximum Likelihood Inversion is displayed in Figure (5.24) and Figure (5.25) respectively.

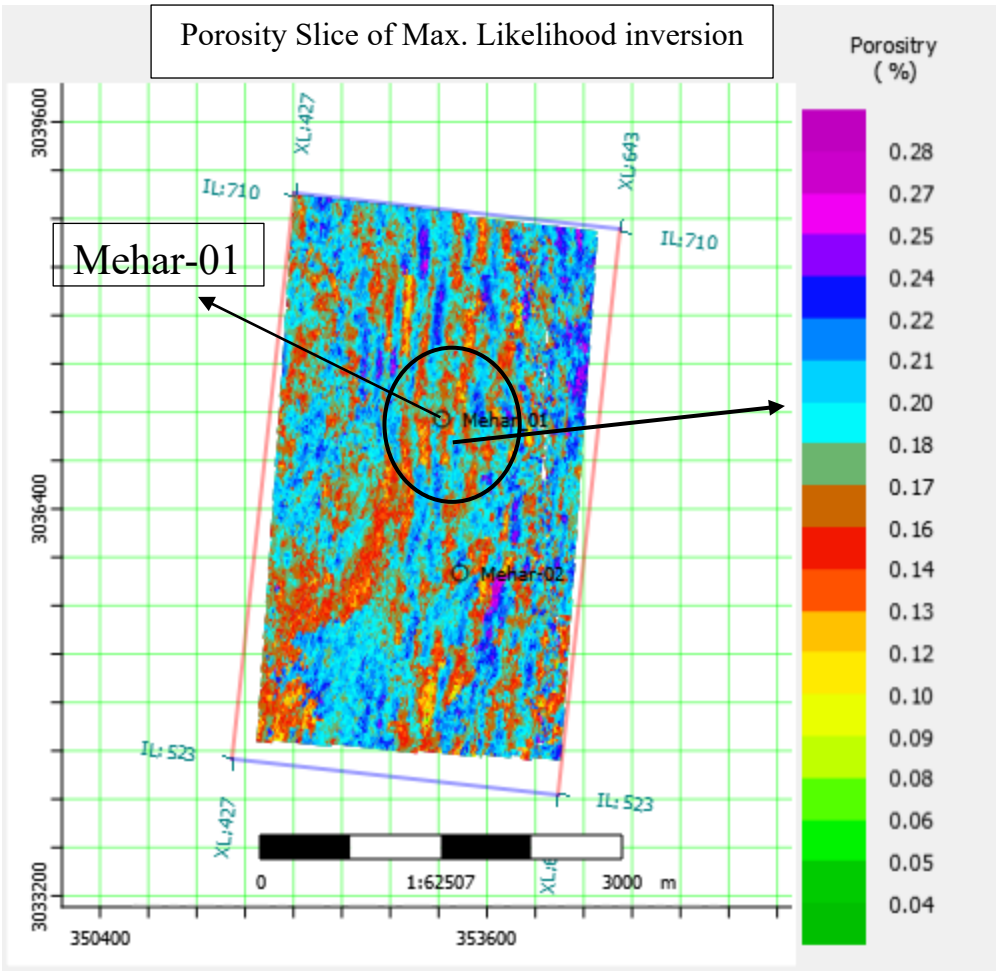

Fig (5.24) Porosity Slice of Maximum Likelihood Inversion

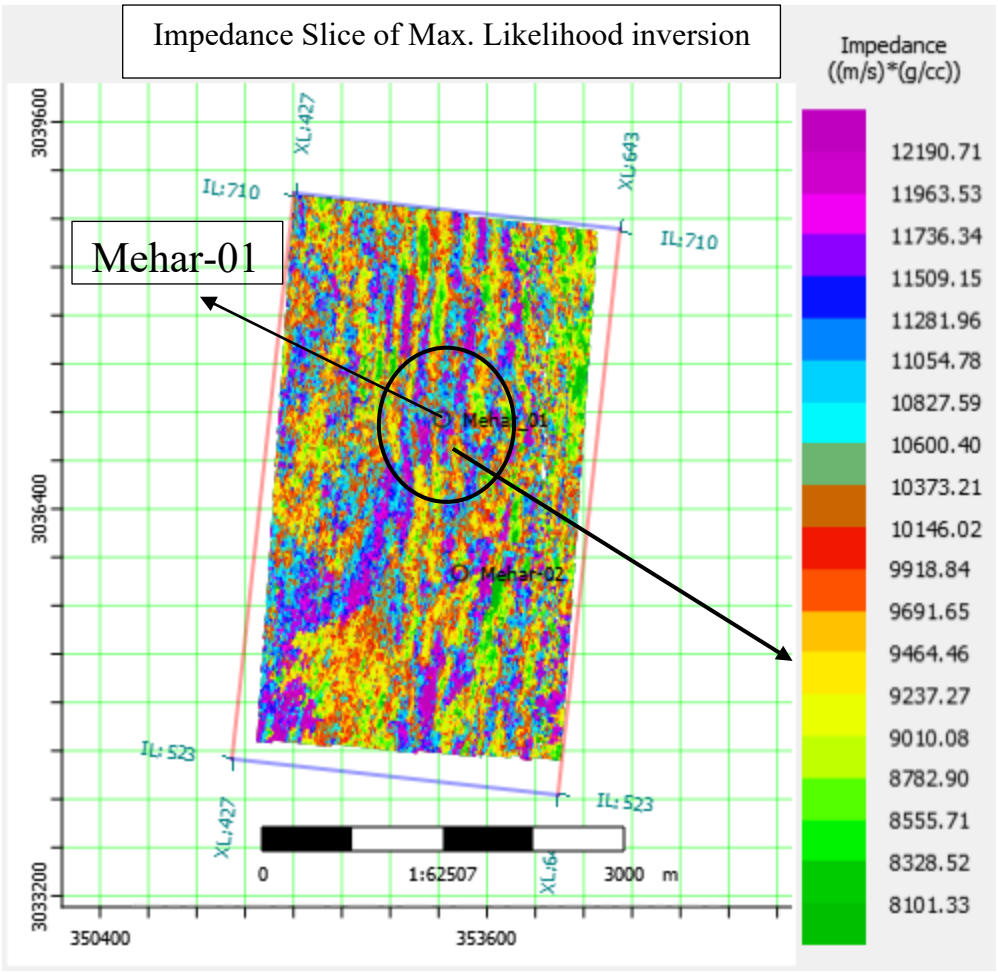

Fig (5.25) Impedance Slice of Maximum Likelihood Inversion

The analogous technique of cross plots is pertained to the Bandlimited Inversion to evaluate the porosity section as well as slice on the root of both impedance and porosity. The subsequent figures signify their visualization.

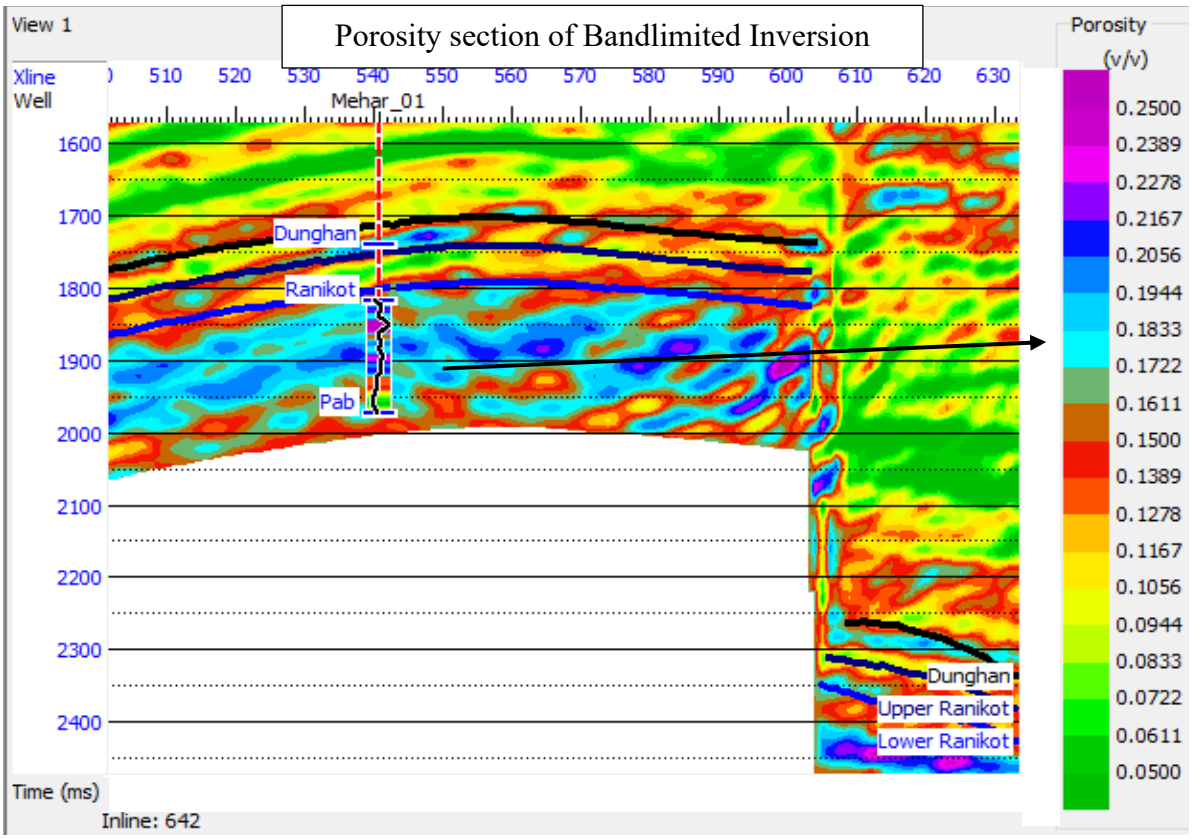

Fig (5.26) Results of Porosity section for Bandlimited Inversion

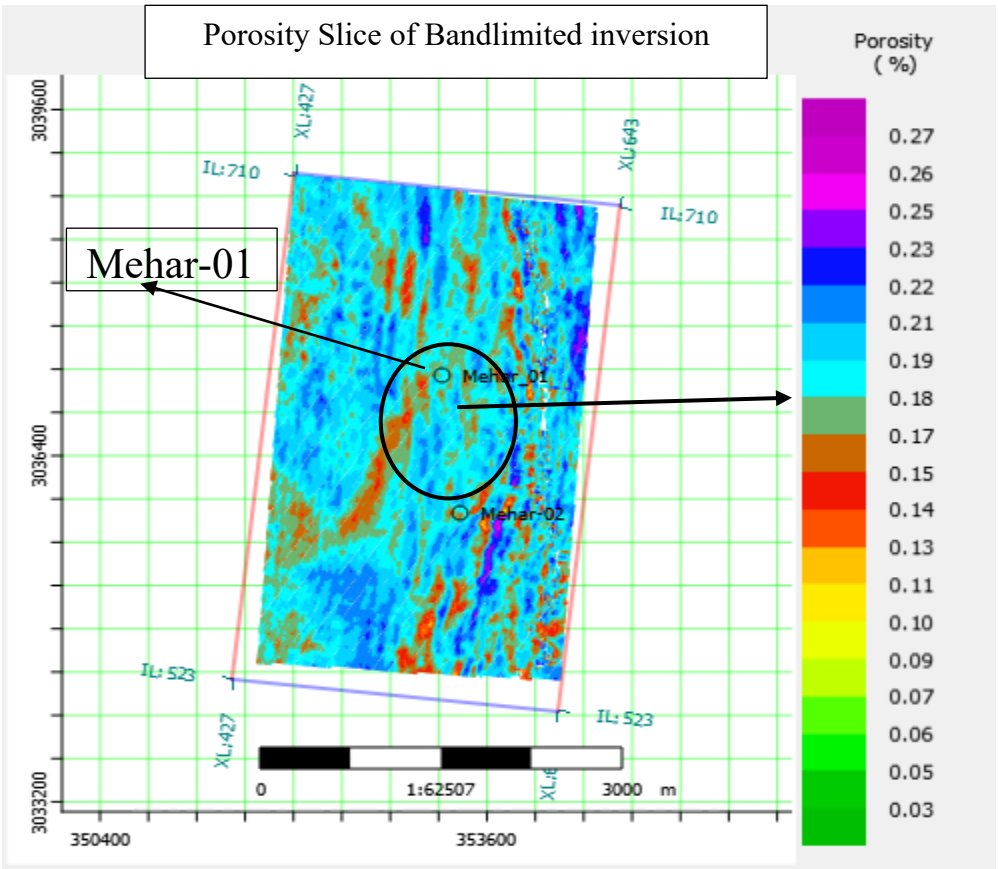

Fig (5.27) Porosity Slice of Bandlimited Inversion

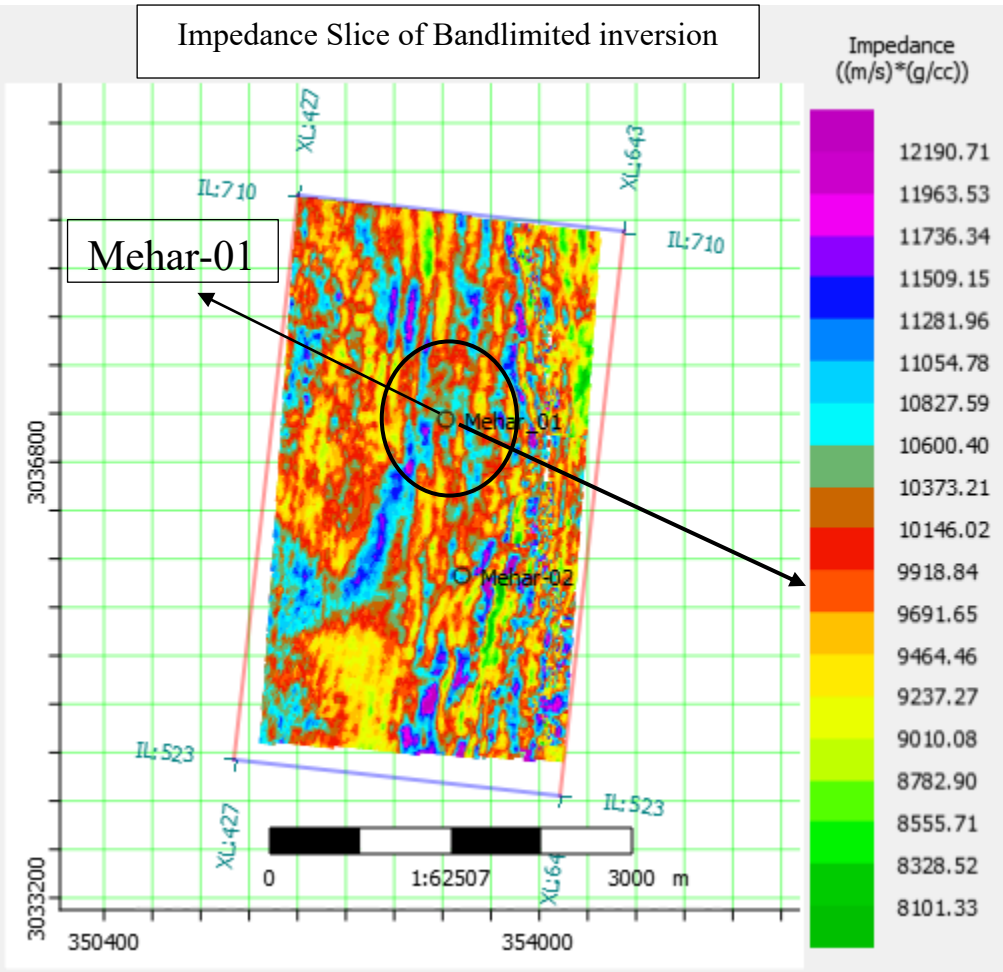

Fig (5.28) Impedance Slice of bandlimited Inversion

5.5) LMR Inversion

Lambda Mu-Rho (LMR) seismic inversion espoused for the integrated delimitation of lithological characterization of hydrocarbon-containing precincts principally gas posture zones (Goodway et al., 2008). The split-up in the retort of together lambda-rho (λρ) and mu-rho (μρρ) in this progression divulge us around the gas sands with respect to shale interims. Diverse lithologies be able to classify after the cross-plots of lambda-rho (λρ) which spectacle that these lithologies partake distinctive rock properties, fluid continence and grain volume. The appropriate considerate of lithological besides fluid characteristics originated after wireline log analysis to attain a comparatively high-pitched gradation of exactness in lithologies plus fluid substances (Anderson et al, 2001). The technique implemented for the reckoning of lambda-rho (λρ) and mu-rho (ρμ) seismic measurements is an AVO impedance scheme by the permutation of P-impedance then S-impedance measurements.

$$\rho\mu = SI^2 \quad (5.2)$$

$$\lambda\rho = AI^2 - 2SI^2 \quad (5.3)$$

The above-mentioned equations epitomize the relation between lambda-rho and mu-rho in terms of acoustic impedance. The LMR sections of Model Based Inversion are implied in the Figures below.

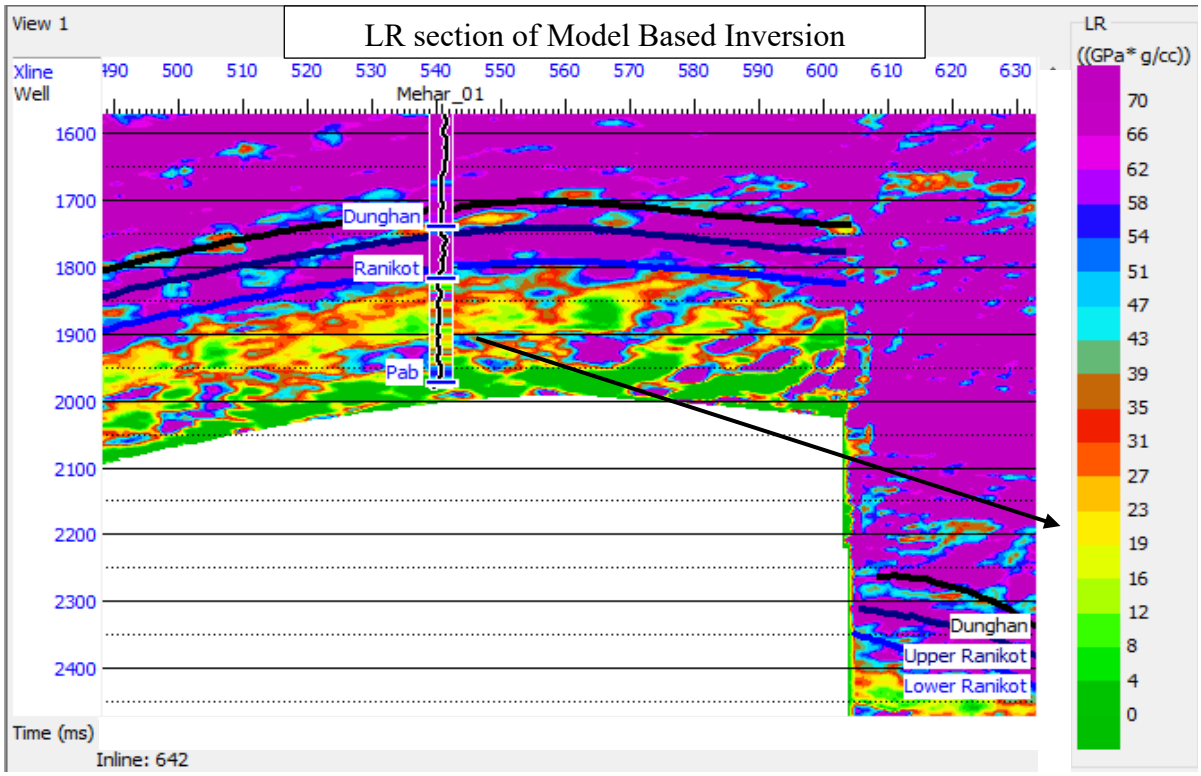

Fig (5.29) Lambda-Rho (λρ) section of Model Based Inversion

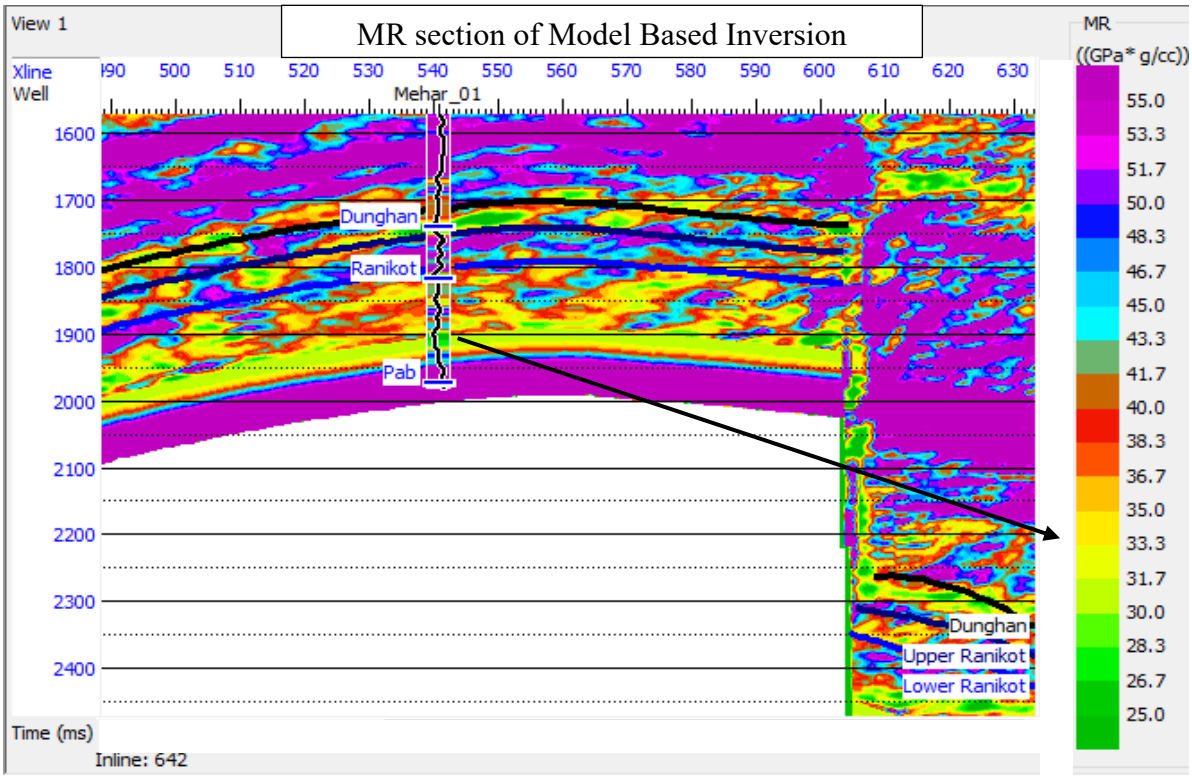

Fig (5.30) Mu-rho (ρμ) section of Model Based Inversion

The LMR sections on Sparse-spike (Maximum likelihood) and Bandlimited inversion are correspondingly presented in the Figure's underneath.

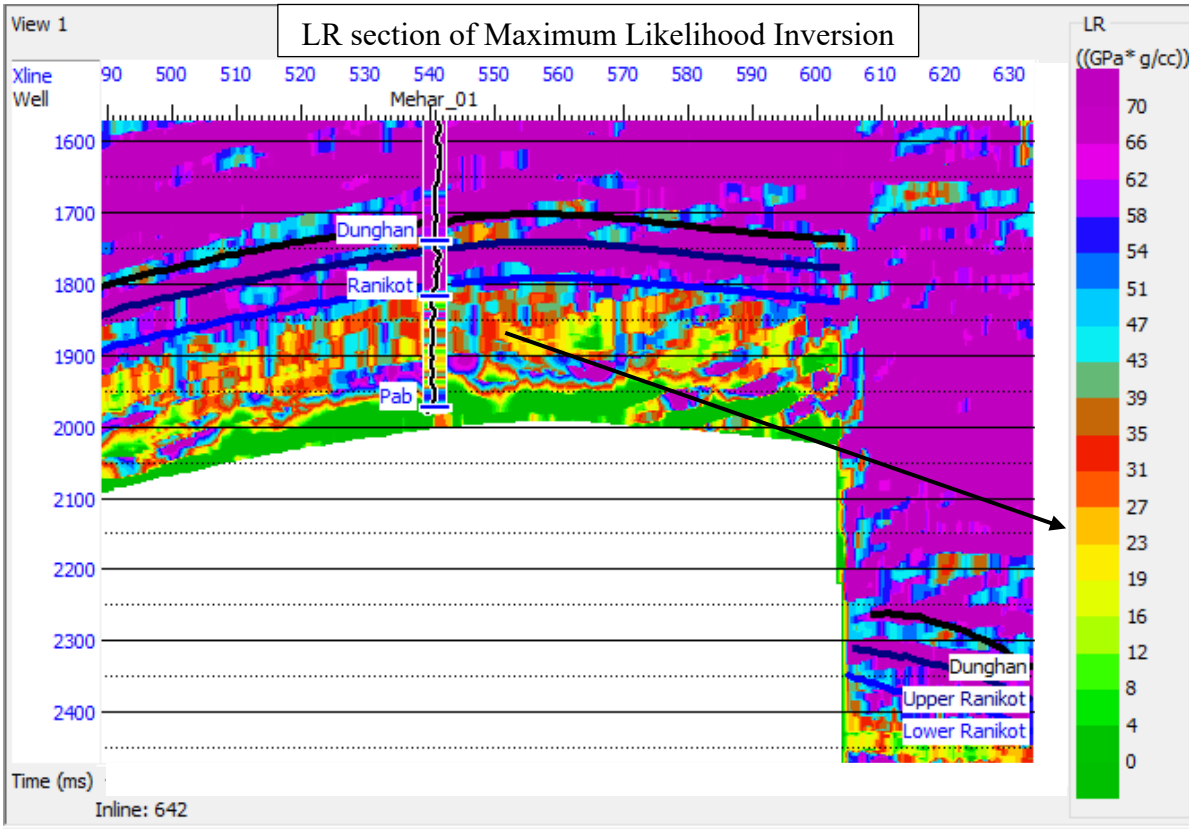

Fig (5.31) Lambda-Rho (λρ) section of Maximum Likelihood Inversion

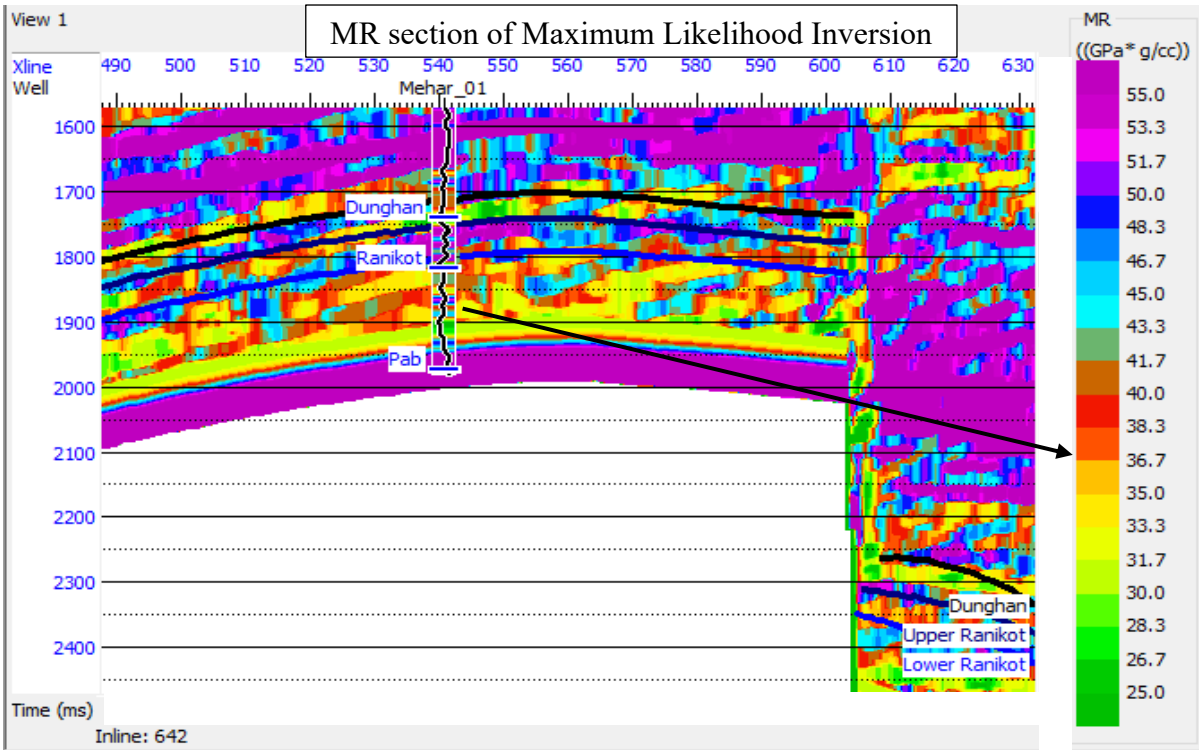

Fig (5.32) Mu-rho (ρμ) section of Maximum Likelihood Inversion

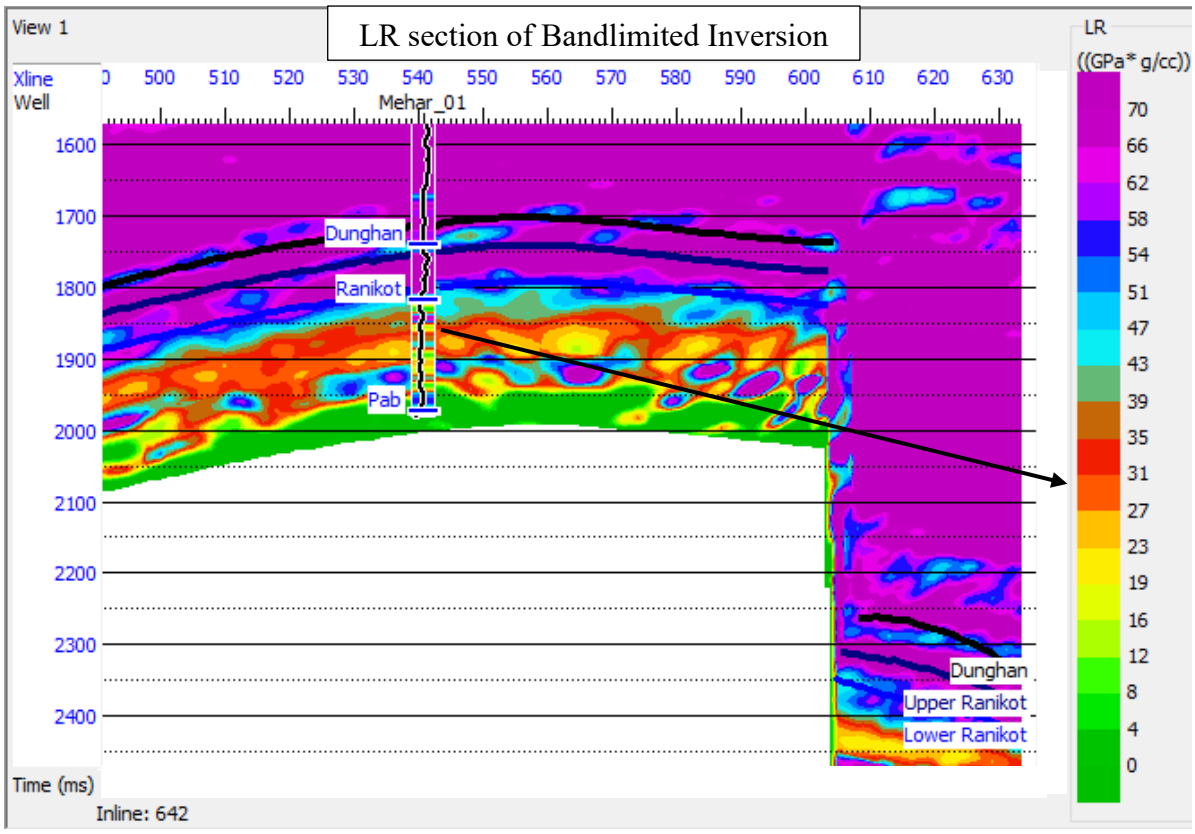

Fig (5.33) Lambda-Rho (λρ) section of Bandlimited Inversion

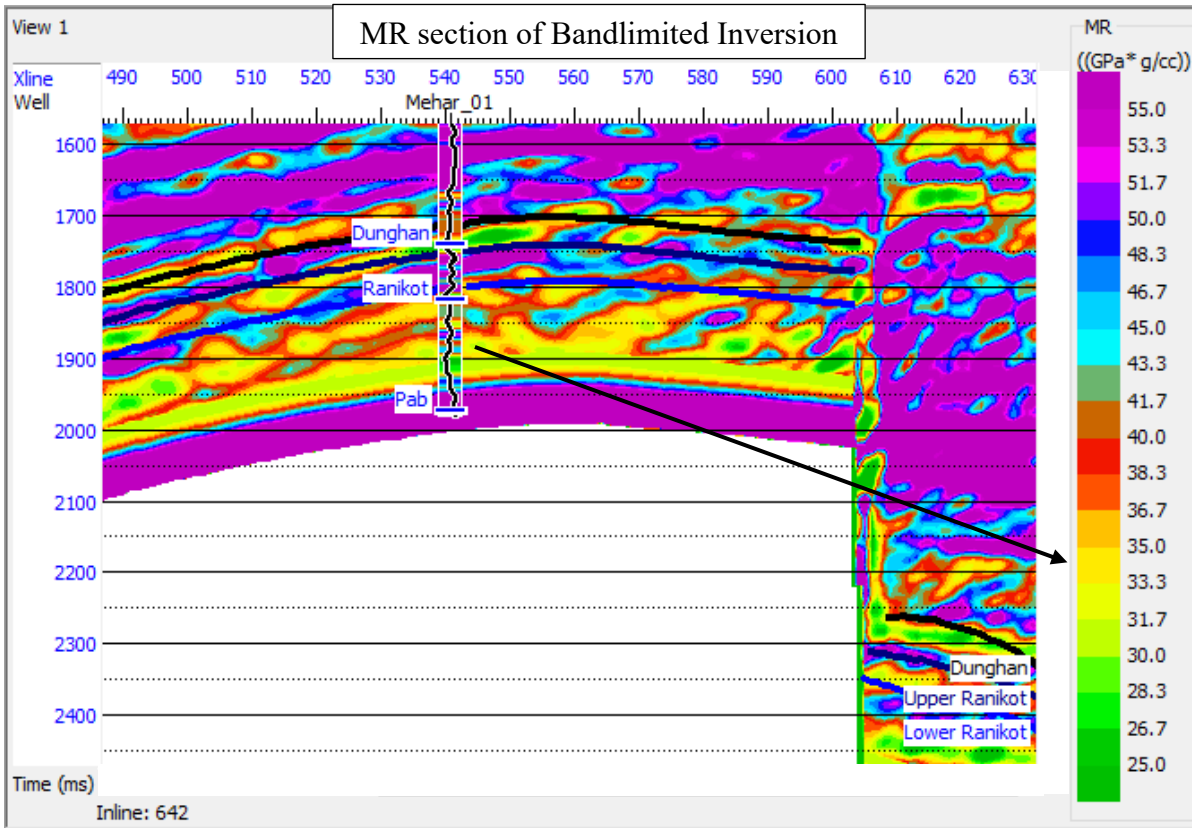

Fig (5.34) Mu-rho (ρμ) section of Bandlimited Inversion

Chapter 6 Evaluation of Porosity and Water Saturation via Machine Learning

6.1) Porosity modeling on the basis of Probabilistic Neural Network (PNN)

Neurons in the human nervous system process information at speeds a million times slower than logical computer gates (Vemuri, 1988).. Probabilistic Neural Network is a logical technique-based practice that make use of certain requisite neural linkage for its accomplishment. The purpose of Probabilistic Neural Network is to foretell the significance of exclusive dependent variable from one or supplementary autonomous variable standards. By the convention of Artificial Intelligence, Probabilistic Neural Networking stipulates enhanced and added steadfast results. The guesstimate of porosity by employing PNN spectacles that no recognizable difference is found between predicted and tangible porosity value. The succeeding Figure (6.1) displays the application of single attribute regression with correlation of 65% and an average of 5%.

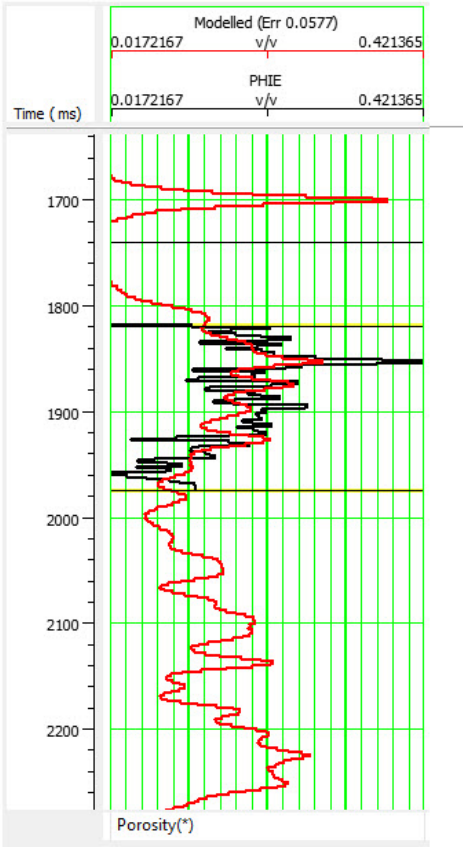

Fig (6.1) Application plot of Single Attribute Regression

The amplitude weighted Frequency versus square root porosity is plotted by using the slope-intercept equation (i.e. y = mx + c). Here, m = 0.50 and x = -3.73899e-06. The correlation of the plot came out to be 60% and error of the plot is 5%. The Figure (6.2) shows the associated plot.

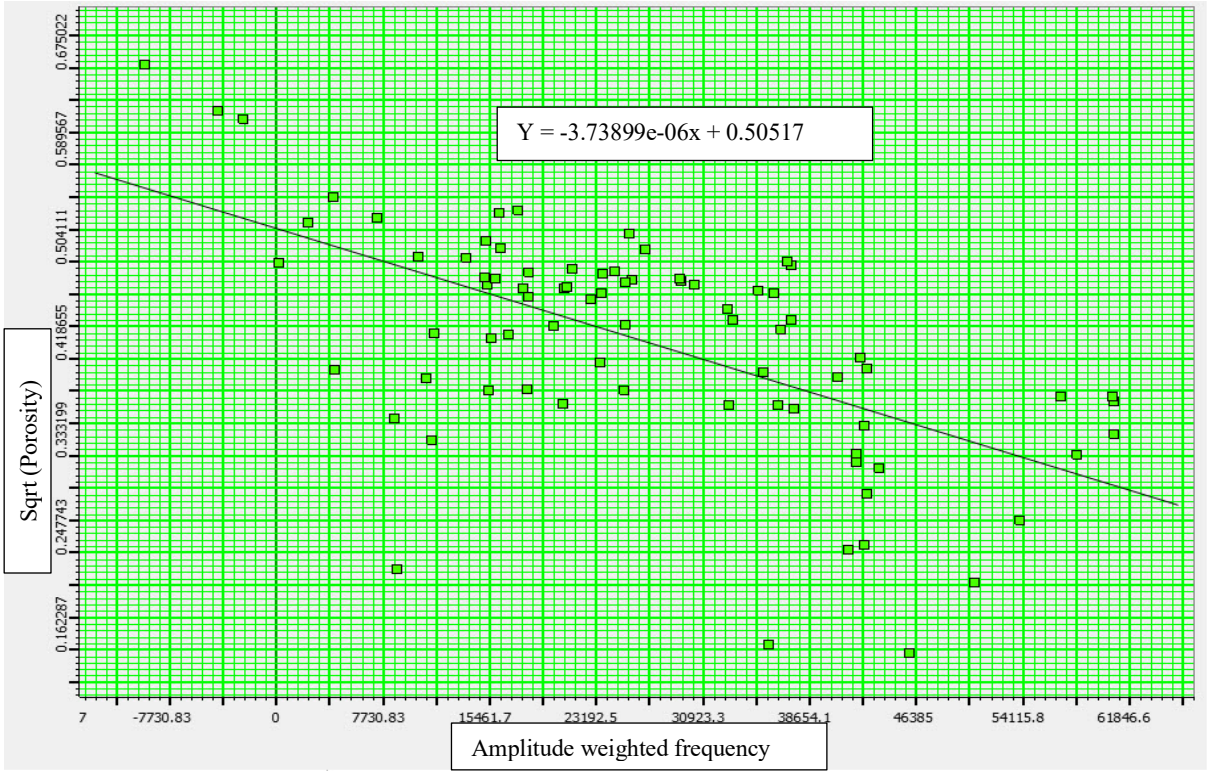

Fig (6.2) Amplitude weighted Frequency vs Square root Porosity

6.1.1) Multiple Attribute Analysis

The average error of the well-used in the process is shown below in the Figure (6.3). The black dots in the figure corresponds to the average error values on the Multiple-Attribute error plot.

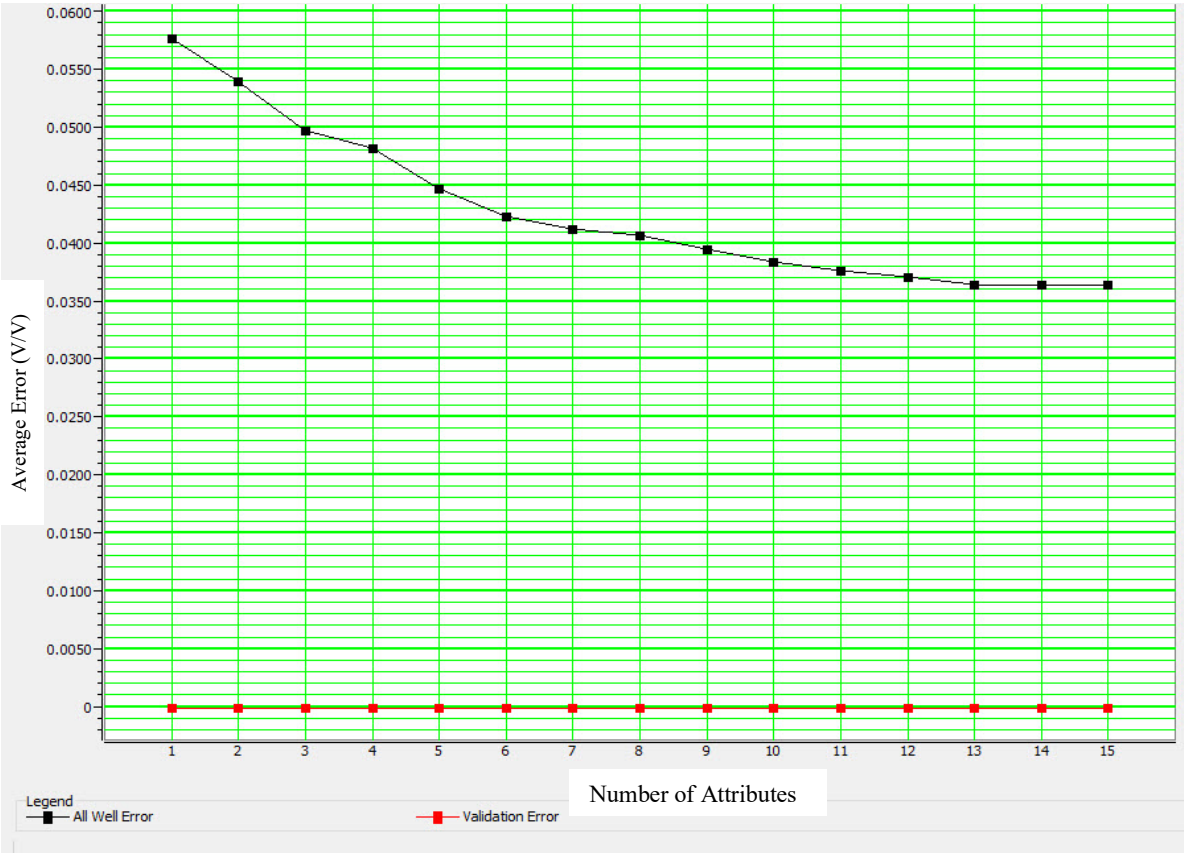

Fig (6.3) Multiple attribute error plot

6.1.2 Actual vs Predicted Porosity

The amplitude for cross-plot of actual porosity versus predicted porosity appeared with the correlation of 65% with 5% error. The subsequent Figure (6.4) illustrates the retrogression on the root of slope-intercept form by using one attribute following neural networking.

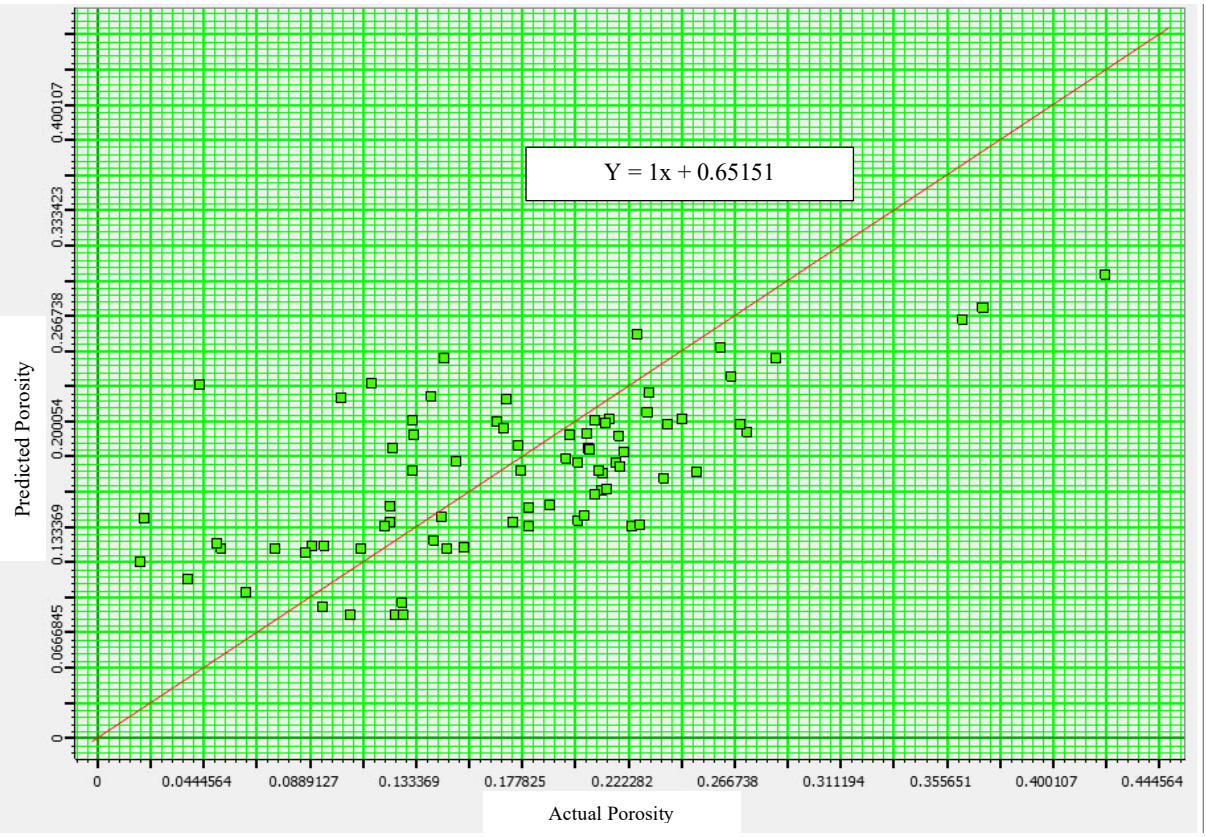

Fig (6.4) Actual porosity versus predicted porosity

6.2) Probabilistic Neural Network

After inputting for single and multiple attribute analysis, the subsequent and absolute phase is to vigor for the assortment of attributes of neural networking for porosity modeling. In the Figure (6.5) underneath, the application plot of neural networking scampered using 15 attributes and the correlation so achieved was 99.4% with the average error of 0.8%.

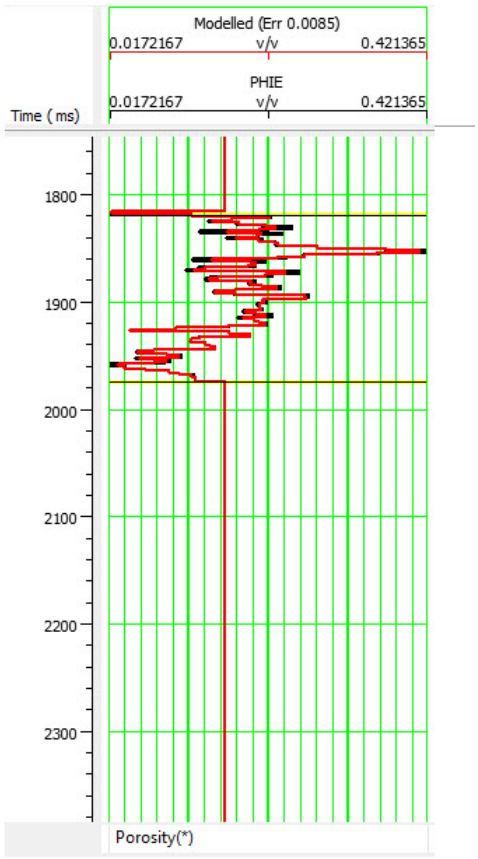

Fig (6.5) Application of Neural Network using 15 attributes with absolute correlation and average error.

6.3) Conclusive Porosity Model

The porosity model attained by applying the fundamentals of Probabilistic Neural Networking has ranges of porosity in between 5% to 25% (Figure, 6.6). The bluish color in the color bar corresponds to the blue pattern in the Ranikot formation that resembles with the actuality in sense of porosity of the same formation. The statistical resemblance amongst porosity of the reservoir formation by PNN, cross plots and wireline log analysis is the authentication of the porosity modeling through Probabilistic Neural Networking.

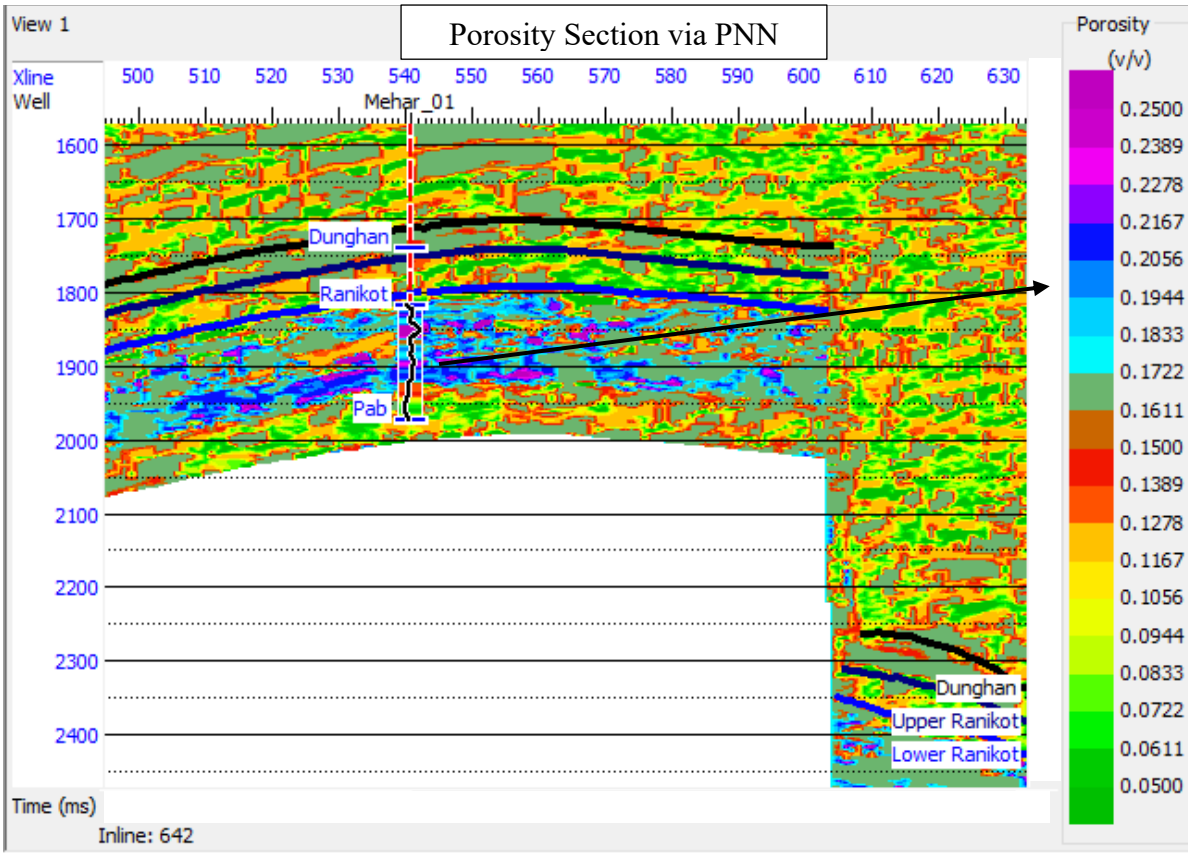

Fig (6.6) Results of PNN porosity estimated by using single and multiple attribute analysis

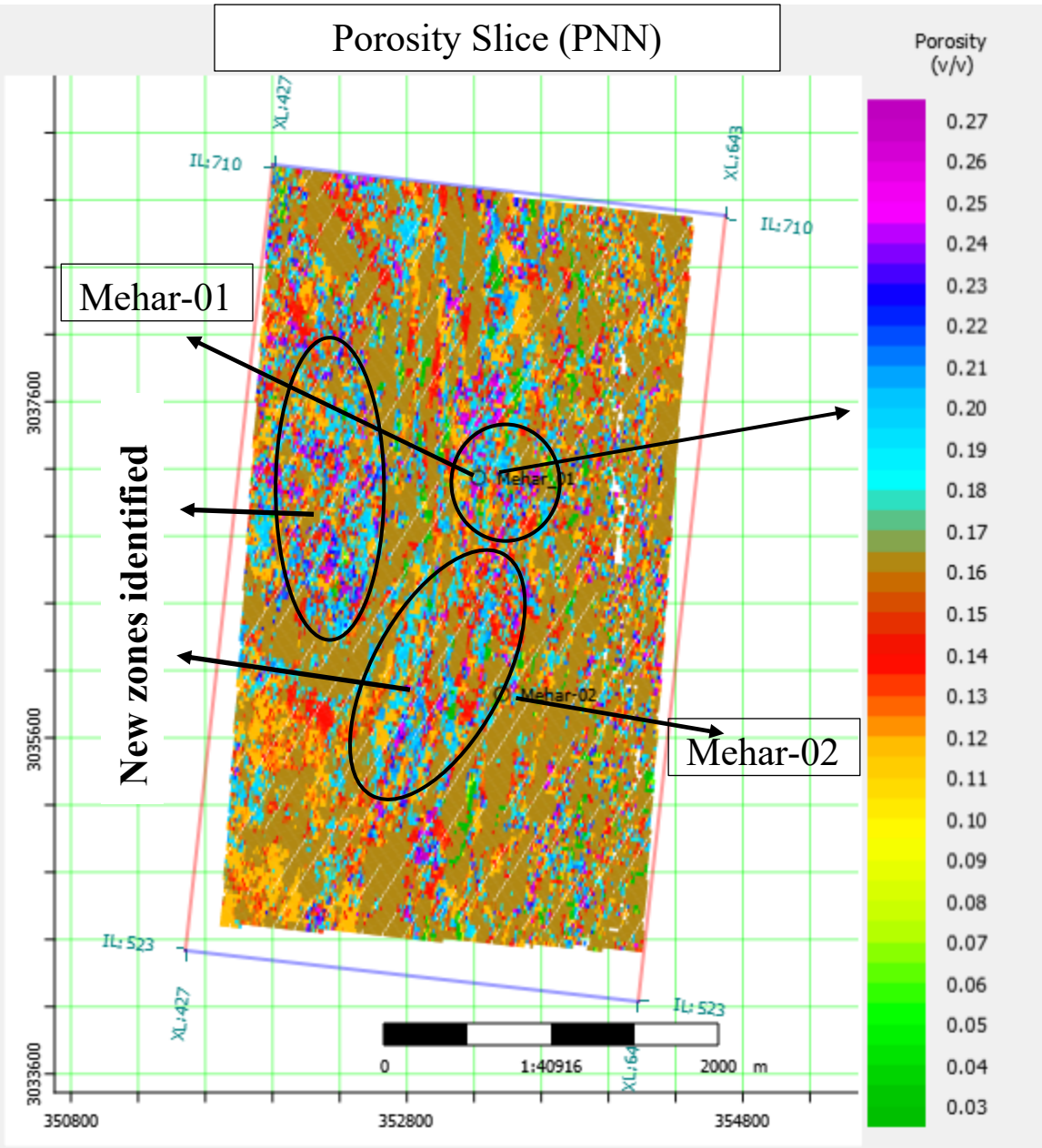

Fig (6.7) Slice of porosity section estimated by PNN

6.4) Estimation of water saturation using Deep Feed Forward Network (DFFN)

Knowledge depends significantly more on the network or structure of architecture than it does on the contents of particular locations (Caudill, 1987). The water saturation is assessed by exploiting Deep Feed Forward Networking (DFFN) via Hampson Russell software. The input parameters required to be chosen as the attributes are existing as the seismic volumes and external attributes. The fundamental footstep is to form an application of Single Attribute Regression. The single attribute analysis is designed using such an attribute which has the

least error and maximum correlation. The below Figure (6.8) is demonstrating the application of single attribute regression.

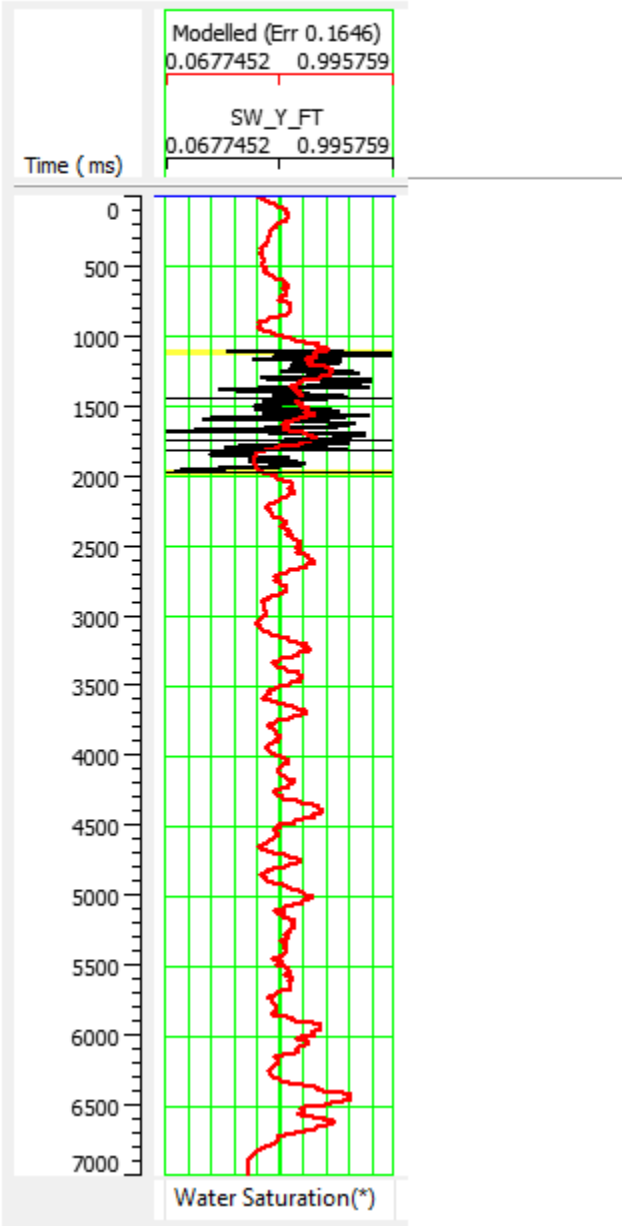

Fig (6.8) Application of single attribute regression

6.4.1) Single Attribute Analysis

The plot of integrated absolute amplitude against water saturation has schemed using single attribute analysis. The apprehensive plot is shown below in the Figure (6.9).

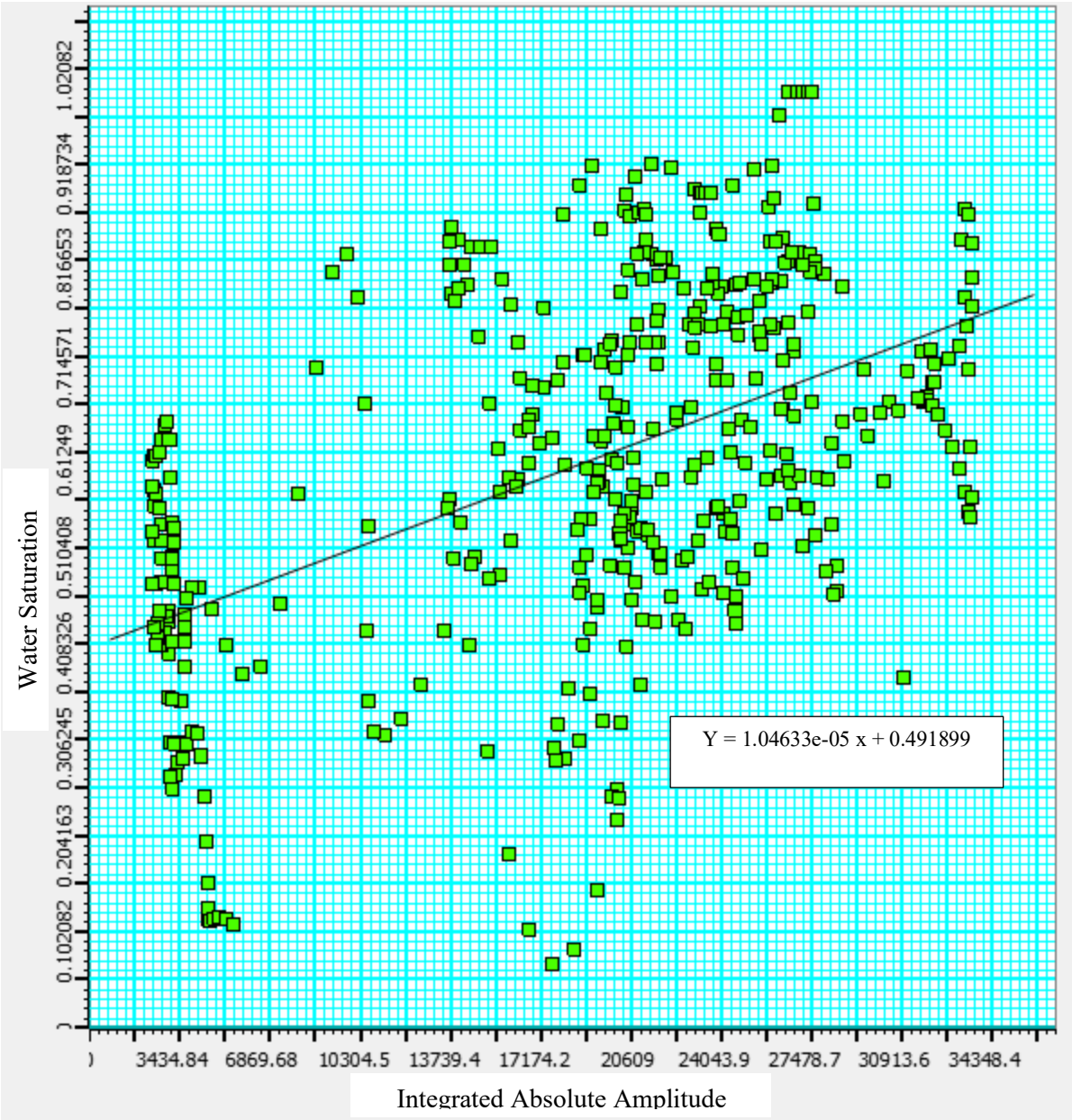

Fig (6.9) Integrated Absolute Amplitude vs Water Saturation

6.4.2) Multiple Attribute Analysis

The accomplishment of single attribute regression then leads to the commencement of multiple attribute regression amongst actual water saturation and predicted water saturation. The error plot of the well Mehar-01 used in the networking is shown below in the Figure (6.10). It can be seen in the Figure of error plot that the validation error is constantly lying at zero. It is because there is only one well utilized in the Deep Feed Forward Networking and no other well picked in the initial output for validation.

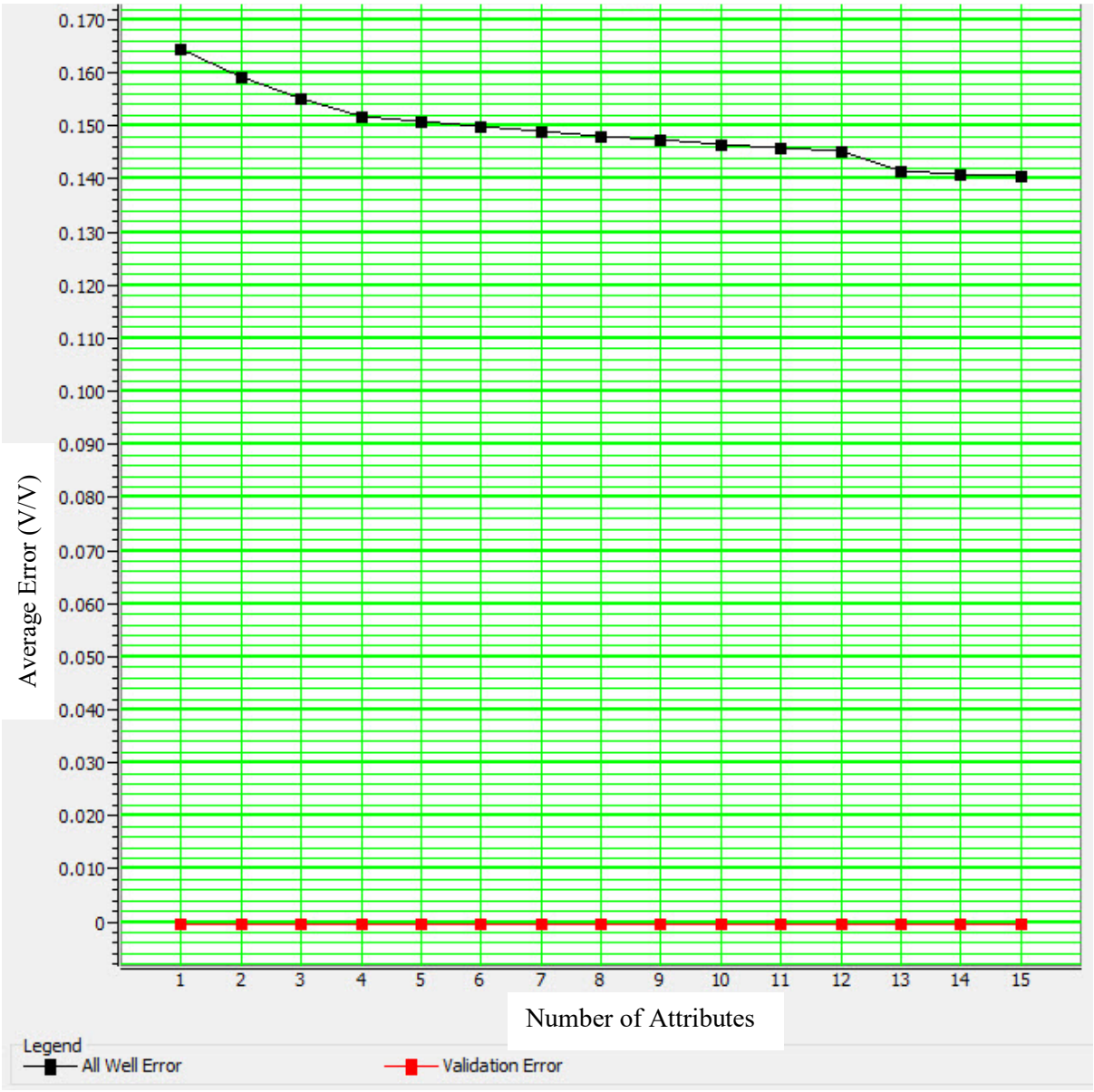

Fig (6.10) Average error plot of Multiple Attribute Anaalysis

There are 15 attributes used in the configuration of actual water saturation against predicted water saturation. The following Figure (6.11) shows the respected plot with correlation of 67%.

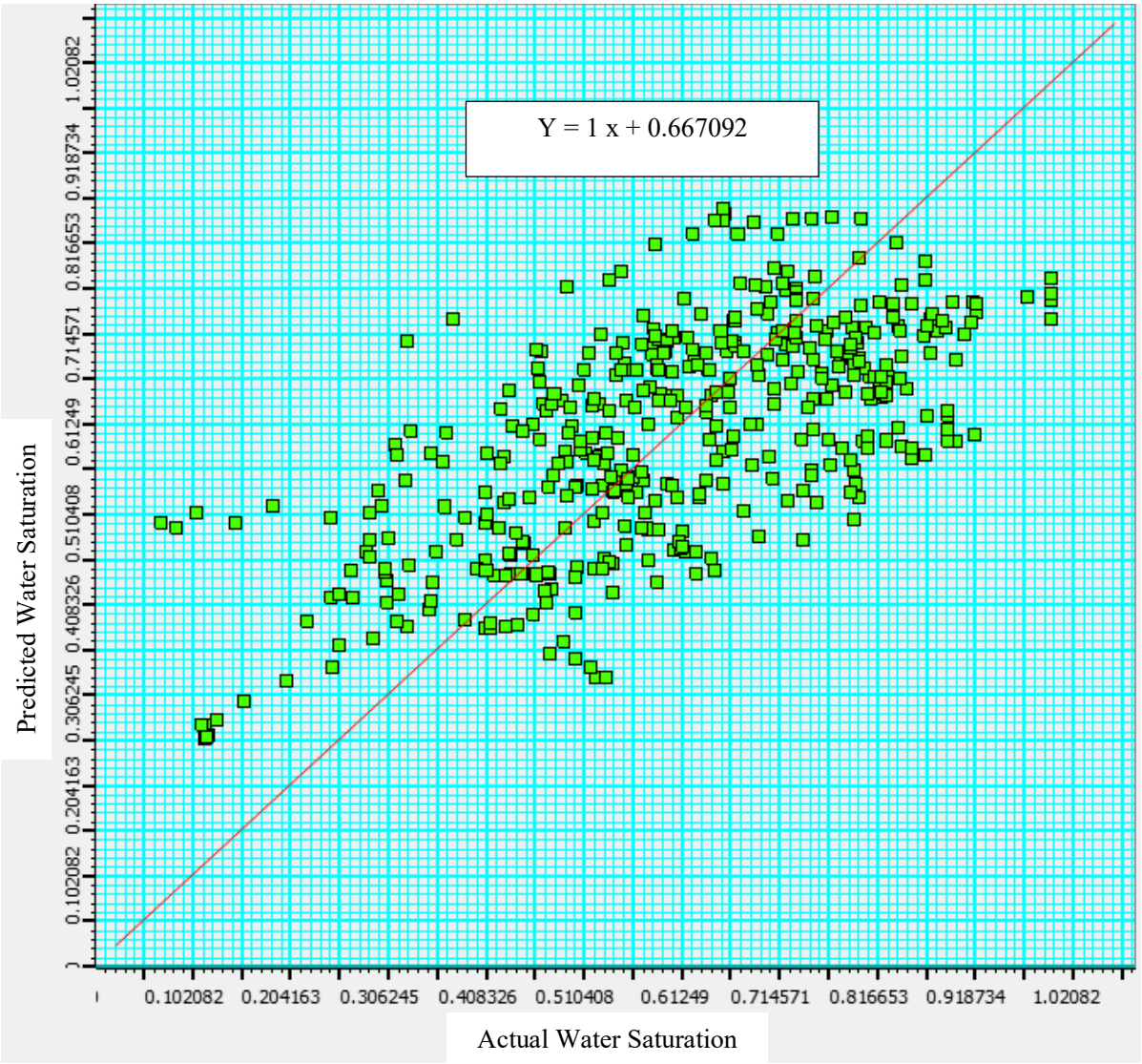

Fig (6.11) Actual Water Saturation vs Predicted Water Saturation

6.5) Results of Water Saturation by Deep Feed Forward Network

The application of Deep Feed-forward Network using 15 attributes with correlation of 88% and average error of 8% is the foundation for the cross plot and the final model of water saturation. The following Figure (6.12) shows the application of Deep Feed-forward Network for water saturation.

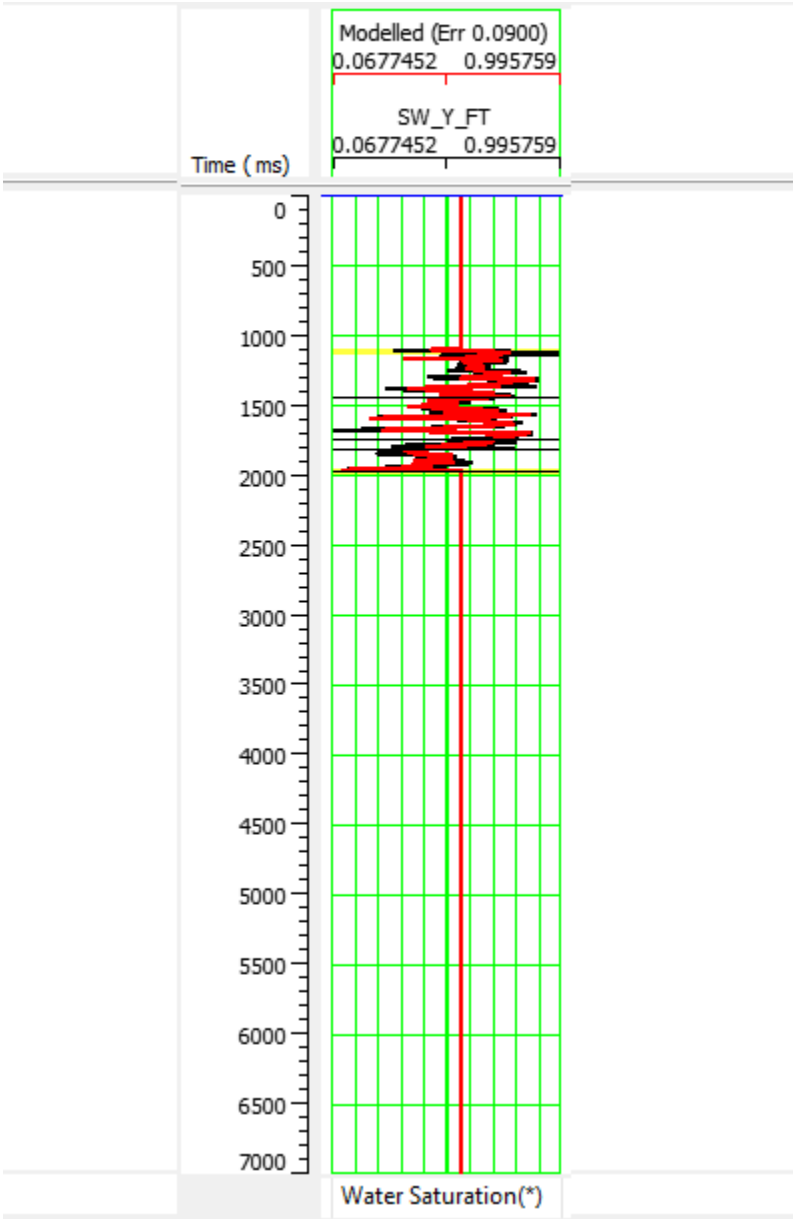

Fig (6.12) Application of Network for Deep Feed-forward Network

After inputting for single and multiple attribute analysis, the subsequent and absolute phase is to drive for the assortment of attributes of neural networking for water saturation modeling via Deep Feed-forward network. In the Figure (6.13) underneath, the application plot of neural networking scuttled using 15 attributes and the correlation so achieved was 88% with the average error of 8%.

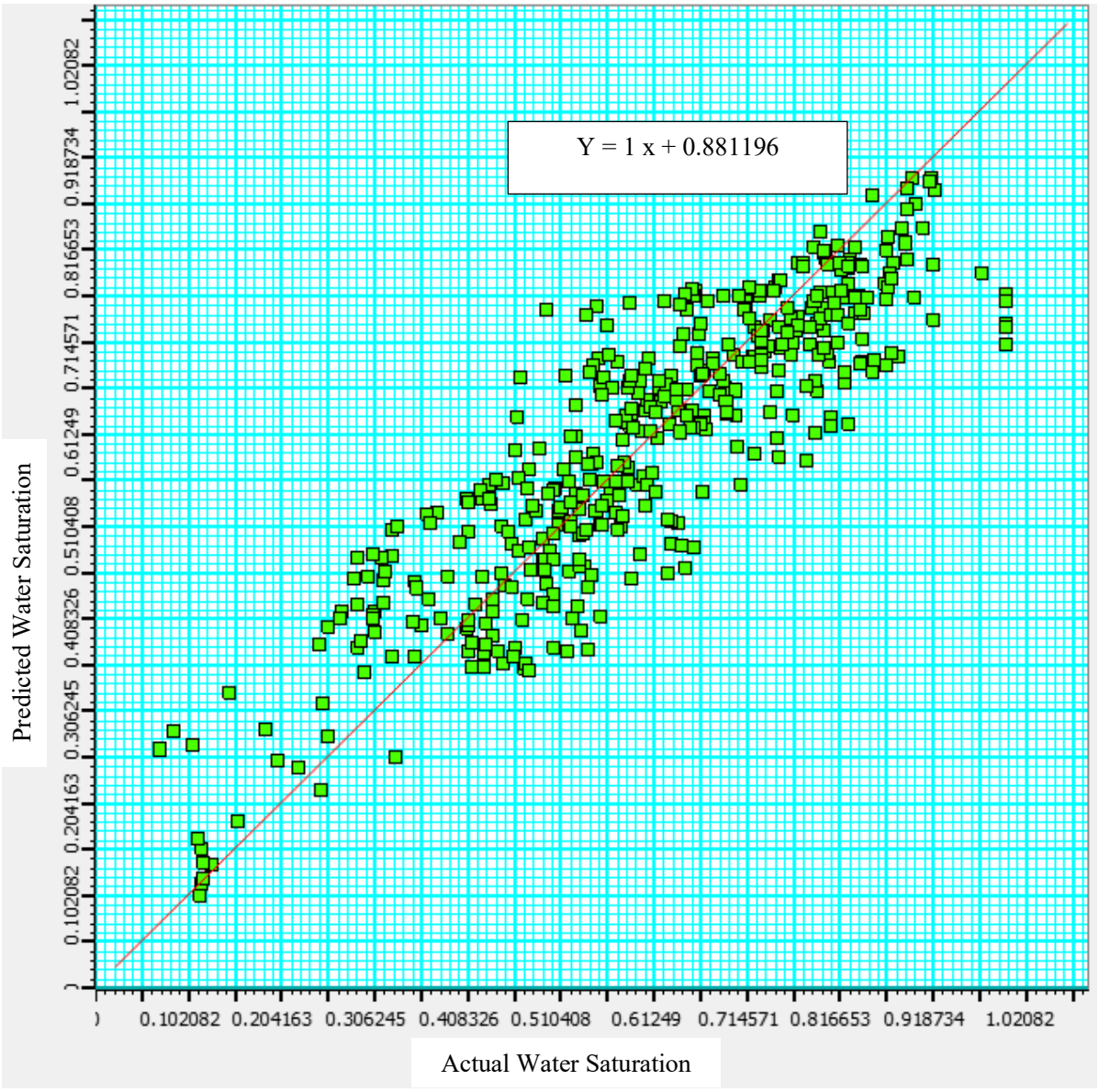

Fig (6.13) Actual water saturation vs Predicted Water saturation

6.6) Conclusive Water Saturation Model

The saturation model accomplished by operating the stipulations of Deep Feed-forward Neural Networking has assortments of saturation in between 20% to 50% in overall of Ranikot formation, (Figure, 6.14). The reddish color in the color bar corresponds to the red pattern in the Ranikot formation that resembles with the certainty in sense of saturation of the same formation. The statistical nearness amongst saturation of the reservoir formation by DFFN and wireline log analysis is the substantiation of the saturation modeling through Deep Feed-forward Neural Networking.

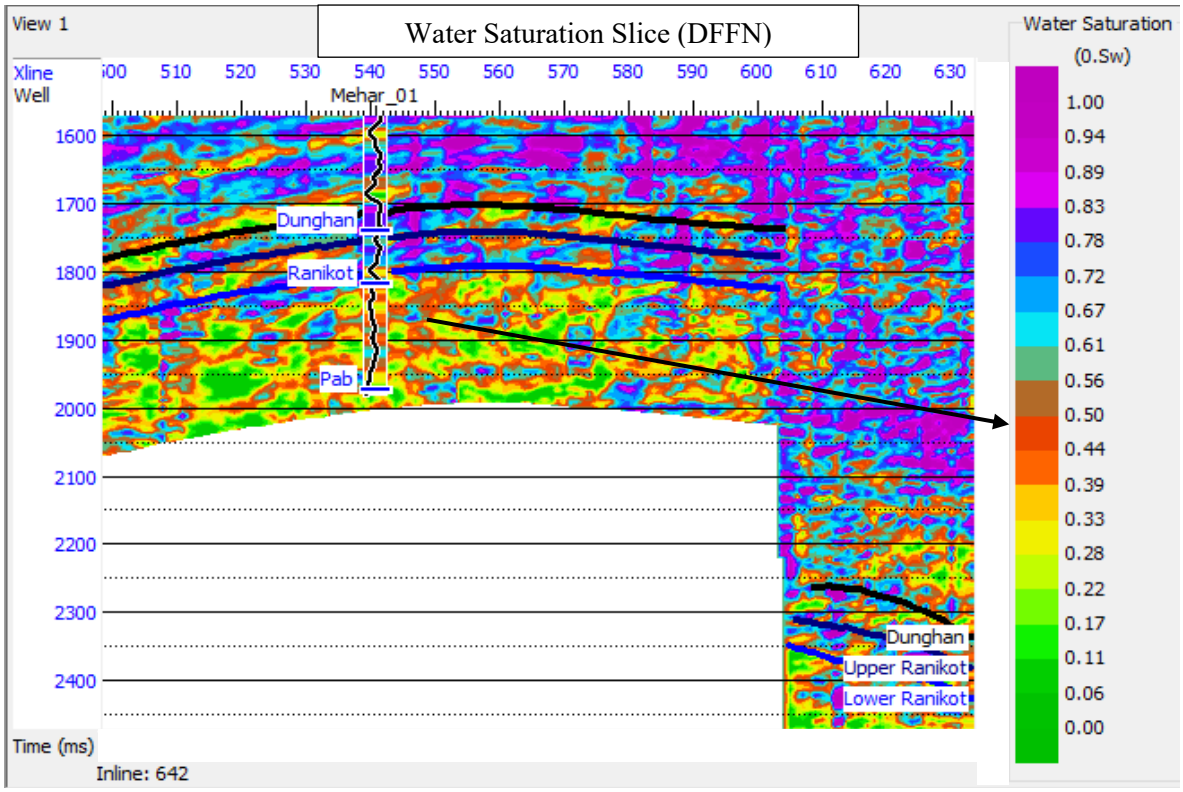

Fig (6.14) Results of DFFN water saturation estimated by using single and multiple attribute analysis

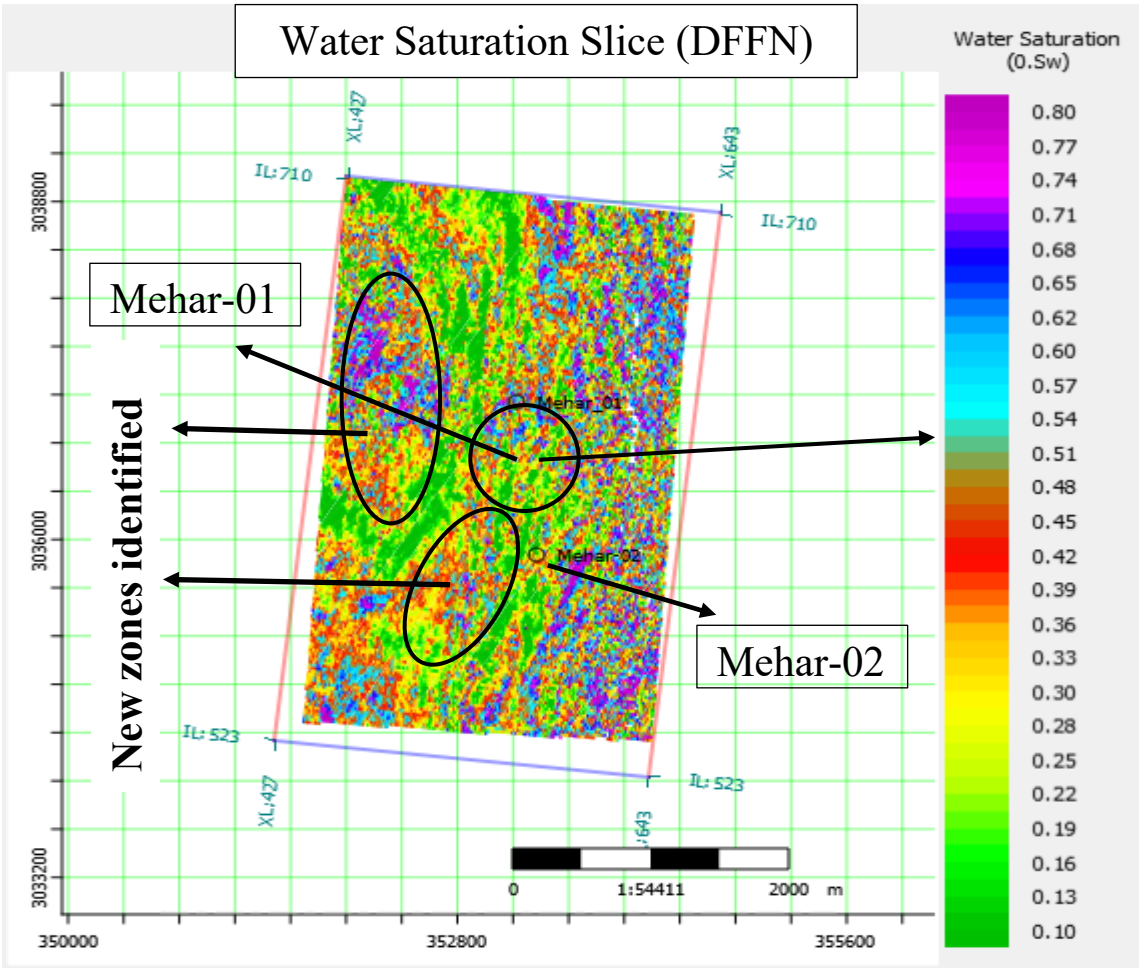

Fig (6.15) Slice of Water Saturation estimated by DFFN

Chapter 7 Discussions and Conclusions

7.1) Discussions

The exploitation of a reservoir can be increased significantly by means of reservoir characterization. To acquire an oil field, reservoir characterization plus model composition are pre-requisite steps (Mahapatra et al., 2003). Although seismic characteristics are also very susceptible to horizontal noise deviations, seismic characteristics are significantly more responsive to horizontal geological changes (Oyeyemi et al., 2015). The aim of this study is to practice the seismic and well log data of Mehar Block, Lower Indus Basin, Pakistan in order to demarcate and subsequently characterize the reservoir formation (i.e. Ranikot). To characterize the potential of the prospective reservoir with a precise geographical distribution is the main goal of reservoir characterization. Information on the amount of reservoir host contains as well as its level of fracking resistance is included in the categorization of resources. Depending on the imperial relationship, a layer feature called acoustic impedance can be utilized to define reservoir characteristics including density, porosity, fluid saturation for the space between wells (Kumar et, al. 2016). Geological, geophysical, petrophysical, and engineering data gathered at different phases of exploration and field production can be expended to anticipate these reservoir attributes. Direct laboratory estimation is done by analyzing samples taken from field outcrops, core/cutting data, quantitative interpretation of surface 2D/3D seismic data, petrophysical interpretation of wireline log data, and assessment of test production data.

Mapping the region's wide-ranging structure is the foremost footstep in seismic interpretation. The fundamental constituent of this structural interpretation is the formation of faults plus horizons with planes. The interpreter generates horizons by selecting and captivating a reflector across the volume. (Bakker, 2002). In order to extract subsurface information about stratigraphy, structure, rock physics and possibly reservoir fluid fluctuations in time and space, seismic interpretation transforms the geological meaning of seismic data (Liner, 1999). A suitable structural interpretation and its deductions are significant in idealizing the geology of the subsurface (Badley, 1985).

In order to extricate subsurface information about stratigraphy, structure, rock physics and conceivably reservoir fluid variabilities in time and space, seismic interpretation transmutes the geological implication of seismic data (Liner, 1999). Recently, seismic data (2D/3D), participated a vibrant function in quantifiable interpretation of conventional shale oil/gas

potential (Mavko et al., 2009; Chopra and Castagna, 2014; Aziz aal, 2019). Seismic data (both pre-stack or post-stack) are recurrently expended in the exploration of oil and gas to guesstimate the potential of reservoirs (Gray et al., 2012; Aziz et al., 2019). The data of well logging, through trailing the compulsory workflow, enumerates the tangible occurence of water or hydrocarbon (either oil or gas or both) in the study area (Asquith and Krygowski, 2004). The repeated use of well logs is made to estimate the reservoir potential to get enough information and also to categorize the thickness (Abd El-Gawad, 2007). A statistical consideration of seismic and well data is seismic inversion (Maurya and Sarkar, 2016). Model Parameters are modified till the model correspondence with experimental data. Concluding geological model adds for approximation of the dissemination of reservoir characteristics (Vecken and Da Silva, 2004). The fundamental aim of the seismic attribute and seismic inversion in this study is not merely to postulate information of acoustic impedances although additionally to represent comprehensive interpretations of other reservoir properties such as TOC, E, Poisson's ratio for locations where no wells are available (Gray et al., 2012; Aziz et al., 2019). Depending on the imperial correlation, a layer feature entitled as acoustic impedance can be utilized to delineate reservoir physiognomies including density, porosity, fluid saturation for the area between wells (Kumar et, al. 2016). Model Parameters outlook commissioned till the model correspondence within the experimental data. Concluding geological model countersigns for approximation of the dissemination of reservoir characteristics (Vecken and Da Silva, 2004). The main goal of wireline log analysis is to adjust the data to the highest standards while approximating the most exact quantitative standards possible. These characteristics include shale volume, net pay, water saturation, porosity, and lithology (Cannon, 2016). The wireline log analysis of the wells Mehar-01, 02 and 03 indicates that the effective porosity (PHIE) in the zone of interest in Mehar-01 is 7.3%, total porosity (PHIT) is 8.1%, shale volume (Vsh) is 10%, and hydrocarbon potential (HS) is 58.2%. In case of Mehar-02, the PHIE in the zone of interest has been estimated to be 7.6%, Vsh is 25%, PHIT is 13% and HS is 68%. Two zones have been demarcated in Mehar-03 well indicating PHIE values of 5.3% and 11.9%, total porosity is 7.8% and 17.9%, shale volume is 11.9% and 12%, and hydrocarbon saturation is 51.2% and 72% respectively. A single parameter is the only thing that "primitive" characteristics, as the name suggests, can quantify. By linking these fundamental characteristics via statistical, neural network, or mathematical operations, "hybrid" attributes are created (Taner, 2001). Probabilistic Neural Network is an analytical technique-based exercise that construct use of certain requisite neural linkage for its execution. The purpose of Probabilistic Neural Network is to prognosticate the implication of exclusive

conditional variable from one or additional independent variable standards. Neurons in the human nervous system process information a million times more slowly than logical computer gates (Vemuri, 1988). By the resolution of Artificial Intelligence, Probabilistic Neural Networking specifies augmented and dividend steadfast results. Knowledge is much more dependent on the architecture of the network or structure than it is on the contents of specific places (Caudill, 1987). The estimation of porosity by commissioning PNN spectacles that no distinguishable difference is discovered between predicted and tangible porosity value. The water saturation is evaluated by utilizing Deep Feed Forward Networking (DFFN). The input parameters are mandatory to be preferred as the attributes that are standing as the seismic volumes and external attributes. This spatially recognized zone is further validated by the low values of the $\lambda\rho$ sections (extracted from each inversion model) demonstrating occurrence of hydrocarbons while the adequate values in the same zone from the $\mu\rho$ sections depict the existence of sand. The spatial distribution of effective porosity using PNN and cross plots depicts high values in the reservoir formation. Furthermore, the DFFN based water saturation values suggest comparatively low saturation values in the zone of interest.

7.2) Conclusions

- The structural seismic interpretation indicated that the regime of the Mehar block is compressional in nature due to the existence of reverse and thrust faulting.
- The wireline log analysis is smeared on the three given wells i.e. Mehar-01, Mehar-02 and Mehar-03 illuminating that the hydrocarbon potential of Mehar-01 is 58% and that of Mehar-02 and Mehar-03 is 68% and 72% respectively.
- Seismic inversion modeling on Model based, maximum likelihood and bandlimited inversion assisted to idealize the reservoir formation using P-impedance and S-impedance. The results of their sections distinctly asserted the appearance of low impedance in the Ranikot formation.
- Probabilistic Neural Networking (PNN) specified the augmented and dividend steadfast results with the statistical proposition of 15% to 20% in overall of the Ranikot formation.
- The water saturation evaluated by exploiting Deep Feed Forward Networking (DFFN) that emanated with the value of 40-50% in the Ranikot formation.

References

Abd El-Gawad, E. A. (2007). The use of well logs to determine the reservoir characteristics of Miocene rocks at the Bahar Northeast field, Gulf of Suez, Egypt. Journal of Petroleum Geology, 30(2), 175-188.

Ahmad, N., Fink, P., Sturrock, S., Mahmood, T. & Ibrahim, M. (2004). Sequence stratigraphy as predictive tool in Lower Goru Fairway, Lower and Middle Indus platform, Pakistan. Proceedings of: PAPG-SPE Annual Technical Conference (pp. 85–104). 8–9 October 2004, Islamabad, Pakistan.

Anderson, K., & Smith, S. J. (2001). Emotional geographies. Transactions of the Institute of British geographers, 26(1), 7-10.

Arshad, K., Imran, M. & Iqbal, M. (2013). Hydrocarbon Perspectivity And Risk Analysis of An Under-Explored Western Kirthar Fold Belt of Pakistan. In Offshore Mediterranean Conference and Exhibition.

Archie, G. E. (1950). Introduction to petrophysics of reservoir rocks. AAPG bulletin, 34(5), 943-961.

Avseth, P., Mukerji, T., and Mavko, G., (2005). Quantitative seismic interpretation: 457 Applying rock physics tools to reduce interpretation risk. Cambridge University Press.

Asquith, G. B., Krygowski, D., & Gibson, C. R. (2004). Basic well log analysis (Vol. 16),Tulsa: American association of petroleum geologists.

Badley, M.E. (1985). Practical seismic interpretation IHRDC press, Boston.

Caudill, M., 1987. Neural networks primer, Part I. AI Expert, Sept. 1987.

Cooke, D., Cant, J., (2010). Model based Seismic Inversion: comparing deterministic and probabilistic approaches. CSEG Rec 35 (4), 28-39.

Da Silva, M., Rauch-Davies, M., Soto Cuervo, A. and Veeken, P. in prep., pre and post-stack attributes for enhancing production from Cocuite gas reservoirs. 66th EAGE Annual Conference, Paris, (2004).

Daud, 2011, Remaining Hydrocarbon Potential in Pakistan – A Statistical Review, https://www.researchgate.net/publication/323143341.

Tectono-Stratigraphic Model for Ghazij Formation in Kirthar Foldbelt, Pakistan* Abrar Ahmad1, Mohsin Ali1, Abid H. Baitu1, and Naeem Sardar1. Search and Discovery Article #50725 (2012).

Bakker, P (2002). Image structure analysis for seismic interpretation, Netherlands Ministry of Economic Affairs, within the framework of Innovation Oriented Research Program (IOP, project number IBV97005).

Bannert, D., Cheema, A., Ahmed, A., & Schäffer, U. (1993). The Structural Development of the Western Fold Belt, -Pakistan.

Cannon, S. (2016). Petrophysics: a practical guide. John Wiley & Sons.

Hoffe, B., Perez, M., & Goodway, W. (2008). AVO interpretation in LMR space: A primer. Back to Exploration, 31-34.

Kadri, I. B. (1995). Petroleum geology of Pakistan. Pakistan Petroleum Limited.

Kazmi, A. H. & Jan, M. Q. 1997. Geology and Tectonics of Pakistan.

Khadri, I.B., 1995, Petroleum geology of Pakistan: Karachi, Pakistan petroleum Ltd., p. 275.

Khan, M. S., Masood, F., Ahmed, Q., Jadoon, I. A. K., & Akram, N. (2017). Structural interpretation and petrophysical analysis for reservoir sands of lower Goru, miano area, Central Indus Basin, Pakistan. International Journal of Geosciences, 8, 379–392.

Kumar. A.R and S. Chopra, (2016). Building more robust low-frequency models for seismic impedance inversion.

Lovell, M., Williamson, G., Harvey, P. (Eds.), 1999. Borehole Imaging; Applications and Case Histories. Geol.Soc., Spec. Publ., vol. 159, 294 pp.

Maurya, S.P., & Sarkar, P. (2016). Comparison of post stack seismic inversion methods: a case study from Blackfoot Field, Canada. Int J Sci Eng Res, 7(8), 1091-1101.

Meissner Jr C, Rahman H (1973) Distribution, thickness, and Lithology of Paleocene Rocks in Pakistan. In: USGS Professional Paper 716-E, US Government Office, Washington.

Mahmud, O. A., & Aziz, S. A. (2002). Sequence stratigraphic study of Pab sandstone, Mehar Block, Middle Indus Basin Pakistan. Warta Geology, 28(5), 7.

Mahapatra, Sailendra N., Imhof, Matthias, G., and Kempner, W., 2003, Deterministic High-Resolution Seismic Reservoir Characterization: Abstract, Aapg Annual Meeting (2003): Energy- Our Monumental Task Technical Program, Salt Lake City, Utah, USA.

Niamatullah, M., & Imran, M. (2012). Structural geometry and tectonics of southern part of Karachi arc—a case study of Pirmangho and Lalji area. Search and Discovery Article, 50581

Liner, C. L., Underwood, W. D., & Gobeli, R (1999). 3-D seismic survey design as an optimization problem. The Leading Edge, 18(9), 1054-1060

Nanda, N. C. (2016). Seismic Wave Propagation and Rock-Fluid Properties. In Seismic Data Interpretation and Evaluation for Hydrocarbon Exploration and Production (pp. 3-17). Springer, Cham.

Oyeyemi, Kehinde & Philips, A. (2015). Seismic attribute analysis for reservoir characterization; Offshore Niger delta. Petroleum and Coal. 57. 619-628.

Ralph Hinsch et al., 2018, Structural Modelling in the Kirthar Fold Belt of Pakistan: From Seismic to Regional Scale, Search and Discovery Article #30546 (2018).

Shakir et, al., 2022, Selection of Sensitive Post-Stack and Pre-Stack Seismic Inversion Attributes for Improved Characterization of Thin Gas-Bearing Sands, https://doi.org/10.1007/s00024-021-02900-1.

Singha, D. K., & Kumar, R (2016). Post stack seismic inversion and attribute analysis in shallow offshore of Krishna-Godavari basin, India. Journal of the Geological society of India, 90(1), 32-40.

Smewing, J. D., Warburton, J., Daley, T., Copestake, P., & Ul-Haq, N. (2002). Sequence stratigraphy of the southern Kirthar fold belt and middle Indus basin, Pakistan. Geological Society, London, Special Publications, 195(1), 273-299.

Stefansson and Steingrimsson. “Geothermal Logging”, National energy authority, Iceland (1980).

Szeliga, W., Bilham, R., Schelling, D., Kakar, D. M., and Lodi, S.: Fold and thrust partitioning in a contracting fold belt: insights from the 1931 Mach earthquake in Baluchistan, Tectonics, 28, TC5019, https://doi.org/10.1029/2008TC002265, 2009.

Tiab, D. and Donaldson, E.C. (2004). Petrophysics- Theory and practice of measuring reservoir rock and fluid transport properties. Gulf Professional Publishing, Oxford, UK. 926 pp.

Taner, M. T., 2001, Seismic attributes, CSEG Recorder, pp. 48-56, September Issue.

Urooj Shakir and Amir Ali, et, al. 2021 Improved gas sand facies classification and enhanced reservoir description based on calibrated rock physics modelling, https://www.degruyter.com/document/doi/10.1515/geo-2020-0311/html.

Van Wagoner, J. C., Mitchum, R. M., Campion, K. M., & Rahmanian, V. D. (1990). Siliciclastic sequence stratigraphy in well logs, cores, and outcrops: concepts for high-resolution correlation of time and facies.

Vemuri, V., 1988. Artificial Neural Networks: Theoretical Con- cepts. IEEE Computer Society Press, Los Alamitos, CA.